TECHNICAL REPORT ITL-87-5

⑫

THEORETICAL MANUAL FOR DESIGN OF CELLULAR SHEET PILE STRUCTURES (COFFERDAMS AND RETAINING STRUCTURES)

by

Mark Rossow

Southern Illinois University

Edward Demsky

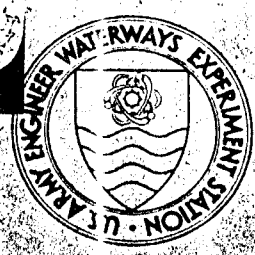US Army Engineer District, St. Louis

Reed Mosher

US Army Engineer Waterways Experiment Station

Information Technology Laboratory

DEPARTMENT OF THE ARMY
Waterways Experiment Station, Corps of Engineers
PO Box 631, Vicksburg, Mississippi 39180-0631

May 1987

Final Report

ADA182903

REPORT DOCUMENTATION PAGE

Form Approved
OMB No 0704-0188
Exp Date Jun 30, 1986

1a REPORT SECURITY CLASSIFICATION	1b. RESTRICTIVE MARKINGS
Unclassified	

2a SECURITY CLASSIFICATION AUTHORITY	3 DISTRIBUTION/AVAILABILITY OF REPORT
2b DECLASSIFICATION/DOWNGRADING SCHEDULE	Approved for public release; distribution unlimited.

4 PERFORMING ORGANIZATION REPORT NUMBER(S)	5. MONITORING ORGANIZATION REPORT NUMBERS
Technical Report ITL-87-5	

6a. NAME OF PERFORMING ORGANIZATION USAEWES Information Technology Laboratory	6b. OFFICE SYMBOL (If applicable) WESKA-E	7a. NAME OF MONITORING ORGANIZATION

DTIC
ELECTE
JUL 2 4 1987
S
D

6c. ADDRESS (City, State, and ZIP Code) PO Box 631 Vicksburg, MS 39180-0631	7b ADDRESS (City, State, and ZIP Code)

8a. NAME OF FUNDING/SPONSORING ORGANIZATION US Army Corps of Engineers	8b OFFICE SYMBOL (If applicable)	9. PROCUREMENT INSTRUMENT IDENTIFICATION NUMBER

8c. ADDRESS (City, State, and ZIP Code)	10. SOURCE OF FUNDING NUMBERS			
Washington, DC 20314-1000	PROGRAM ELEMENT NO.	PROJECT NO	TASK NO.	WORK UNIT ACCESSION NO

11 TITLE (Include Security Classification)
Theoretical Manual for Design of Cellular Sheet Pile Structures (Cofferdams and Retaining Structures

12 PERSONAL AUTHOR(S)
Rossow, Mark; Demsky, Edward; Mosher, Reed

13a. TYPE OF REPORT Final report	13b TIME COVERED FROM _____ TO _____	14 DATE OF REPORT (Year, Month, Day) May 1987	15. PAGE COUNT 122

16. SUPPLEMENTARY NOTATION

17	COSATI CODES		18. SUBJECT TERMS (Continue on reverse if necessary and identify by block number)
FIELD	GROUP	SUB-GROUP	CCELL (Computer program) Sheet-piling (LC)
			Coffer-dams (LC) Steel piling (LC)
			Piling (Civil engineering) (LC)

19 ABSTRACT (Continue on reverse if necessary and identify by block number)

This theoretical manual contains derivations and discussions of procedures for cellular sheet pile cofferdam design. As a companion volume to the planned Engineer Manual, "Design of Cellular Sheet Pile Structures," it is intended to provide theoretical background for that EM as well as to the user of the computer program for cellular-cofferdam design, CCELL. Numerical examples illustrating the design methods' use, along with a broad list of references, are included.

Failure modes involving soil-structure interactions are the primary consideration. The approach herein is intended to provide the reader with the basic analysis procedure to be used for a particular failure mode.

20 DISTRIBUTION/AVAILABILITY OF ABSTRACT [X] UNCLASSIFIED/UNLIMITED ☐ SAME AS RPT ☐ DTIC USERS	21 ABSTRACT SECURITY CLASSIFICATION Unclassified
22a NAME OF RESPONSIBLE INDIVIDUAL	22b TELEPHONE (Include Area Code)	22c OFFICE SYMBOL

DD FORM 1473, 84 MAR

83 APR edition may be used until exhausted
All other editions are obsolete

PREFACE

This report provides the derivations and describes the procedures for the design of cellular sheet pile cofferdams. The work was accomplished by the US Army Engineer Waterways Experiment Station (WES) and sponsored under funds provided by the Civil Works Directorate, Office, Chief of Engineers (OCE), in an effort to update the Corps' Engineer Manuals.

The first draft of the manual was written by Dr. Mark Rossow, Department of Civil Engineering, Southern Illinois University at Edwardsville, under the direction of Mr. Reed Mosher, Engineering Applications Office (EAO), formerly the Engineering Applications Group (EAG), Scientific and Engineering Application Division (SEAD), Automation Technology Center (ATC), WES. Additional sections were written by Mr. Edward Demsky, Foundation Section, Geotechnical Branch, US Army Engineer District, St. Louis, and Mr. Mosher. Example problems were developed by Mr. Demsky. The work accomplished at WES was under the general supervision of Dr. N. Radhakrishnan, A/Chief, Information Technology Laboratory (ITL), formerly chief, ATC, and under the direct supervision of Mr. Paul Senter, A/Chief, Information Research Division, ITL, formerly chief, SEAD. The technical monitor for OCE was Mr. Don Dressler. This manual was edited by Ms. Gilda Miller, Information Products Division, ITL, WES.

COL Allen F. Grum, USA, was the previous Director of WES. COL Dwayne G. Lee, CE, is the present Commander and Director. Dr. Robert W. Whalin is Technical Director.

Accesion For

NTIS CRA&I	☑
DTIC TAB	☐
Unannounced	☐
Justification	

By

Distribution /

Availability Codes

| Dist | Avail and/or Special |

A-1

1

CONTENTS

3

CONVERSION FACTORS, NON-SI TO SI (METRIC)
UNITS OF MEASUREMENT

Non-SI units of measurement used in this report can be converted to SI (metric) units as follows:

Multiply	By	To Obtain
degrees	0.01745329	radians
feet	0.3048	metres
inches	2.54	centimetres
kip/inches	112.9848	newton-metres
pounds (force)	4.448222	newtons
pounds (force) per foot	14.5939	newtons per metre
pounds (force) per inch	175.1268	newtons per metre
pounds (force) per square foot	47.88026	pascals
pounds (mass) per cubic foot	16.01846	kilograms per cubic metre
pounds (mass) per cubic inch	27.6799	grams per cubic centimetre
seconds	4.848137	radians

THEORETICAL MANUAL FOR DESIGN OF CELLULAR SHEET PILE
STRUCTURES (COFFERDAMS AND RETAINING STRUCTURES)

PART I: INTRODUCTION

Purpose

1. This manual is a companion volume to the planned Engineer Manual (EM), "Design of Cellular Sheet Pile Structures," and is intended to provide theoretical background for that EM to the reader. It is also designed to present the background for the computer program CCELL (X0040) for the analysis/design of sheet pile cellular cofferdams.

Scope

2. The manual contains derivations and discussions of procedures used in CCELL. It includes several procedures mentioned in the technical literature but found inadequate, and therefore omitted from CCELL. Several numerical examples illustrating the use of the design methods and an extensive list of references on cellular cofferdams are included in the manual.

Design Methods Presented in Rational Form

3. Most of the design methods discussed in this report are expressed in terms of a factor of safety (FS)* as

$$FS = \frac{\text{Maximum available resisting force (or moment)}}{\text{Driving force (or moment)}} \qquad (1)$$

That is, the design methods are based on a comparison of resisting effect to driving effect. For this comparison to be meaningful, the following two criteria must be satisfied:

    a. Identification of a single free body must be possible.

    b. Both the driving and resisting forces (or moments) must act on this free body.

---

* For convenience, symbols and abbreviations are listed in the Notation (Appendix B).

Criteria and Design Procedures

4. Although these criteria may seem obvious, some statements of design procedures in the literature do not satisfy them, and these procedures had to be modified or reinterpreted for inclusion in the manual. Thus, several of the design procedures presented herein differ somewhat from the formulations in the references cited.

Limitations of the Manual

5. The question of what constitutes a minimum acceptable value of a safety factor for a given failure mode is as much a policy issue as a technical issue and thus is not treated herein; values of safety factors are available in the EM.

6. Consideration is limited primarily to failure modes involving soil-structure interactions. Other important potential failure modes, such as undermining or piping caused by excessive seepage, are not considered.

Basic Combinations

7. Not every possible combination of foundation conditions (e.g., bare rock, rock with overburden, deep-sand, clay, berm or no berm) is considered. Instead, one or sometimes two sets of conditions have been chosen for each failure mode, and the corresponding free body and acting forces are identified. The intent of this approach is to provide the reader with the basic analysis procedure to be used for a particular failure mode. Once the procedure is understood, modification for different foundation conditions should be straightforward.

Soil-Structure Interaction in a Cellular Cofferdam

8. A cofferdam cell consists of a flexible steel membrane enclosing a granular soil fill. The soil-structure interaction in a structure of this type is a complex process involving composite action of the fill and the membrane. For example, the gravity forces acting on the fill cause it to exert pressure on the membrane and as a result of the pressure, tensile forces are

6

produced in the membrane. These forces stiffen the membrane against further extension, thus providing a confining effect on the fill. This effect, in turn, stiffens the fill and enables it to develop the large compressive and shearing stresses it needs to transmit the hydrostatic and gravity loads to the foundation. Hence, the fill serves as the principal load-bearing element in the structure, but could not perform its task without the aid of the steel membrane.

Two Possible Analogies

9. To clarify the behavior of a cellular cofferdam further, it is helpful to consider two analogies, one good and the other poor. The better analogy consists of a thin polyethylene bag, such as the type used to wrap sandwiches, filled with sand. When a distributed horizontal force of reasonable size is applied to the bag, its only resistance is through the mobilization of shear resistance within the sand. Thus, the sand will be seen to displace within the bag. This behavior is a valid comparison for a cofferdam cell. By contrast, a poor analogy would be a typical, kitchen-size metal can, filled with sand. When a horizontal force of reasonable magnitude is applied to the sand-filled can, the can tips over, or if sufficient friction is present between it and the surface upon which it rests, the can simply remains at rest with no change of shape. In either event, the external load is carried primarily by the shell (the can) rather than by the fill. Such behavior is not representative of a cofferdam cell. Of course, all analogies have limitations. The behavior of an actual cofferdam lies somewhere between that of a sand-filled bag and a can, although it is much closer to that of a bag.

State of the Art

10. Beginning with the construction of the first steel sheet-pile cellular cofferdam at Black Rock Harbor, near Buffalo, N. Y., in 1908 and lasting at least until the publication of Terzaghi's famous paper (Terzaghi 1945), most cellular cofferdams were designed as gravity walls. Terzaghi pointed out the error in this approach and introduced the concept of designing the fill on a vertical plane to prevent shear failure, an idea which had been used, but not published, by TVA engineers some time earlier (TVA 1957). In the same paper, Terzaghi discussed the possibility of slip between the fill and the

7

sheet-pile walls, and of penetration of the inboard walls into the foundation. Several currently-used design rules concerned with these phenomena appear to have been derived, at least in part, from his discussions. Other types of internal-stability failure modes have also been hypothesized by Hansen (1953, 1957), Ovesen (1962), and Cummings (1957). Some notable cofferdam failures attributable to excessive underseepage or lack of bearing capacity of the foundation (ORD 1974) have given rise to yet more potential failure modes for the designer to consider.

Hypothesized Failure Modes

11. Thus, over the years a rather large number of hypothesized failure modes have accumulated. Several model studies (Cummings 1957, EM 1110-2-2906, Maitland 1977, Ovesen 1962, Rimstad 1940, TVA 1957, Kurata and Kitajima 1967) have been conducted to determine which failure modes are likely and which are improbable. With one recent exception (Maitland 1977, Maitland and Schroeder 1979, Schroeder and Maitland 1979), these studies have not been of great help. Indeed, some of the studies have actually hindered the understanding of cellular-cofferdam behavior. The use of relatively small models with overly stiff walls led the experimenters to postulate failure modes which are highly unlikely to appear in a full-sized cell. In addition to model studies, field measurements (Summary Report Lock and Dam No. 26 (Replacement) 1983; Khuayjarernpanishk 1975; Moore and Alizadeh 1983; Schroeder, Marker, and Khuayjarernpanishk 1977; Sorota, Kinner, and Haley 1981; Sorota and Kinner 1981; TVA 1957; Naval Research Laboratory 1979; White, Cheney, and Duke 1971) of full-sized cells have also been conducted. Although valuable data on operating conditions have been obtained, no instrumented, full-sized cell has failed, and thus no data are available on cell behavior during failure.

12. Given the plethora of hypothesized failure-modes and the lack of sound experimental data, it is not surprising that "most designers in this field still rely heavily on past practice and experience" (USS 1972). At the present time, theoretical calculations, alone or even in large part, do not suffice for cellular cofferdam design.

13. In the next 5 to 10 years, this situation may change as finite element programs, polished and specialized for everyday use by the cofferdam designer, are developed. Such programs are not available at present.

8

PART II: ANALYSIS OF FAILURE MODES

Conventional Simplifications and Equivalent Layout

14. The analysis of many failure modes is simplified if the original cofferdam geometry is replaced by an equivalent straight-walled cofferdam. The literature contains several different procedures for calculating the dimensions of this equivalent cofferdam. The procedure adopted herein is to choose the distance L between crosswalls in the equivalent layout that equals the average distance between crosswalls in the original cofferdam (Lacroix, Esrig, and Lusher 1970) as shown in Figure 1. The equivalent width b is then computed by equating plan areas of the original and equivalent layouts. For example, in the case of a circular cofferdam, this procedure leads to the equation

$$b = \frac{\text{Area of main cell and one arc cell}}{2L} \tag{2}$$

Average vertical slice

15. Another simplifying approximation made often is the calculation of resultant forces and moments. Included are those arising from the crosswall, for a length L of the equivalent cofferdam and dividing these quantities by L to get the average force and moment per unit length of cofferdam. This procedure is equivalent to assuming that the behavior of the entire cofferdam can be represented by a single "average" vertical slice such as that shown in Figure 2.

Flat walls

16. An obvious consequence of analyzing the equivalent rather than the actual cofferdam is that the curvature of the walls is neglected. For certain choices of free body, this amounts to neglecting the effect of interlock tension.

17. For example, Figure 2c shows a free body consisting of unit widths of both the outboard and inboard walls. Typical forces which act on this free body are also shown. Note that the interlock tension is not included. In effect, the walls are assumed to be flat. This latter statement may be clarified by considering Figure 3, in which is shown a free body consisting of

9
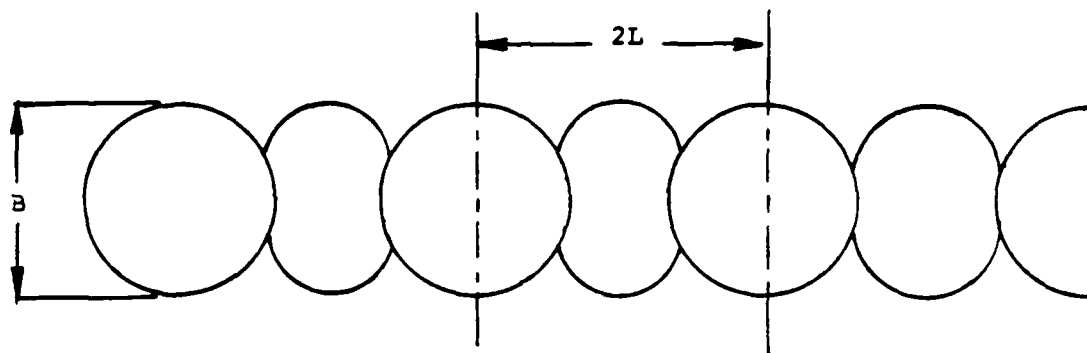
a. Circular cofferdam
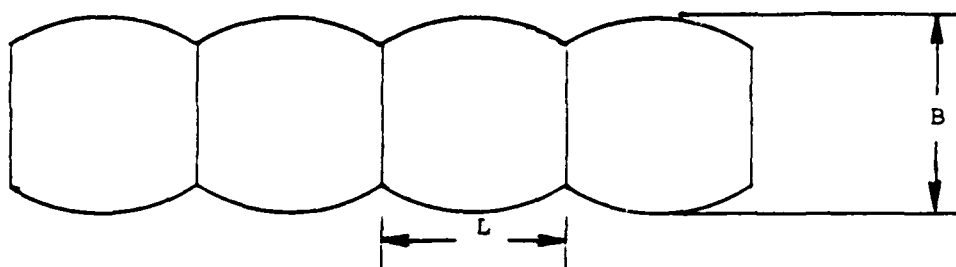
b. Diaphragm cofferdam
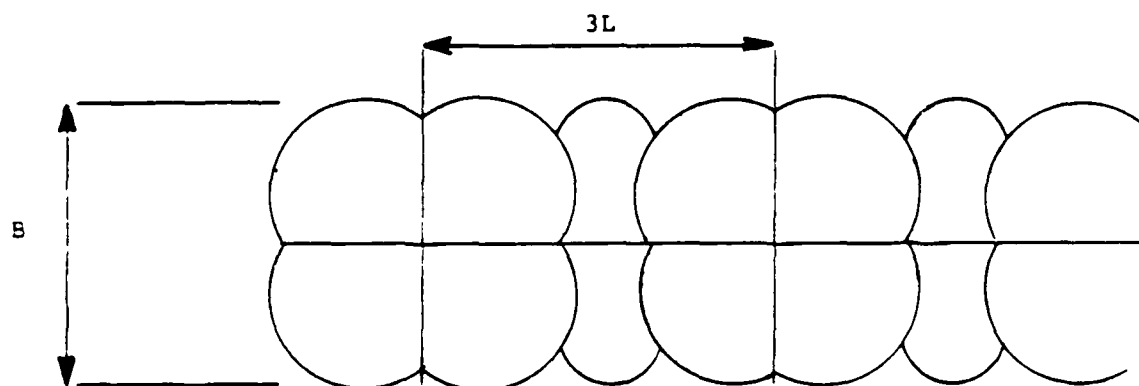
c. Cloverleaf cofferdam
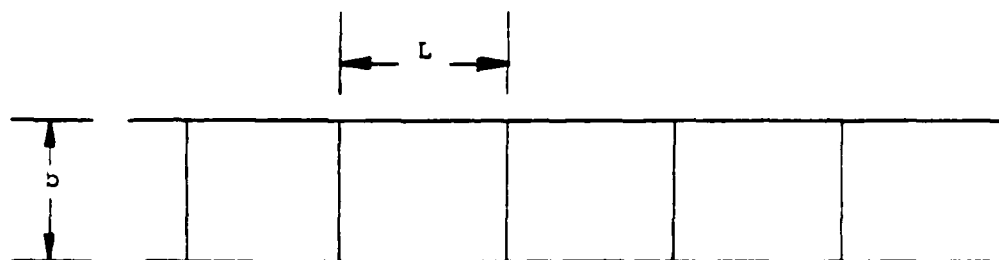
d. Equivalent rectangular cofferdam

Figure 1. Actual cofferdams replaced by rectangular equivalent

10
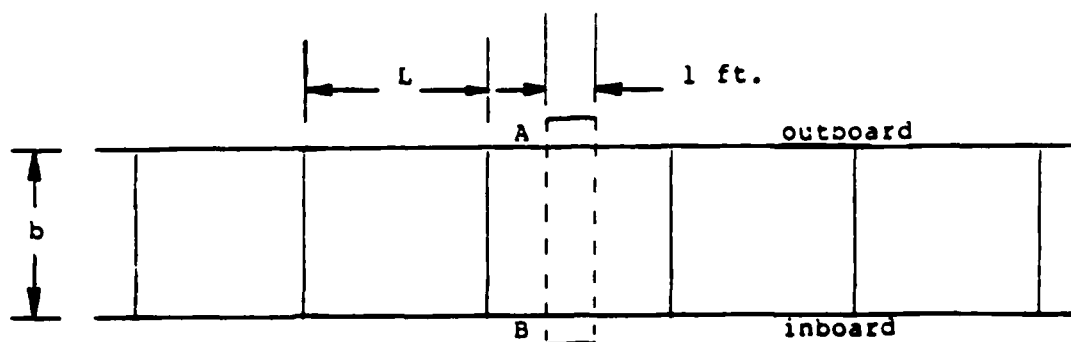
a. Portion of equivalent cofferdam selected for analysis
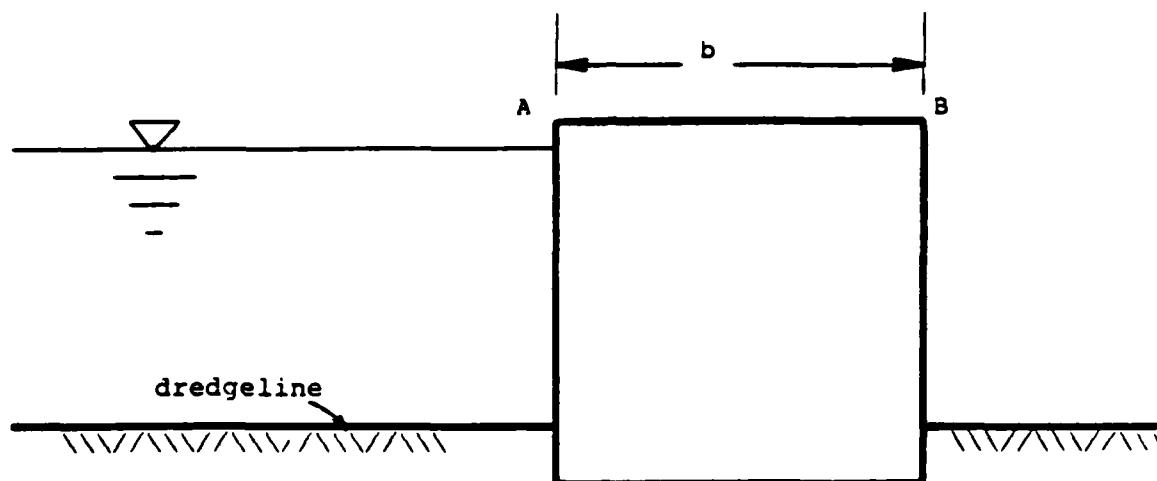
b. Elevation view of region in a

P_1 = force from water outside cell

P_2, P_3 = forces from foundation

P_4, P_5 = forces from fill and water inside cell
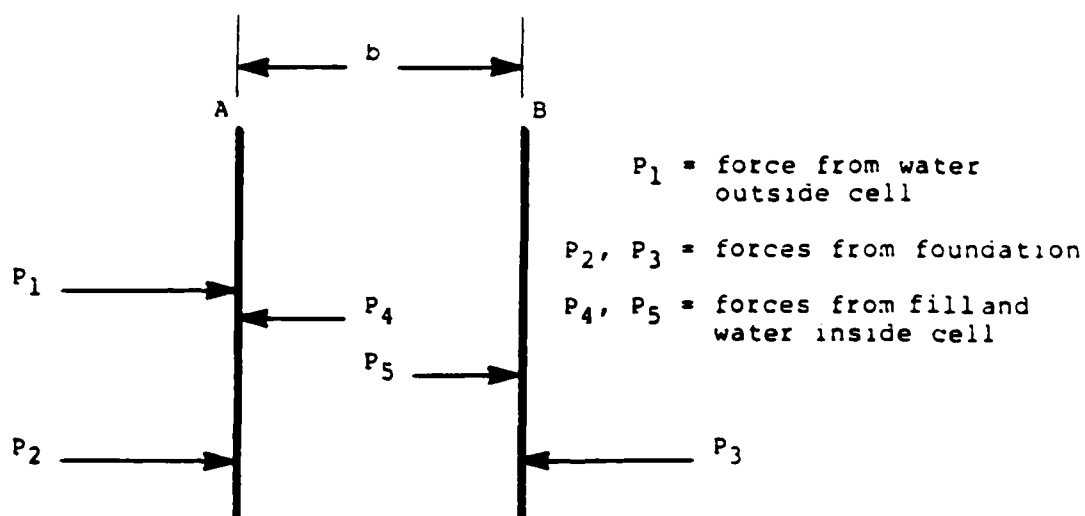
c. Free body comprised of unit widths of outboard and inboard walls

Figure 2. Average vertical slice of cofferdam

11
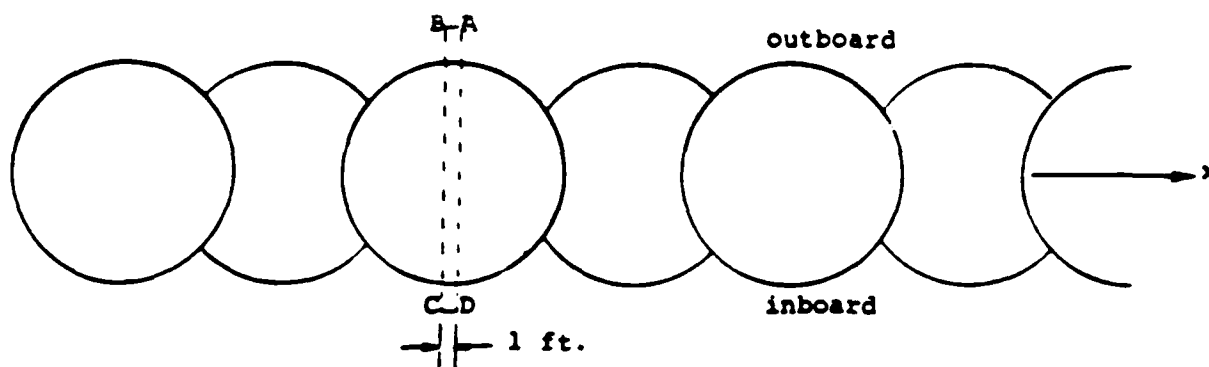
a. Portion of actual (not the equivalent)
cofferdam selected for analysis
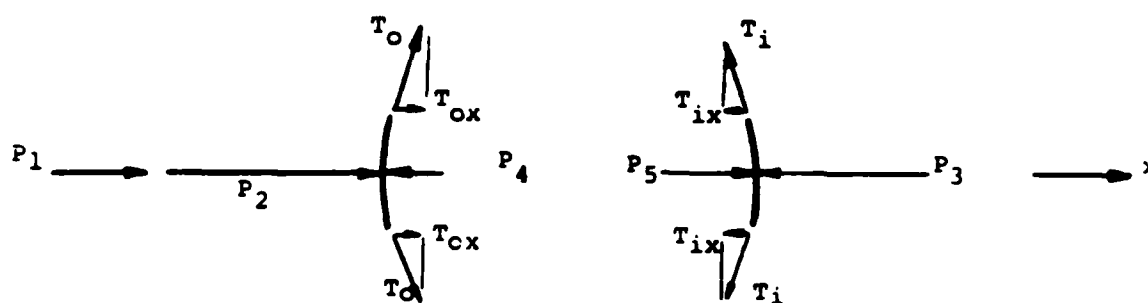
b. Plan view of free body (P_1 - P_5 defined in Figure 2)
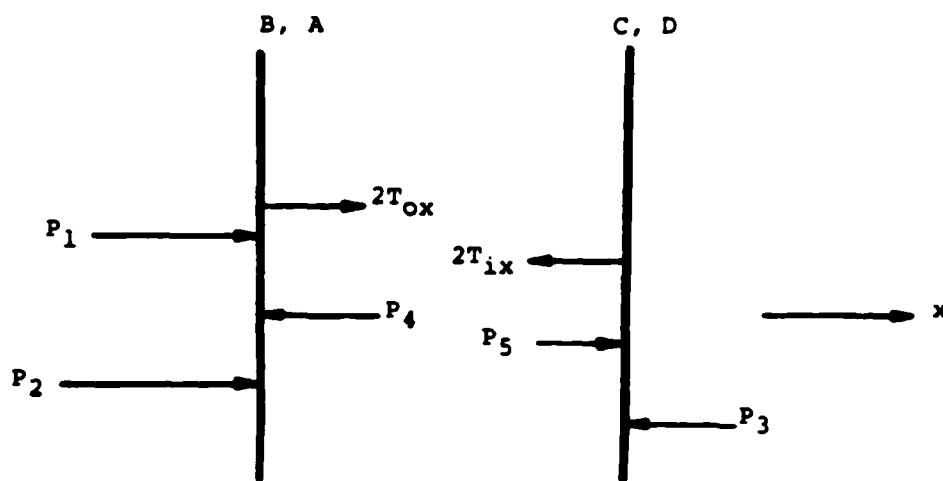
c. Elevation view of free body

Figure 3. Free body showing effect of wall curvature

unit widths of opposing walls in an actual (not an equivalent) cofferdam. Because of the curvature of the cell walls, the interlock tensions T_o and T_i have components T_{ox} and T_{ix} acting in the x-direction. This can be seen in Figures 3b and c. These components are neglected in the free body shown in Figure 2c.

Critique of Simplifications

18. Although statements are frequently found in technical literature that it is "correct" to analyze a cofferdam by replacing it with an equivalent rectangular layout, no studies have been published which estimate the error involved in making the approximation.

<u>a</u>. The alternative to replacing the cofferdam with its rectangular equivalent is to perform a three-dimensional FE analysis. At the present time, this is not a feasible approach for a design office.

<u>b</u>. Similarly, analyses are based on an average vertical slice, not because the error in doing so is known to be small, but because of the lack of a feasible alternative.

<u>c</u>. For analyses based on a free body consisting of a <u>single wall</u>, the flat-wall assumption appears questionable. The component of interlock tension acting in the x-direction in Figures 3b and c is the primary means by which the wall resists the force from the fill and should not be neglected. This may be graphically demonstrated by considering the wall on the right in Figure 3c as a single free body. If the component of interlock tension $2T_{ix}$ is neglected, moment equilibrium cannot be satisfied.

<u>d</u>. For analyses based on a free body consisting of <u>both the inboard and outboard walls</u>, the flat-wall assumption is somewhat more defensible, although the magnitude of the error implied by this assumption is not known. Consideration of the free body consisting of <u>both</u> walls in Figure 3c shows that the components of interlock tension will cancel each other provided that the magnitude of the interlock tension in the outboard wall equals that in the inboard wall, and the two tensions have the same line of action. This means that the resultant tensions in the inboard and outboard walls act at the same elevation. To the extent that these conditions are not satisfied, a net horizontal force and a moment arise from the interlock tensions acting on the free body.

<u>e</u>. Finally, point should be made of the development of FE models which use elastic springs to connect the outboard and inboard walls of a vertical slice of the cofferdam (Clough and Duncan

13

1977; Hansen and Clough 1982). In this way, the effect of wall
curvature can be included.

Failure Modes and Example Problems

19. Detailed descriptions and discussions of ten failure modes follow
in the next 10 parts. Further explanation through example problems, illu-
strated by step-by-step solutions, is presented in Appendix A.

PART III: BURSTING

Effects of Internal Lateral Stresses

20. The lateral stresses exerted by the fill and acting on the walls produce hoop forces which cause the interlocks to separate (Figure 4). The fill is lost and the cell may collapse.
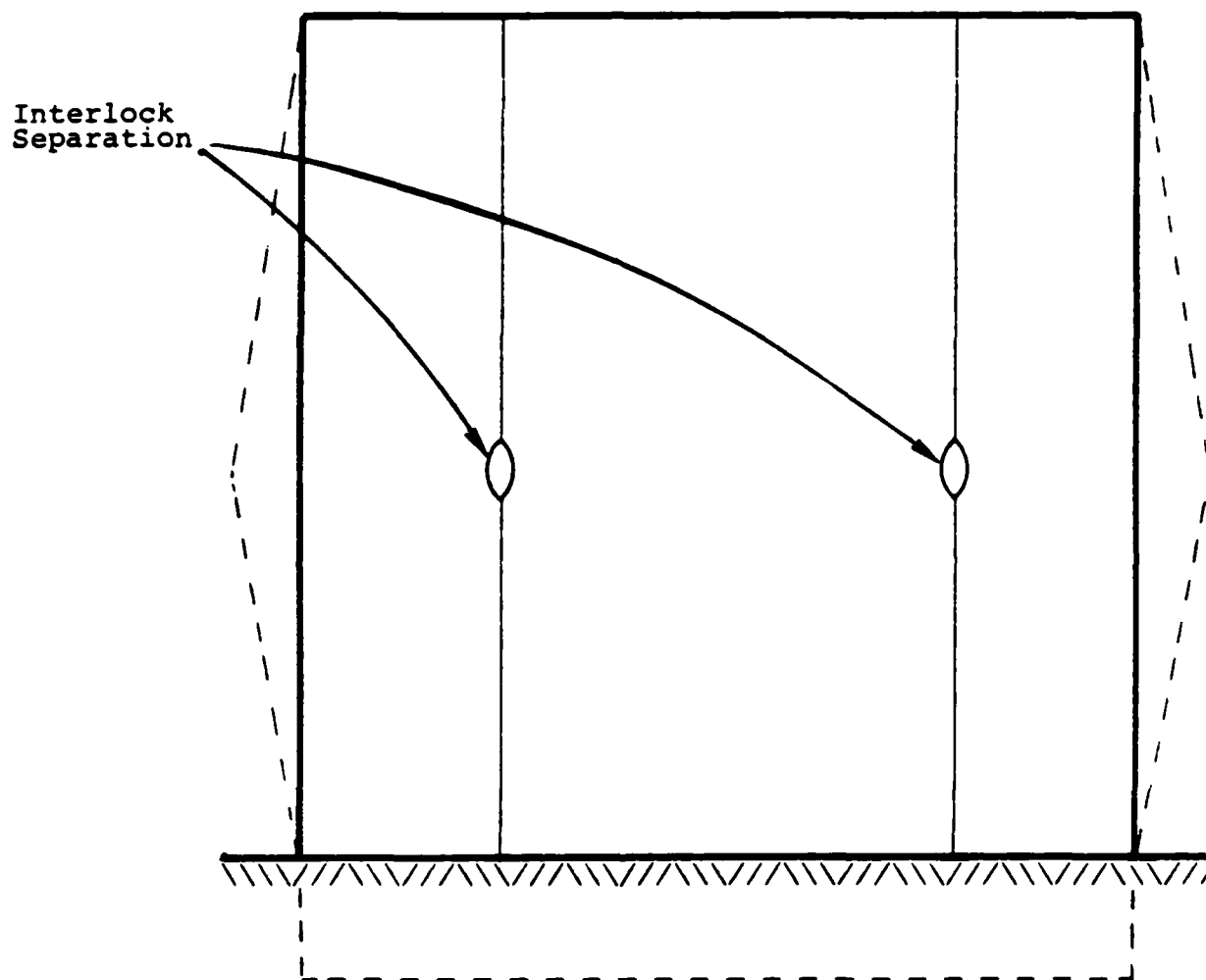

Figure 4. Failure by interlock separation (Dismuke 1975)

21. The FS against bursting is shown by:

$$FS = \frac{t_{ult}}{t_{max}} \tag{3}$$

where

t_{ult} = maximum permissible interlock tension (per unit length of sheet) as specified by the sheet-pile manufacturer

t_{max} = maximum interlock tension (per unit length of sheet) existing in the cell wall

Critical Loading Cases

22. The following discussion on interlock tension is primarily concerned with the case of an isolated main cell, both after filling and at low water. This loading state usually represents the most important condition producing interlock tension in the main cell. The lateral forces associated with dewatering and the presence of a berm will also affect the interlock tension, although the effect does not appear to be great (Schroeder and Maitland 1979; White, Cheney, and Duke 1971; St. Louis District, CE 1983). In unusual circumstances such as anticipated removal of an interior beam during high water, a FE analysis may be necessary (Clough and Duncan 1977, 1978; Hansen and Clough 1982; St. Louis District, CE 1983) to resolve doubts over possible excessive interlock-tension.

Considerations in Interlock-Tension Calculations

Plane of fixity

23. The interlock tension and the lateral earth pressure acting on the cofferdam cell wall are each at a maximum at the same elevation. Both intuition and field measurements indicate that this elevation is close to the elevation at which maximum bulging of the cell occurs (Schroeder and Maitland 1979; St. Louis District, CE 1983). The location of the point of maximum bulging depends on the degree of restraint provided by the foundation acting on the embedded portion of the sheet-pile walls and may best be estimated by use of the concept of the plane of fixity.

24. The plane of fixity is defined as the plane below which the interlock tension in the sheet piling is small, or, alternatively, as the plane of potential plastic hinges in the piling (Figure 5). Analytically, for a cell founded on a weak or a strong soil foundation, the plane of fixity may be located by using established results for the behavior of laterally-loaded
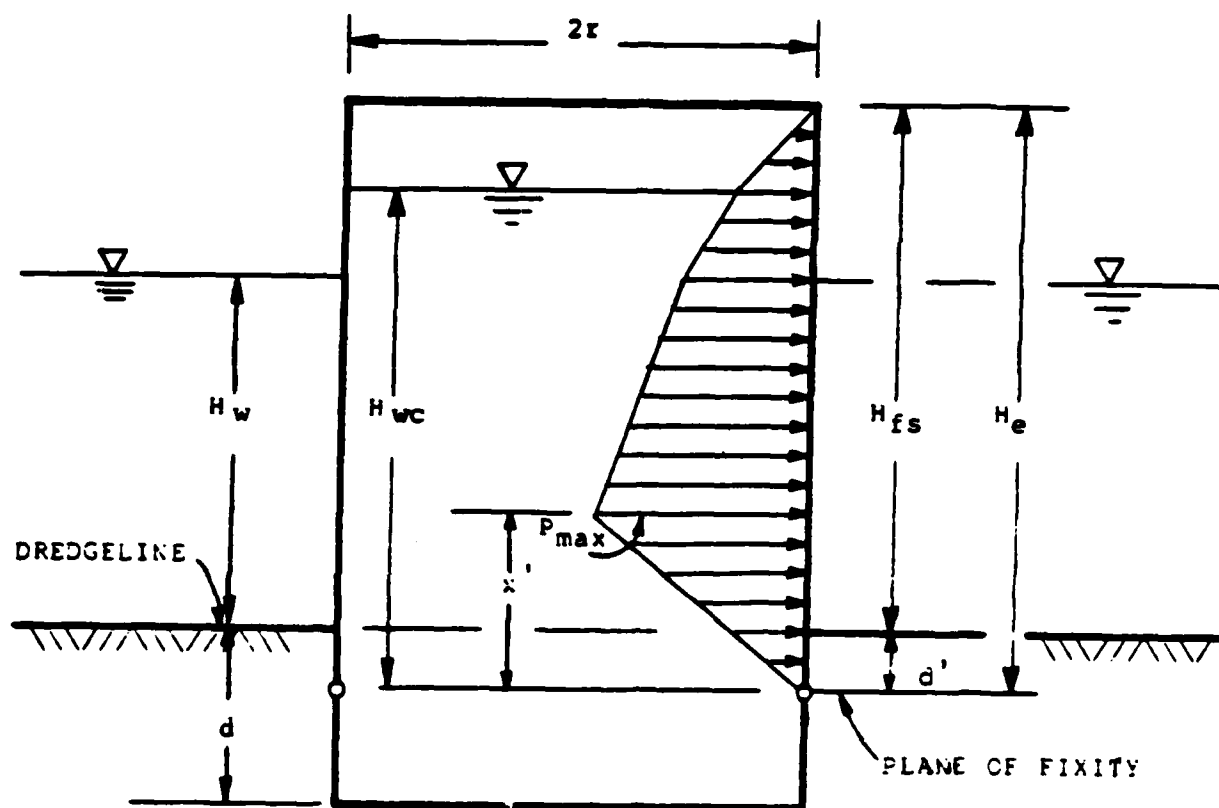
Figure 5. Definitions used in interlock force calculations

piles. In deriving Equations 4 and 6, the assumption is made that the plane
of fixity occurs at the point of zero rotation.

Sand foundation

25. For cofferdam cells in a sand foundation, the depth-to-fixity d'
(= distance from plane of fixity to dredgeline, Figure 5) is given by the
equation (Schroeder and Maitland 1979)

$$d' = 3.1 \left(\frac{EI}{n_h} \right)^{1/5} \tag{4}$$

where

E = modulus of elasticity of the pile

I = moment of inertia of the pile section

n_h = constant of horizontal subgrade reaction

For Equation 4 to be valid, the embedment depth of the cofferdam cell, d ,
must satisfy the relation

$$d \geq 5 \left(\frac{EI}{n_h}\right)^{1/5} \qquad (5)$$

Note that the effect of the foundation characteristics on the depth-to-fixity enters the calculations through the appearance of the parameter n_h .

Clay foundation

26. For cofferdam cells in a clay foundation the depth-to-fixity is given by the equation

$$d' = 3.3 \left(\frac{EI}{E_s}\right)^{1/4} \qquad (6)$$

where E_s equals a horizontal spring modulus representing the behavior of the soil-pile system. For Equation 6 to be valid, the embedment depth of the cofferdam cell must satisfy the relation

$$d \geq 4 \left(\frac{EI}{E_s}\right)^{1/4} \qquad (7)$$

Equations 4 through 7 are derived from the theory of beams on elastic foundation (Hetenyi 1946). Thus, the above equations depend on the assumptions made in deriving that theory and also on the assumption that the bending response of the cofferdam cell can be represented by the theory of beams on elastic foundation.

27. The value of n_h for sheet-pile walls can be calculated by the following equation.

$$n_h = \frac{b_s}{d'} \ell_h \qquad (8)$$

The value of E_s for sheet-pile walls can be calculated by the following equation

$$E_s = \frac{1}{3} b_s k_{s1} \frac{1}{d'} \qquad (9)$$

Values of k_{s1} and ℓ_h are given by Terzaghi (1955) in Tables 2 and 4. The terms in the above equations not previously defined are:

18

b_s = width of a single sheet pile

ℓ_h = constant of horizontal subgrade reaction for anchored bulkhead with free earth support

k_{s1} = basic value of coefficient of vertical subgrade reaction

It should be noted that in Equation 9 the 1 term above the d' term has units of feet associated with it, thus d' should also have units of feet. The assumption is made in the above equations that the cofferdam walls are flat. The curvature of the cofferdam cells is neglected.

Alternate Method for Locating Plane of Fixity

28. Another method for finding the plane of fixity is derived by equating the internal and external pressure acting on the equivalent coffer-dam. In this method the plane of fixity is assumed to occur at the point where the internal cell pressure is equal to the external pressure. This method assumes that active earth pressure is mobilized inside the cell and passive earth pressure is mobilized outside of the cell. The assumption of neglecting the interlock force as stated in paragraph 16 for the equivalent cofferdam is also made.

29. For a cofferdam in a sand foundation where the water level inside and outside of the cell is at different levels, the plane of fixity is given by the equation

$$d' = \frac{K_a[\gamma_m(H_{fs} + d - H_{w4}) + \gamma'(H_{w4} - d)] + \Delta H_w \gamma_w}{\gamma'(K_p - K_a)} \qquad (10)$$

Terms not previously defined are:

K_a = active earth-pressure coefficient

K_p = passive earth-pressure coefficient

H_{fs} = vertical distance from dredgeline to top of cell (free-standing height)

H_{w4} = vertical distance from sheet-pile tips to water level inside of cell

ΔH_w = differential water head between the inside and outside of the cell, the water level inside of the cell minus the water level outside of the cell

γ_m = unit weight of moist fill

γ_w = unit weight of water

γ' = effective unit weight of soil

An equation similar to Equation 10 can be derived for cells in a clay foundation by equating internal and external pressures.

30. Once the plane of fixity has been located, the point of maximum bulging and interlock tension can be calculated from the empirical formula (Schroeder and Maitland 1979; St. Louis District, CE 1983)

$$x' = \frac{(H_{fs} + d')}{3} \qquad (11)$$

where

x' = distance from the plane of fixity to the point of maximum interlock-tension

Rock foundation

31. For the case of a cell founded on rock, where the embedment of the sheet-pile tips is sufficient to prevent radial displacement when the cell is filled, Equation 11 may still be applied by substituting $d' = o$. A plane of fixity cannot be said, strictly speaking, to exist since the slope of the sheet at the tips cannot be considered small. However, the rock foundation provides enough radial restraint to reduce interlock tension to near zero at the base of the cell. Note that substituting $d' = o$ in Equation 11 in this case gives $x' = H_{fs}/3$, a result similar to that given by the Tennessee Valley Authority (TVA) rule (TVA 1957), which specifies that the maximum interlock tension be calculated at $H_{fs}/3$ or $H_{fs}/4$.

32. A final observation on the use of Equation 11 is that it is based on the assumption that at some point along the length of the sheetpiling, the radial displacement of the piling is restrained. It is inappropriate to use Equation 11 if this assumption is not valid. An example would be the case for a cell founded on very hard rock, into which piling penetration is very small, or in the case of a weak soil foundation for which no depth-to-fixity could be established (that is, Equations 5 or 7 are not satisfied). In these instances, the foundation provides little lateral restraint, and the point of maximum interlock stresses may be very close to the bottom of the piling.

Hoop-stress equation

33. The interlock tension in the main or arc cell outside the crosswall is computed from the hoop-stress equation

$$t_{max} = p_{max} r \qquad (12)$$

20

where

p_{max} = maximum lateral pressure acting against the wall

r = radius of the cell

34. The maximum pressure p_{max} is assumed to occur at the elevation of the point of maximum bulging and is calculated by summing the effective lateral-earth pressure and the difference in water pressure inside and outside the cell. Based on the water depths shown in Figure 5, the equation for p_{max} is

$$p_{max} = K \left\{ \gamma_f (H_e - H_{wc}) + \gamma_f' \left[\frac{2H_e}{3} - (H_e - H_{wc}) \right] \right\} + \gamma_w (H_{wc} - H_w - d') \qquad (13)$$

This equation will work only when the differential water-level height inside the cell is above point at which p_{max} is being calculated. If the water level is the same, inside and outside of the cell, Equation 13 is suitable, regardless of the water level.

where

K = lateral earth-pressure coefficient

γ_f = unit weight of dry fill

γ_f' = submerged unit weight of fill

H_e = vertical distance from plane of fixity to top of cell (effective length of the sheet piles)

H_w = vertical distance from dredgeline to surface of water outside of cell

H_{wc} = vertical distance from plane of fixity to intersection of phreatic surface with center line of cell

The other terms retain their previous meanings. Selecting a value of K will be discussed in paragraph 39.

Interlock-Tension Calculations in Crosswall

Swatek's equation

35. When both the main cell and an adjacent arc cell are filled, the crosswall near the arc connection must provide sufficient tension to support the tension from the main cell and the arc cell. An equation for the interlock tension in the crosswall may be derived by considering the free body

21

shown in Figure 6. Since the total force acting on a unit depth of wall in
this figure is $p_{max}L$, a balance of forces gives

$$t_{cw} = p_{max}L \qquad (14)$$

in which t_{cw} is the interlock tension (per unit length of sheet) in the
crosswall, and the pressure p_{max} is computed from Equation 13. Equation 14
is commonly referred to as Swatek's equation, since it was first used by Paul
Swatek.

TVA secant equation

36. An alternative equation, the TVA secant equation (TVA 1957),
especially intended for use near the arc connection, is

$$t_{cw} = p_{max}L[\sec (\theta)] \qquad (15)$$

where (Figure 7a) θ is the angle measured from the cofferdam axis to the
connecting pile.
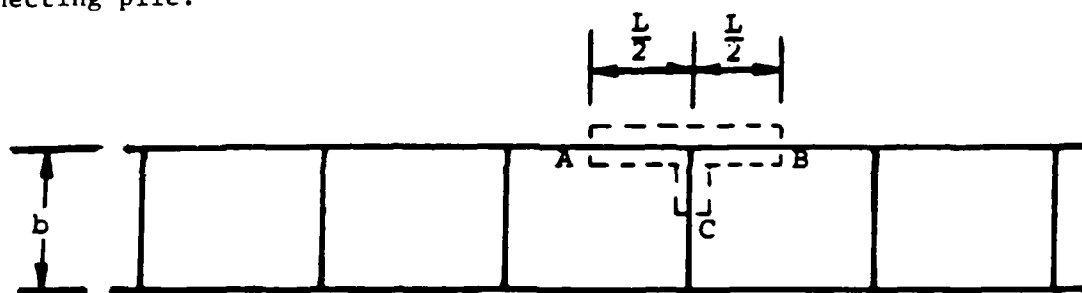
a. Portion of equivalent cofferdam selected for analysis
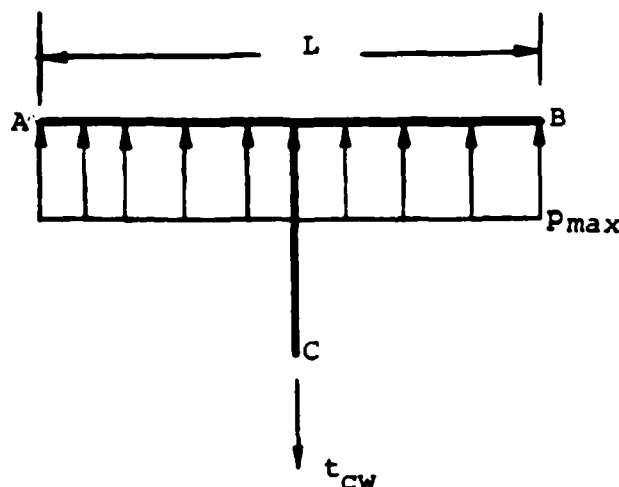
b. Free body of unit depth
into plane of figure

Figure 6. Geometry and free body for derivation of Swatek's equation

22
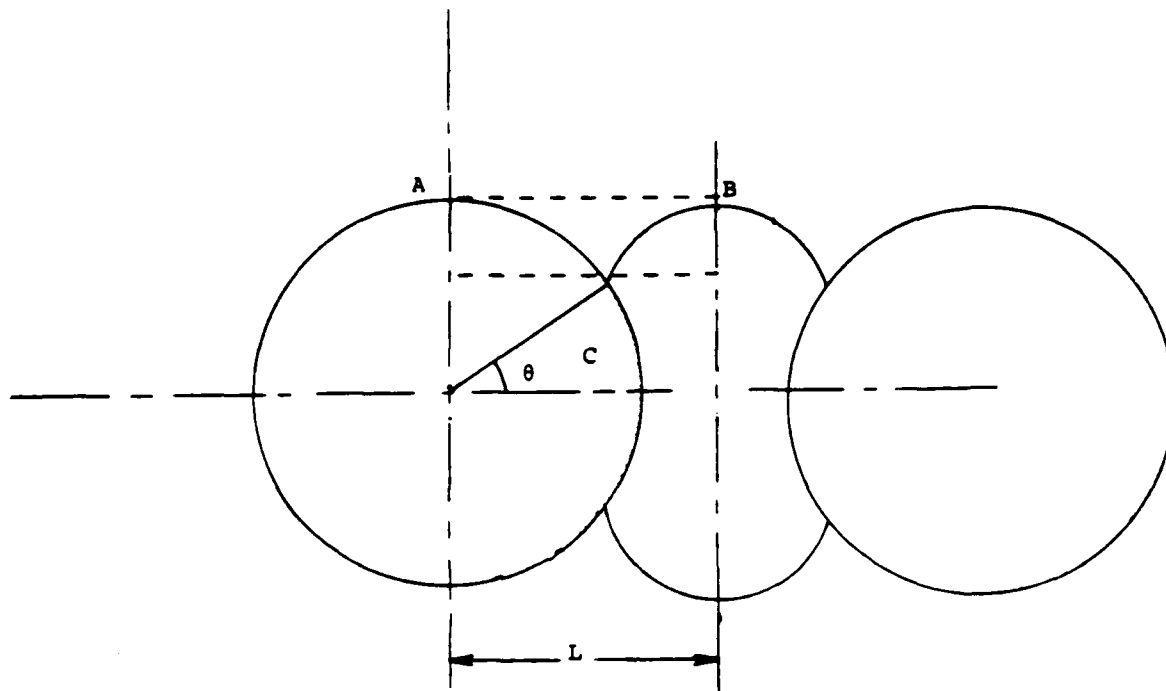
a. Region selected for analysis
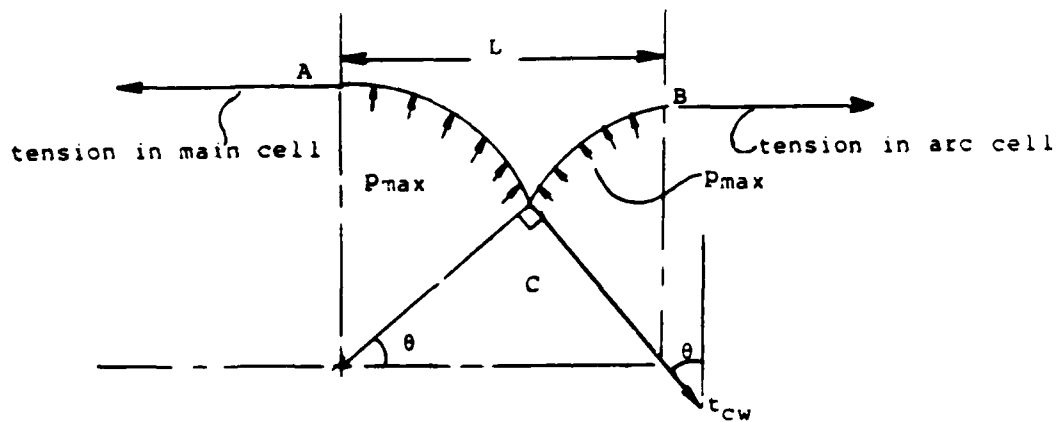
b. Free body of unit depth into plane of figure

Figure 7. Geometry and free body for derivation of TVA-secant formula

37. Equation 15 may be derived by referring to Figure 7b and noting that the resultant $p_{max}L$ is equilibrated by the inboard component of t_{cw} , giving

$$t_{cw}[\cos (\theta)] = p_{max}L \qquad (16)$$

from which Equation 15 follows by dividing through by $\cos (\theta)$.

Rational Design Procedure to Avoid Bursting

38. Because the elevation of the point of maximum bulging (and hence, the point of maximum interlock tension) depends on the stiffness of the foundation, traditional design rules such as "the interlock tension should be calculated at one-third to one-fourth the free-standing height of the cell" are necessarily subject to interpretation and modification each time a cell is designed for different foundation conditions. However, if the plane-of-fixity concept is used, the effect of different foundation conditions is automatically taken into account: the maximum interlock tension is calculated at a lower level for weak soils compared to strong soils, and may even occur at or below the dredgeline (Schroeder and Maitland 1979). Thus, use of the concept provides a rational basis for considering the stiffness of the foundation when calculating the interlock tension.

Selecting a value of K

39. Because of the take up of slack and stretching of the interlocks during cell filling, some movement of the fill occurs, and the earth-pressure coefficient is reduced from its at-rest value. The degree to which the pressure is reduced, however, is controversial, and the theoretical arguments, field data, and model studies reported in the literature give a wide range of values of K to choose from. It should be noted that no reliable direct measurements of soil pressure inside cells have been reported. (Several investigators have installed soil pressure cells, but little data were obtained which could be viewed with confidence.) Instead, soil pressure has generally been calculated from the hoop-stress equation, Equation 12, in which the interlock tension has in turn been calculated from the generalized Hooke's law for the steel sheet pile and from strains measured by strain gages. Thus, even soil-pressure values purportedly obtained experimentally are based on theoretical assumptions such as how the strain in the sheet pile is distributed across the cross section, or whether or not vertical strain and the associated Poisson effect are present.

40. Further complicating the question of what value of K to use is the fact that for a given fill material K will be influenced by a host of factors. Examples of these factors include the method and rate of filling, the presence of a surcharge, internal drainage conditions, and the method of compaction of the fill. In light of these uncertainties, K values are best

24

chosen by relying on previous experience, rather than on theoretical arguments (Sorota, Kinner, and Haley 1981; Sorota and Kinner 1981). Values of 1.2 to 1.6 times the Rankine active coefficient have been proposed (Schroeder and Maitland 1979; St. Louis District, CE 1983); alternatively, Terzaghi (1945) proposed using a value of 0.4. Since some movement of the fill within the cell does occur, it would be overly conservative to use the at rest earth pressure coefficient.

41. Finally, it is important to see the uncertainty of the K value in proper perspective. For example, the interlock safety of the cell is much more strongly affected by the assumption made for the height of saturation within the cell than it is by choosing K equal to, for instance, 0.4 or 0.5. Thus, for protection against bursting, much more attention should be paid to ensuring proper drainage of the cell than to lengthly deliberations about what value of K to use (Swatek 1970).

Secant formula

42. Although the field and model-test data reported in the literature (St. Louis District, CE 1983; Schroeder and Maitland 1979; Sorota, Kinner, and Haley 1981; Sorota and Kinner 1981) are not completely consistent, at least some measurements indicate that the interlock tension in the crosswall near the arc connection may be as much as 20 percent higher than the main-cell tension. Thus, it appears reasonable to design for higher values of interlock tension in the crosswall than in the rest of the cell walls. The secant formula, Equation 15, was developed by TVA engineers (TVA 1957) to estimate the crosswall tension near the connecting pile, but for the following reasons its use is not recommended.

    <u>a</u>. The derivation of Equation 15 implies that forces are balanced in the inboard-to-outboard direction only; using the value of t_{cw} given in Equation 15 and summing forces in the direction of the axis of the cofferdam shows that equilibrium is violated in this latter direction.

    <u>b</u>. The angle θ appearing in Equation 15 corresponds to the angle which could be measured in the field <u>before</u> the main arc cells are filled. Since the sheet-pile walls can transmit only membrane forces (bending resistance is negligible), once the cells are filled the walls must deform and reorient themselves in order to accommodate the load from the fill. In particular, the connecting pile at the juncture of the main and arc cells must rotate and deform (some plastic yielding will be present (Grayman 1970)) to equilibrate the three tensile forces meeting there, and thus the value of the angle θ of Figure 7b must

25

change. Alternatively, inspection of free-body diagrams of the connecting pile (Dismuke 1975 and Swatek 1970) also show that θ must change under loading. Thus, in any derivation based on Figure 7b, both t_{cw} and θ should be considered as unknowns to be determined by equilibrium requirements.

43. The implication of these observations is that Equation 15 is based on premises which violate one of the fundamental principles upon which a cofferdam cell depends for its ability to carry its loads. Namely, large deformations of the sheet-pile skin are necessary to permit shearing resistance to develop in the fill. As a result, it is not surprising to find that both model and field data indicate that interlock tensions predicted by Equation 15 are overly conservative, and that its use is not recommended (Schroeder and Maitland 1979; Sorota and Kinner 1981; St. Louis District, CE 1983; Lacroix, Esrig, and Lusher 1970).

Swatek's equation

44. In place of the TVA secant equation, Swatek's equation, Equation 14, is recommended for the following reasons:

a. The approximation made in basing the derivation of Equation 14 on the equivalent rectangular cofferdam is consistent with the approximation made in analyzing other failure modes.

b. Equation 14 predicts results in better agreement with measured field data (St. Louis District, CE 1983; Moore and Alizadeh 1983; Sorota, Kinner, and Haley 1981; and Naval Research Laboratory 1979).

c. Equation 14 may be shown to yield good agreement with that obtained from an analysis which satisfies equilibrium and compatibility and is based on the actual positions of the loaded walls (Rossow 1984).

d. Finally, most bursting failures which have occurred can be traced to sheets being driven out of interlock, to damage or fabrication errors (e.g., welding-related problems) associated with the connector pile, or to the extreme deformations required of a tee connector (Belz 1970; OCE 1974; Grayman 1970; ORD 1974). Most designers consider separation of the interlocks a prime candidate as a cause of cell failure. A striking fact, however, is that the literature contains no reports of failures for which underdesigning for interlock tension was identified as the principle cause, at least for Y rather than tee connections. This fact offers evidence for using a less conservative formula for the common-wall tension near a Y pile, such as Equation 14.

Equation comparisons

45. A final observation may be made here to summarize the essential difference between the TVA secant equation and Swatek's equation. Swatek's

26

equation is based on using a crude model of the cofferdam (that is, the equivalent rectangular cofferdam) to estimate an average interlock tension for the entire crosswall. The equations of statics are satisfied. In contrast, the TVA secant equation is based on a geometrical model which takes into account wall curvature, and an estimate is obtained for the crosswall interlock-tension at a specific point--adjacent to the Y . However, an equation of statics is violated, and, furthermore, the geometrical model is flawed, since it does not take into account the movement and rotation of the walls which occurs as the cell is filled.

PART IV: SLIP ON VERTICAL CENTER PLANE IN FILL

Effects of External Lateral Forces

46. The lateral force acting on the cell causes shear failure on vertical planes within the fill. Large distortions of cell shape occur and the cell may collapse towards the inboard side of the cofferdam. See Figure 8.
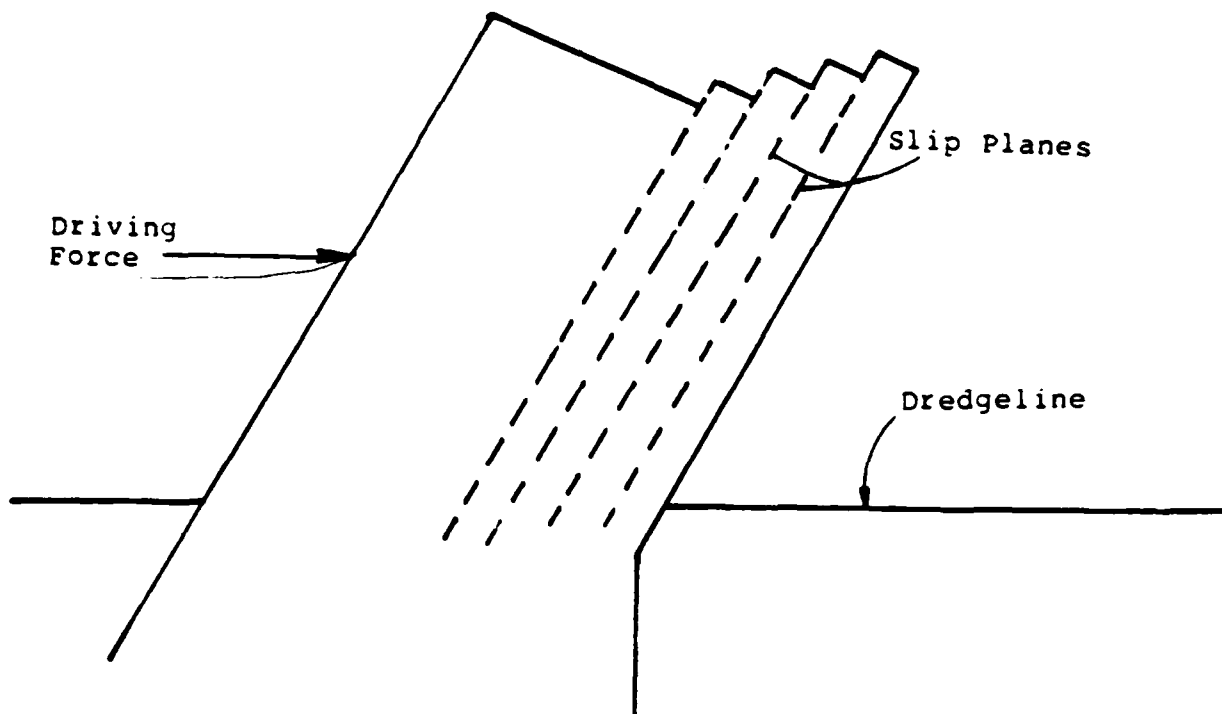

Figure 8. Failure by slip on vertical center plane

47. The FS against failure by slip on vertical center plane (Terzaghi 1945) is written as:

$$FS = \frac{\text{Maximum available resisting force}}{\text{Driving force}}$$

$$= \frac{S'_m + S''_m}{S' + S''} \tag{17}$$

28

where

    S' = actual shearing force acting on vertical centerplane of cell

    S'_m = maximum possible value of shearing force on vertical centerplane of
         cell

    S" = actual friction force from interlocks in crosswall

    S''_m = maximum possible value of friction force from interlocks in
         crosswall

It should be noted that all quantities are calculated for a unit length of the
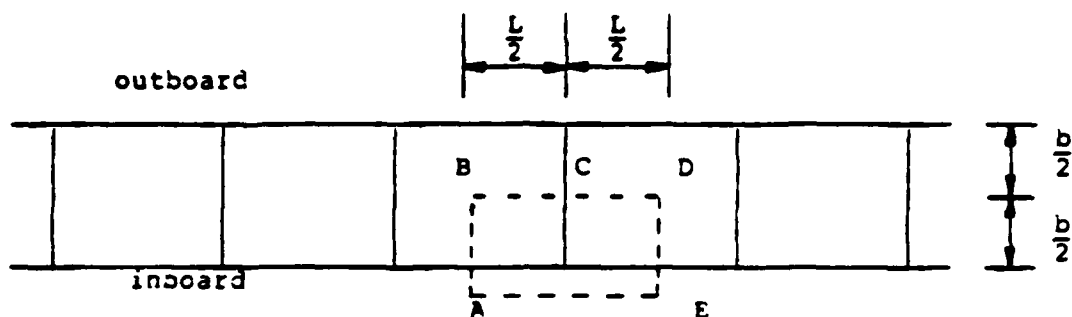cofferdam.

Cell Foundation

48. The discussion of this failure mode is based on the assumption that
the cell is founded on a rock, sand, or hard clay foundation. Thus, the foun-
dation is able to resist the unequal pressure distribution resulting from the
combined vertical and horizontal forces acting on the cell. As a consequence,
shearing resistance on vertical planes within the fill can be mobilized. The
magnitude of this resistance is an important consideration in evaluating the
stability of the cell. In contrast, the design of cofferdams founded on soft
clay or other compressible soils tends to be governed by the bearing capacity
of the foundation, rather than by considerations of internal stability. The
stability calculations can still be made, however, based on the resisting
moment provided by interlock friction (Jumikis 1971; Terzaghi 1945; USS 1972).

Considerations in Analysis of Failure by Vertical
Shear on Center Plane

49. The individual driving forces S' and S" cannot be easily cal-
culated; their sum, however, can be expressed in terms of the overturning
moment. The relevant free body is shown in plan view in Figure 9a and in an
isometric view in Figure 9b. Only vertical forces are shown. These forces
are:

    a. F , the friction force in the interlock of the crosswall.

    b. S'L , the shear force acting on the center plane DGHB (S' is
       produced by the cell fill on one side of the center plane
       acting on the fill on the other side.).

    c. W/2 , the weight of half the contents of the cell.

29

a. Portion of equivalent cofferdam selected for analysis
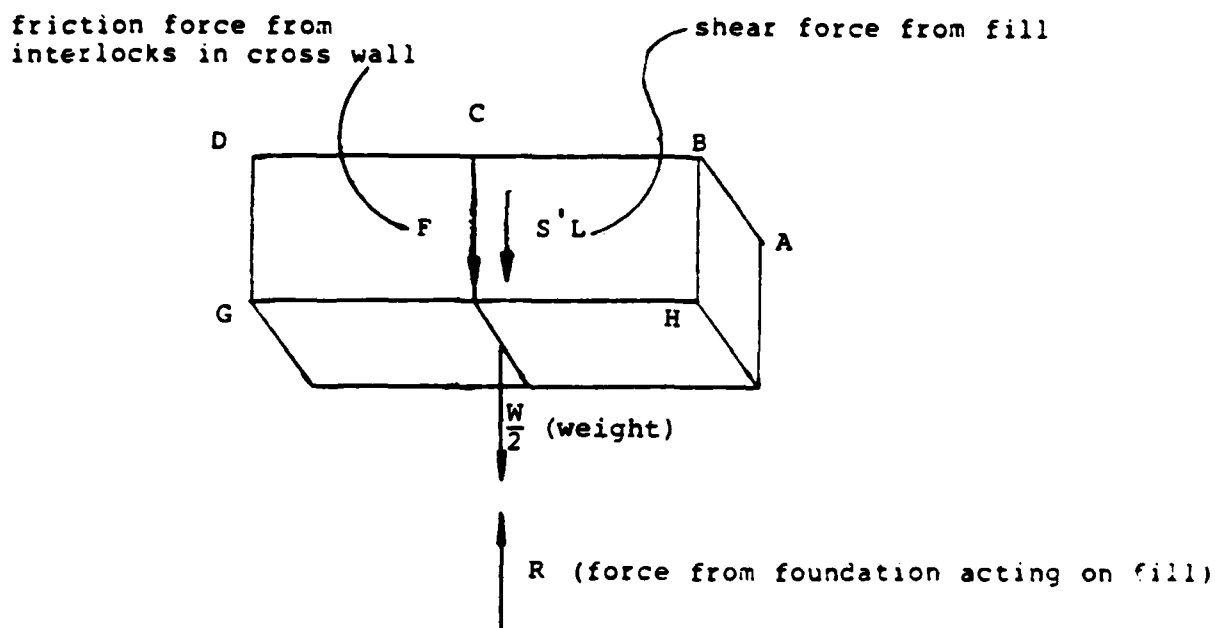

Figure 9. Free-body diagram showing driving forces

_d_. R , the upward reaction from the foundation.

Summing vertical forces and equation to zero gives

$$S'L + F + \frac{W}{2} - R = 0 \qquad (18)$$

Dividing through by L and using the definition of S'' as friction force per unit length, namely,

30

$$S'' = \frac{F}{L} \tag{19}$$

gives, after some re-arrangement,

$$S' + S'' = \frac{\left(R - \frac{W}{2}\right)}{L} \tag{20}$$

Thus, the driving force $(S' + S'')$ has been expressed in terms of the weight and the upward reaction R on the inboard half of the cell.

50. In turn, R may be expressed in terms of the overturning moment. Figure 10a shows the portion of the cofferdam selected for analysis, and an elevation view is shown in part b of that figure. Also shown in Figure 10b is the distributed force from the foundation which acts upward on the cell. Since only the weight W of the cell (no lateral forces) is considered in this sketch, the distributed force is uniform. In Figure 10c, the overturning effect of lateral forces has been included through the presence of the over- turning moment. If the symbol M denotes moment per length, then the magni- tude of the overturning moment is ML . The force distribution has now been altered and is assumed to vary linearly across the base of the cell (USS 1979). As shown in Figure 10d, this latter force distribution may be replaced by the sum of a uniform distribution and a linearly varying symmetric distri- bution. But these two distributions may be replaced by a pair of concentrated loads of magnitude $W/2$ and a couple defined by two forces of unspecified magnitude Q . Thus R , the vertical reaction from the foundation acting upward on the inboard half of the cell, can be expressed in terms of Q as

$$R = Q + \frac{W}{2} \tag{21}$$

51. It remains to express Q in terms of the overturning moment. Since in Figure 10d each force Q represents the resultant of a triangular distribution, each force must act through the centroid of the triangle; thus the distance between the Q forces is $2b/3$, and the magnitude of the couple

31

a. Portion of equivalent cofferdam selected for analysis

Resultant = W
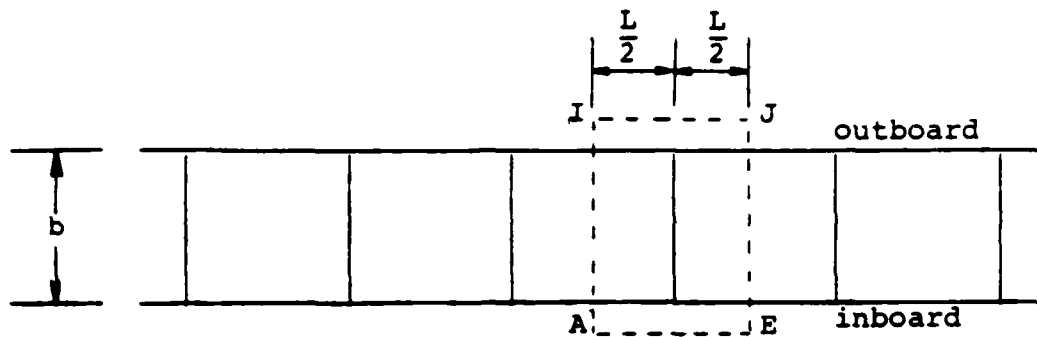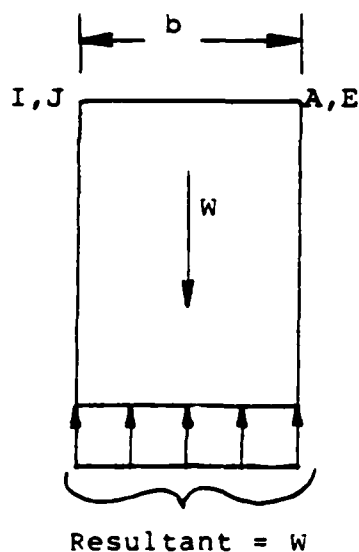
b. Free body with no overturning moment
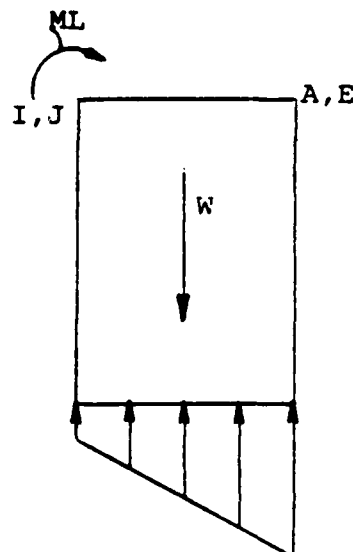
c. Free body with overturning moment
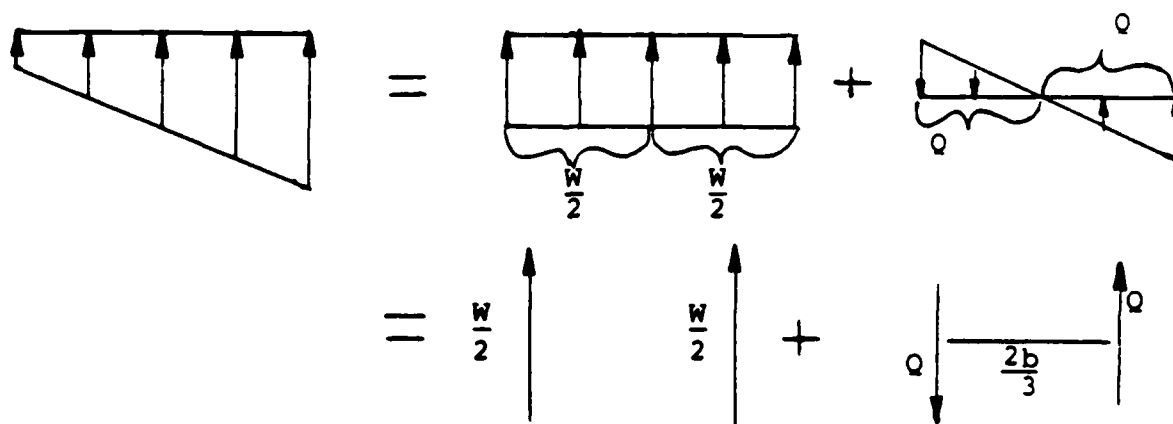
d. Statically equivalent reactions

Figure 10. Pressure distribution from foundation acting on cell

32

produced by the foundation pressures is $2bQ/3$. Since the cell is in equilibrium, this couple must balance the overturning moment ML ; that is,

$$ML = \frac{2bQ}{3} \tag{22}$$

52. Equation 22 may be solved for Q in terms of the overturning moment and the result substituted in Equation 21 to yield an expression for R in terms of M . Substituting this latter expression into Equation 20 then yields

$$S' + S'' = \frac{3M}{2b} \tag{23}$$

Overturning Moment

53. The lengths used in the calculation of the overturning moment M are defined in Figure 11a. Here, the quantities H_{w1} , H_{w2} , and H_{w3} are the vertical distances from the sheet-pile tips to the intersection of the phreatic surface with the inboard sheeting and the center line, respectively. $H_{wo}$ is the vertical distance from the tips of the sheet-pile to the water level outside of the cofferdam. The forces are defined in Figure 11b. Here, P_w and P_{w1} represent the resultants (per unit length of cofferdam) of the water pressure on the exterior faces of the outboard and inboard walls of the cell, and are given by the relations

$$P_w = \frac{\gamma_w (H_{wo})^2}{2} \tag{24}$$

and

$$P_{w1} = \frac{\gamma_w (H_{w1})^2}{2} \tag{25}$$

33
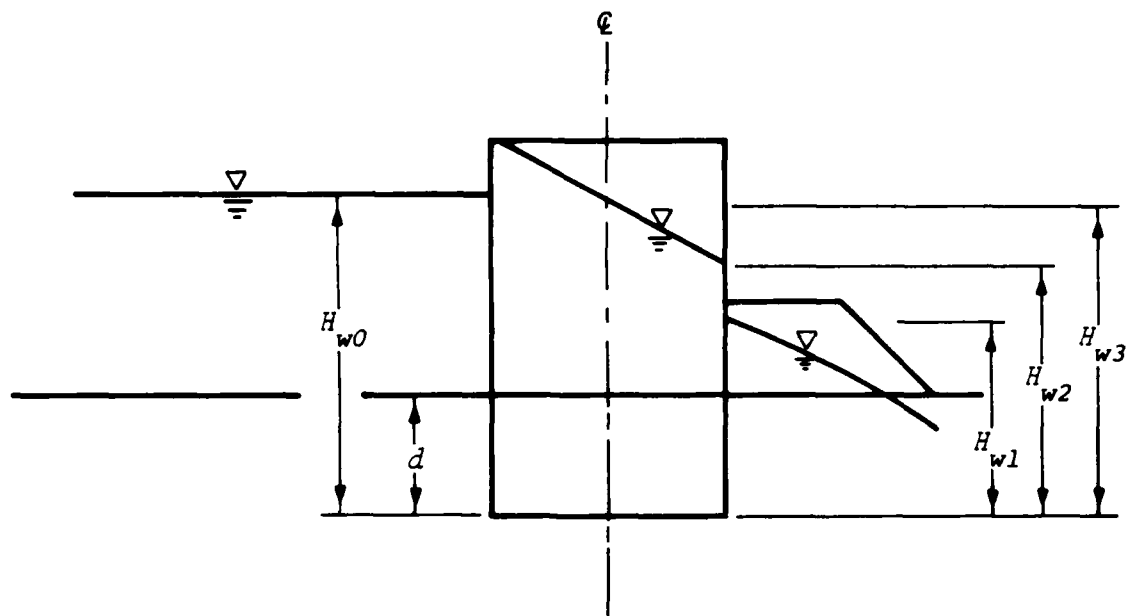
a. Definition of lengths used in M calculation
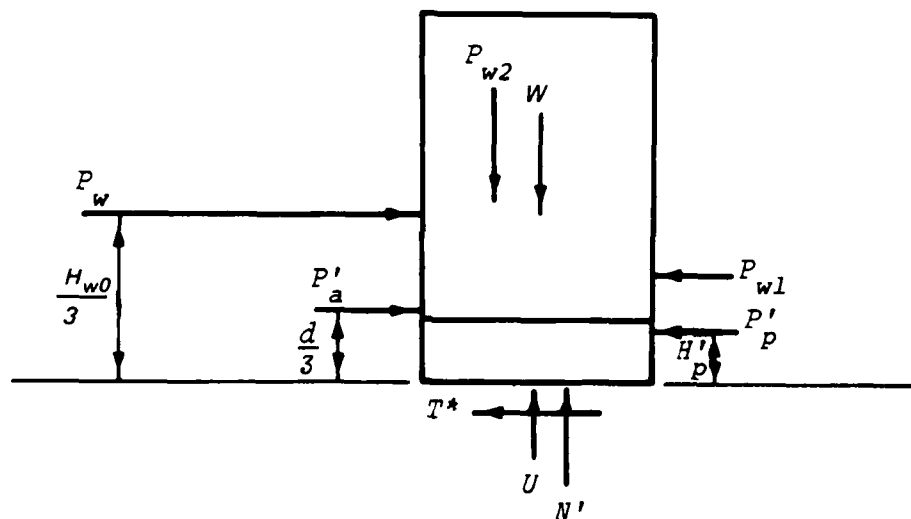
b. External forces considered in calculation of overturning moment

Figure 11. Calculation of overturning moment

P'_a , the horizontal effective force of the foundation soil acting on the outboard sheeting, is calculated using the Rankine active earth pressure coefficient K_a :

$$P'_a = \frac{K_a \gamma'_s d^2}{2}$$

(26)

in which γ'_s is the submerged unit weight of the foundation soil.

54. The calculation of P_p', the horizontal effective force from the berm and foundation soil acting on the inboard sheeting, is problematical. One approach is to calculate it using the sliding-wedge theory, the Coulomb theory modified by the presence of the back slope of the berm or the friction circle method. However, under certain conditions this procedure may lead to such a large value of P_p' that the overturning moment and, hence, the factor of safety become negative. Clearly, this is physically unrealistic, since the passive resistance of the berm and foundation acting on the inboard wall is mobilized only in response to the driving forces P_w and P_a'.

55. Since horizontal equilibrium must be maintained, it can be seen from Figure 11b that the value of P_p' cannot exceed the following equation:

$$P_p' = P_a' + P_w - P_{w1} - T* \qquad (27)$$

where $T*$ is the horizontal shear force on the base of the cofferdam per unit length of cofferdam. The value of P_p' for use in Equation 28 can be calculated as follows: calculate the maximum passive earth force P_p^* acting on the cofferdam. This may be calculated using the trial-wedge method, Coulomb theory modified by the presence of the back slope of the berm, or the friction-circle method. Compare P_p^* to the results of Equation 27 with $T*$ taken as zero. Let P_p' be the smaller of these two terms. Assume that H_p', the moment arm at which P_p' acts about the base of the cell, for P_p' is the same as for P_p^*. When P_p' is taken as the value of P_p^*, equilibrium is maintained by increasing $T*$ so that Equation 27 is satisfied. Note that $T*$ must be less than $N'\tan\phi$ to prevent sliding along the base of the cell where N' is the resultant effective soil force acting on the base of the cofferdam per unit length of cofferdam. The $T*$ term does not enter into the calculation of the overturning moment since it passes through the point about which the moment is summed.

56. In terms of the quantities which have now been defined, the overturning moment per unit length of cofferdam can be calculated by summing moments about the point where the center line of the cell intersects the base.

$$M = \frac{P_w H_{wo}}{3} + \frac{P_a' d}{3} - P_p' H_p' - P_{w1}\frac{H_{w1}}{3} \qquad (28)$$

57. In deriving Equation 28, the assumption is made that water forces P_{w2} and U (Figure 11) act through the same point, thus cancelling each other in determining the overturning moment. If the cofferdam designer does not believe this to be the case, the P_{w2} and U terms should be included in Equation 28. The weight of the contents of the cell along the center line of the cell thus has no contribution to the overturning moment.

Calculation of S_m'

58. The maximum possible value of the shear on the vertical centerplane of the cell may be estimated as the product of the effective normal force P_c' acting on the center plane times the coefficient of friction of the fill. That is,

$$S_m' = P_c' \tan (\phi) \tag{29}$$

where ϕ equals the angle of internal friction of fill. The normal force P_c' may be computed from the pressure diagram shown in Figure 12. The question of what value to use for the lateral earth pressure coefficient K will be deferred to paragraph 60.

Calculation of S_m''

59. Figure 13 shows the relevant free body. T_{cw} is the resultant tensile force in the crosswall. If f denotes the coefficient of friction of the interlock (steel-on-steel), then the maximum possible friction force in the crosswall is fT_{cw}. Thus, the maximum friction force S_m'' per unit length of wall is given by the equation

$$S_m'' = \frac{fT_{cw}}{L} \tag{30}$$

The tension T_{cw} may be found by summing forces on the free body shown in Figure 13b. In Figure 13b the pressure diagram goes to zero at the plane of fixity or the tip of the sheet pile. This is a choice left up to the cofferdam designer. There is still some tension in the crosswall below the plane of fixity because, as mentioned earlier, the plane of fixity is calculated at the point of zero slope, not zero deflection. Sometimes there is tension in the crosswall all the way to the tip of the sheetpiling. But this is not always

$(H-H_{w3})$

$(H_{w3}- d)$

d

$K\gamma'_s d$ $K\gamma'_f(H_{w3}-d)$ $K\gamma'_f(H - H_{w3})$
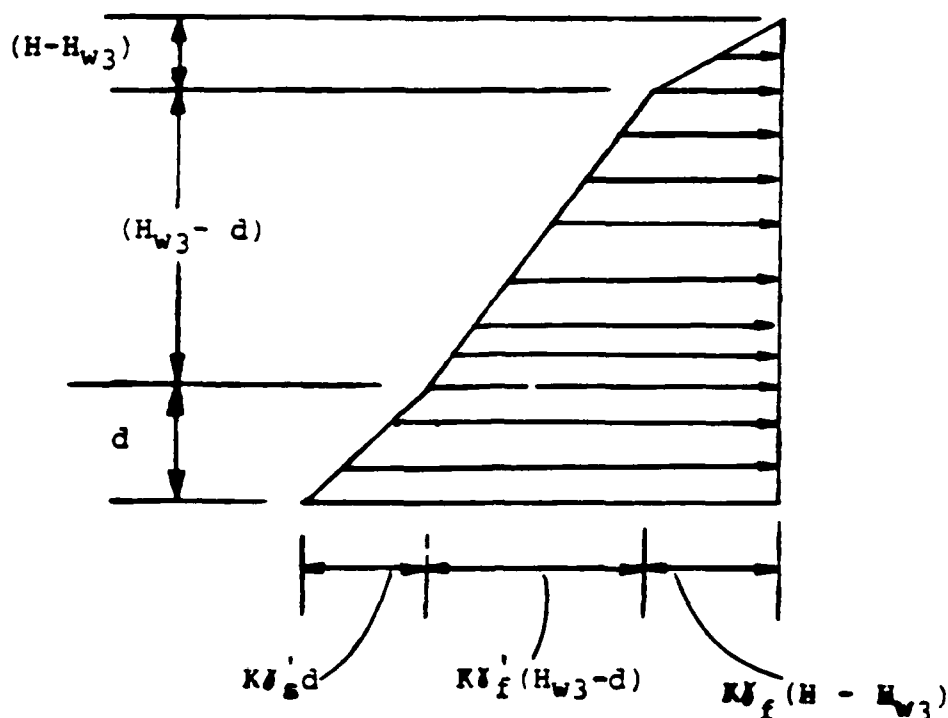
Figure 12. Pressure diagram for calculation of P'_c effective force on center plane

the case, especially for cofferdam cells with deep embedment into the foundation. It should be noted that in some cases for cofferdams on rock, the pressure diagram may not go to zero at the tip of the sheet piling. The pressure diagram will still decrease from the P_{max} value, but it may not be zero at the tip.

Discussion of
vertical-shear failure mode

60. The staircase-type surface shown at the top of the cell in Figure 8 has been observed in mooring cells which have been struck by barges. This suggests that the vertical-shear failure mode does occur in a full-sized cell.

61. In the most realistic model tests which have been conducted to date (Maitland and Schroeder 1979), the vertical-shear mode was found to be the actual mode of failure under lateral load. Controversy remains, however, as to the appropriate value to use for the lateral earth pressure coefficient K. In his original work, Terzaghi (1945) suggested use of the Rankine coefficient, K_a. In a discussion of Terzaghi's paper, however, Krynine (1945)

37
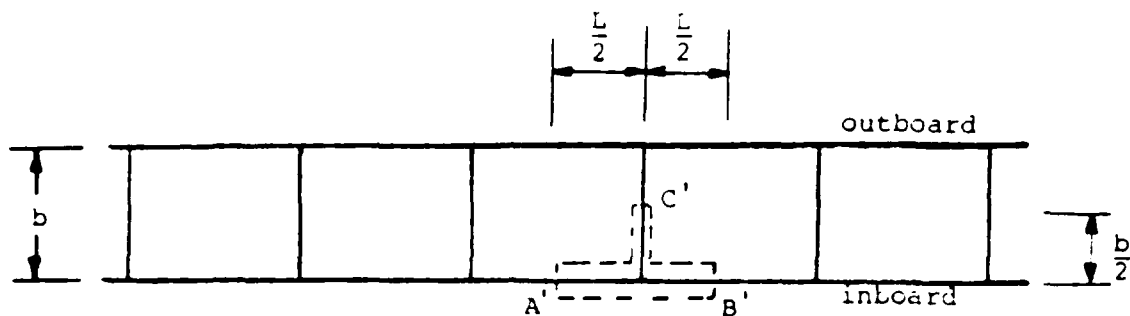
a. Portion of equivalent cofferdam selected for analysis
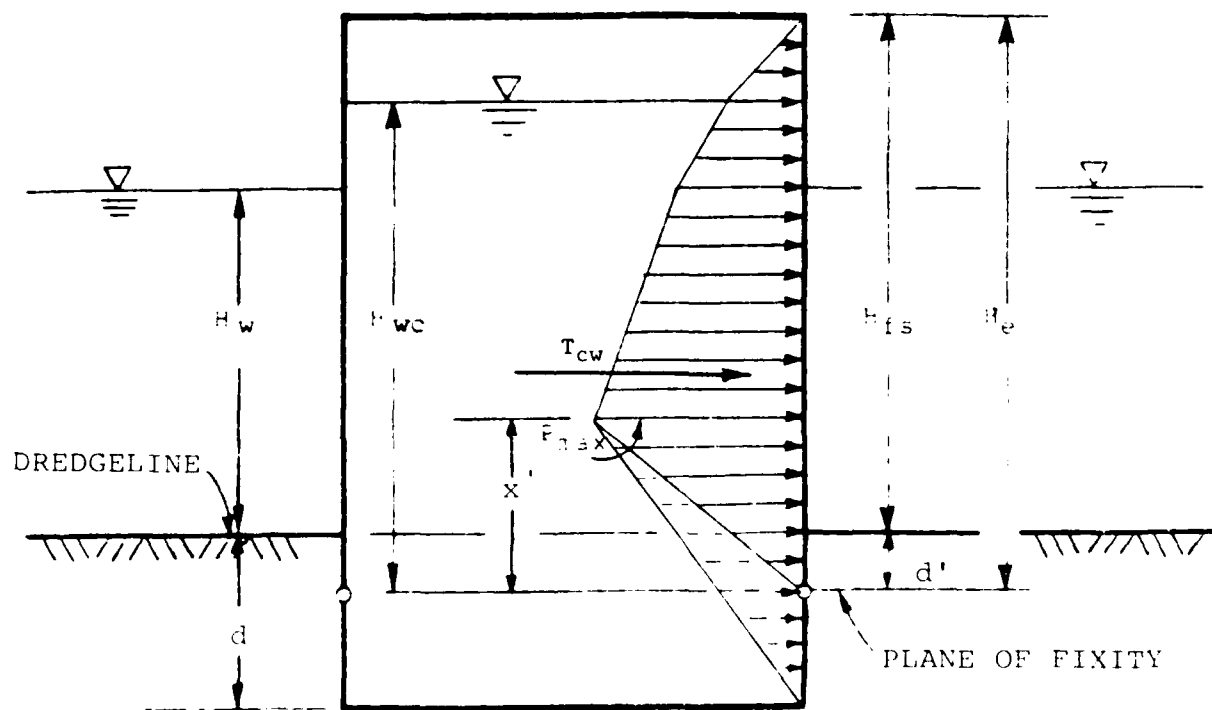
b. Free body for calculation of force in cross wall

Figure 13. Free body for calculation of T_{cw}

pointed out that it is incorrect to use the Rankine coefficient. The reason
for this is that the assumed failure plane (the vertical plane) cannot be a
principal plane because shear acts on it. Using a Mohr's circle analysis,
Krynine derived the equation

$$K = \frac{\cos^2 \phi}{2 - \cos^2 \phi} \tag{31}$$

62. It was subsequently pointed out by Cummings (1957) and Esrig (1970)
that Krynine's expression for K had the physically unrealistic property that
K decreased with increasing values of the angle of friction ϕ , and this
result led Esrig to doubt the value of the entire vertical-shear failure mode.
Based on their model studies, however, Schroeder and Maitland (Maitland and
Schroeder 1979; Schroeder and Maitland 1979) argued that the overturning
moment applied to the cell tends to compress the fill significantly on the
inboard side and, as a result, the lateral-earth pressure coefficient is
appreciably increased. They suggest using the empirical value K = 1 . This
approach yielded calculated values of ultimate overturning moment in good
agreement with values determined experimentally in their model study. Using
K = 1 , however, does not appear sufficiently justified by experience at this
time, especially since currently used safety factors are based on much lower
values of K . Thus, it is recommended to use the Krynine earth pressure
coefficient when calculating P'_c . Schroeder and Maitland also suggest that
pressure calculations be based on the effective height H_e of the cell.

63. For some fill materials, interlock friction $S'' = fT_{cw}/L$ may
account for 30 to 40 percent of the total resisting force (Terzaghi 1945).

64. The approximation of the base pressure distribution by a straight
line in Figure 10c is valid only if the base remains in compression over its
entire length. This condition will be satisfied only if the resultant force
acting on the cell from the foundation acts within the middle third of the
base. If the resultant does not act within the middle third, the entire
analysis for shear on the vertical center plane is questionable.

65. The free body used to calculate the overturning moment, Figure 11b,
neglects the interlock tensions occurring in the actual curved-wall cell. The
error involved in using free bodies which neglect the curvature of the walls
has been discussed in paragraph 18.

39

PART V: SLIP ON HORIZONTAL PLANES IN FILL (CUMMINGS' (1957) METHOD)

Horizontal Plane Sliding Due to Lateral Forces

66. Under the action of the resultant lateral force P , a plane of rupture forms. This is illustrated in Figure 14. The plane extends from the toe of the cell at B upward at an angle ϕ to the outboard wall at A . ϕ is the angle of friction of the fill. Shear failure of the fill occurs on horizontal planes within the triangle bounded by the plane of rupture, the bottom of the cell, and the outboard wall (region AOB). As a result of the shear failure of the fill, the cell tilts excessively and may collapse through excessive deformations of the interlocks and consequent loss of fill.

67. The FS against failure by slip on horizontal planes in fill is shown as:

$$FS = \frac{\text{Maximum available resisting moment}}{\text{Driving moment}}$$

$$= \frac{M_f + M_{shear}}{M} \tag{32}$$

where (Figure 15, the free body shown consists of a unit width of the outboard and inboard walls, as shown in Figure 2)

M_f = moment caused by the friction force in the interlocks of the crosswall

M_{shear} = moment caused by the pressure of that portion of the fill which fails in shear on horizontal planes

Considerations in Horizontal Shear Calculations

Discussion of the theory

68. Figure 16a shows a vertical slice of the fill within a cell. The slice is assumed to be of unit thickness into the plane of the figure. Line AGJN defines the assumed phreatic surface, and line BQLO , which makes an angle $\dot{\tau}$ with the base of the cell, defines the plane of rupture. According to Cummings (1957), as the cell begins to tilt under lateral pressure, the fill above the rupture plane begins to slide down the plane. This motion is,
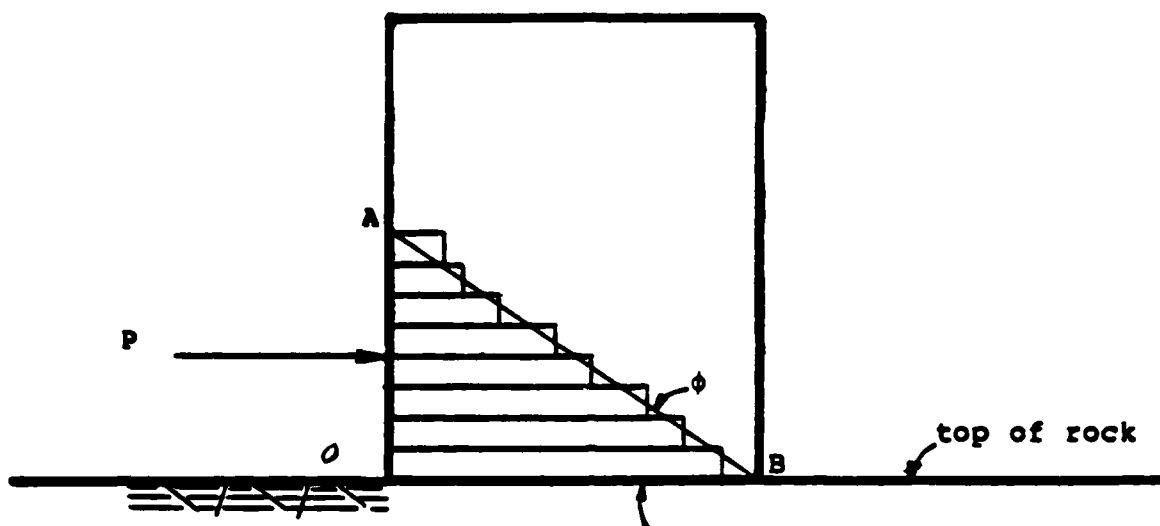
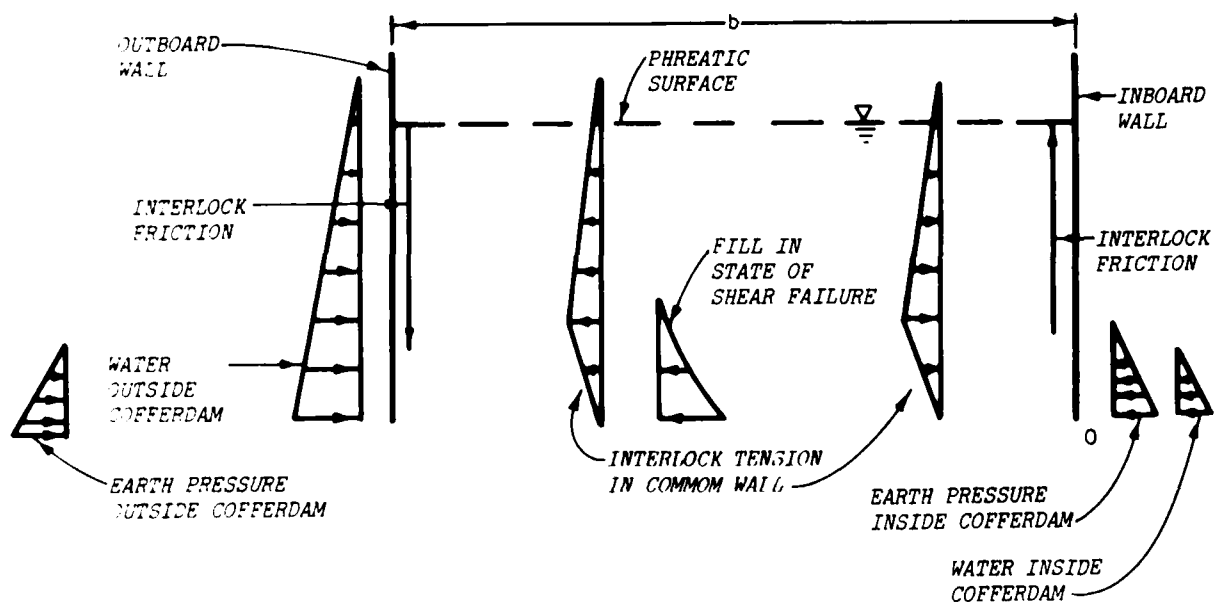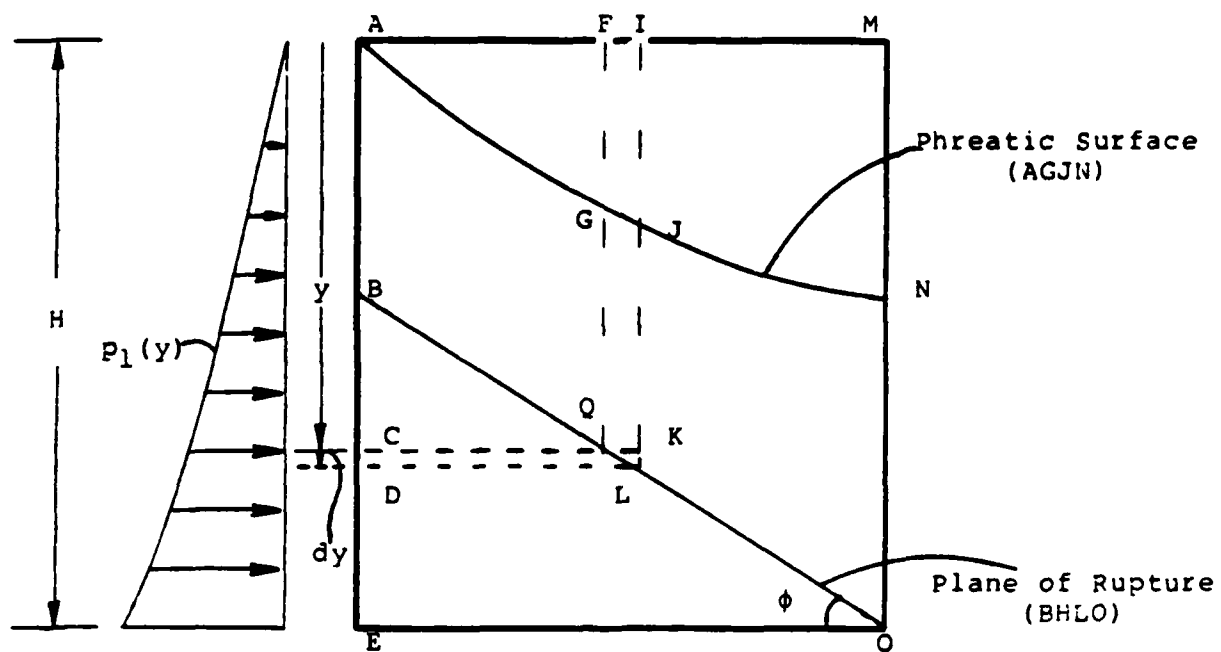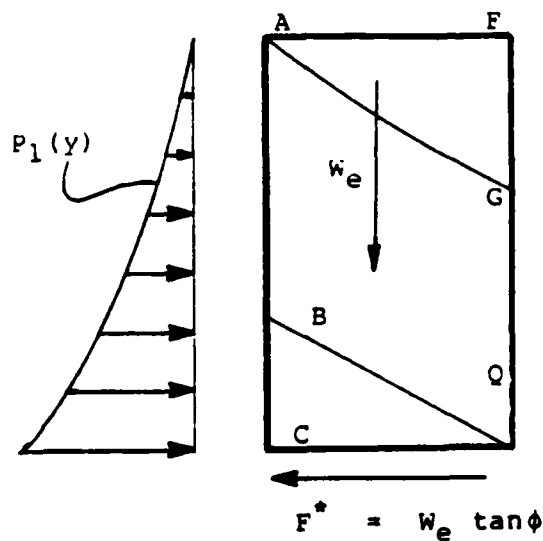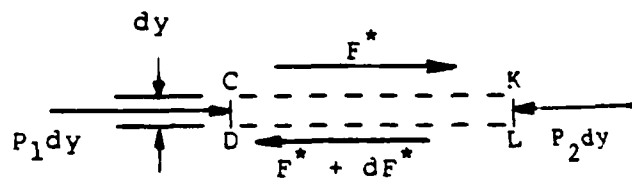Figure 14. Failure by sliding on horizontal planes
within fill

Figure 15. Free body for calculation of moments in Cummings'
Method. Moments are summed about point O

a. Cross section of cell fill, with pressure P_1 from sheetpiling

b. Shear force F^* on
   horizontal plane CH

c. Free body for relating
   P_1, F^*, and P_2

Figure 16. Lateral forces on fill

of course, inhibited to a large extent by the confining effect of the sheet-pile envelope. The fill below the rupture plane (within the prism BEO) is transformed into a passive state by the combined effect of the lateral forces acting on the cofferdam exterior and the weight of the fill above the rupture plane. The latter body of material, that is, the fill <u>above</u> the rupture plane, is assumed to remain in an active state.

Resisting moment acting on outboard wall

69. Figure 16a shows the pressure distribution p_1 of the outboard sheet-pile wall acting on the fill. By Newton's Third Law, this pressure is equal and opposite to the pressure of the fill acting on the wall. Above point B , where the plane of rupture intersects the wall, p_1 is the sum of the pressure produced by water inside the cell and by fill in the active state. That is,

for
$$o < y < y_B$$

$$p_1(y) = (\gamma_w + \gamma_f' K_a)y \tag{33}$$

in which y is the distance measured downward from the top of the cell.

70. Below point B , the pressure distribution is more complex since the resisting shear on the horizontal sliding planes within the fill must be taken into account. In Figure 16b, region ABCQGF has been drawn isolated from the rest of the cell, and the shear F* is shown acting to resist the lateral pressure. F* can be calculated from the relation

$$F^* = W_e \tan(\phi) \tag{34}$$

in which W_e equals the effective weight of the fill above the base of the free body, that is,

$$W_e = \gamma_f V_{AGF} + \gamma_f' V_{ACQG} \tag{35}$$

where

V_{AGF} = volume of prism AGF

V_{ACQG} = volume of prism ACQG

71. To develop the relation between the shear F^* and the pressure p_1, consider the infinitesimal region CDLK extending from the wall to the plane of rupture (Figure 16c). Note that the pressure p_2 acting on the right end of the free body has been included. Summing the horizontal forces acting in the figure gives

$$p_1 \, dy - p_2 \, dy - dF^* = 0 \tag{36}$$

from which it follows, through use of Equation 34, that

$$p_1 = p_2 + \frac{dF^*}{dy}$$

$$= p_2 + \frac{dW_e}{dy} \tan(\phi) \tag{37}$$

72. At this point in the derivation, to arrive at Cummings' expressions for the resisting moment, the following equation for p_2 must be assumed:

$$p_2 = (\gamma_w + \gamma_f' K_a) y \tag{38}$$

That is, the lateral pressure acting at points on the rupture plane is the sum of the hydrostatic pressure and the active earth pressure corresponding to a completely saturated cell--the downward slope of the phreatic surface is ignored, even though it is included in the calculation of the effective weight W_e given by Equation 35. Since the pressure p_2 contributes to the resisting pressure p_1 of the cell through Equation 37, it is conservative to assume that the unit weight of the fill has the submerged value γ_f' over the entire depth y. However, it is nonconservative to assume that the water pressure term in Equation 38 is based on the entire depth y.

73. With p_2 now defined, the pressure p_1 of the wall on the fill below point B can be written using Equations 37 and 38:

for
$$y_B < y < H$$

44

$$p_1 = (\gamma_w + \gamma_f' K_a)y + \frac{dW_e}{dy} \tan (\phi) \tag{39}$$

Pressure distribution defined

74. Equations 33 and 39 together completely define the pressure distribution of the outboard wall acting on the fill. The equal and opposite pressure acting on the outboard wall is shown in Figure 17.
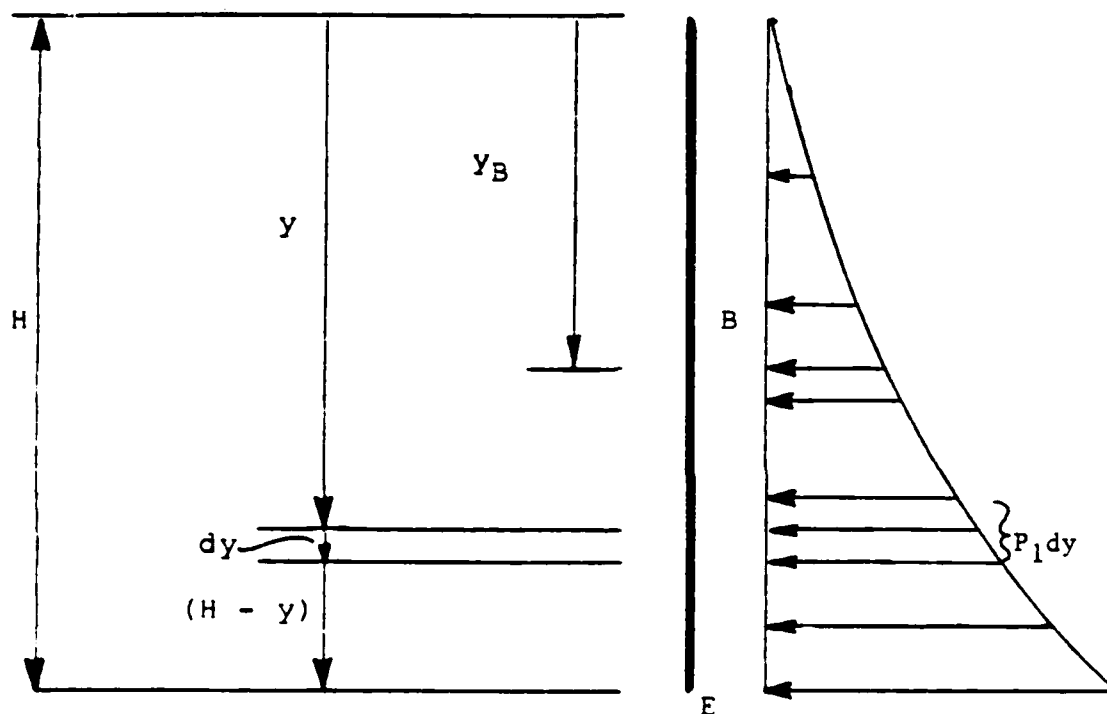
Figure 17. Resisting pressure acting on outboard wall

The total moment about the base produced by this pressure is

$$M^\star = \int_0^H (H - y)p_1 \; dy$$

which can be written, with the use of Equations 33 and 39, as

$$M^* = \int_0^{y_B} (H - y)(\gamma_w + \gamma_f' K_a)y \, dy + \int_{y_B}^{H} (H - y)\left[(\gamma_w + \gamma_f' K_a)y \right.$$

$$\left. + \frac{dW_e}{dy} \tan (\phi) \right] dy$$

$$= \int_0^{H} (H - y)\gamma_w y \, dy + \int_0^{H} (H - y)\gamma_f' K_a y \, dy + \int_{y_B}^{H} (H - y) \frac{dW_e}{dy} \tan (\phi) \, dy \qquad (40)$$

Representative Integrals

75. Examination of the right-hand side of the last equation shows that the three integrals appearing there represent terms in the expression for the resisting moment in Equation 32:

$$M_{wo} = \int_0^{H} (H - y)\gamma_w y \, dy \qquad (41)$$

$$M_{ao} = \int_0^{H} (H - y)\gamma_f' K_a y \, dy \qquad (42)$$

$$M_{shear} = \int_{y_B}^{H} (H - y) \frac{dW_e}{dy} \tan (\phi) \, dy \qquad (43)$$

The effective weight W_e, which appears in the last integral, depends on the location of the phreatic surface within the cell (Equation 35 and Figure 16).

46

Since this surface may vary in a nonlinear manner within the cell, Cummings suggests that an "incremental method" (in effect, a low-order numerical integration rule) be used to evaluate Equation 43:

$$M_{shear} = \tan{(\phi)} \sum \left[(\Delta W_e)_i (H - y_i) \right] \tag{44}$$

where

$(\Delta W_e)_i$ = effective weight of the cross-hatched region shown in Figure 18

y_i = distance measured downward from the top of the cell to the midpoint of increment i in Figure 18

76. Equation 44 could be replaced by a more accurate numerical integration method such as Simpson's rule. The equation given for M_{shear} by
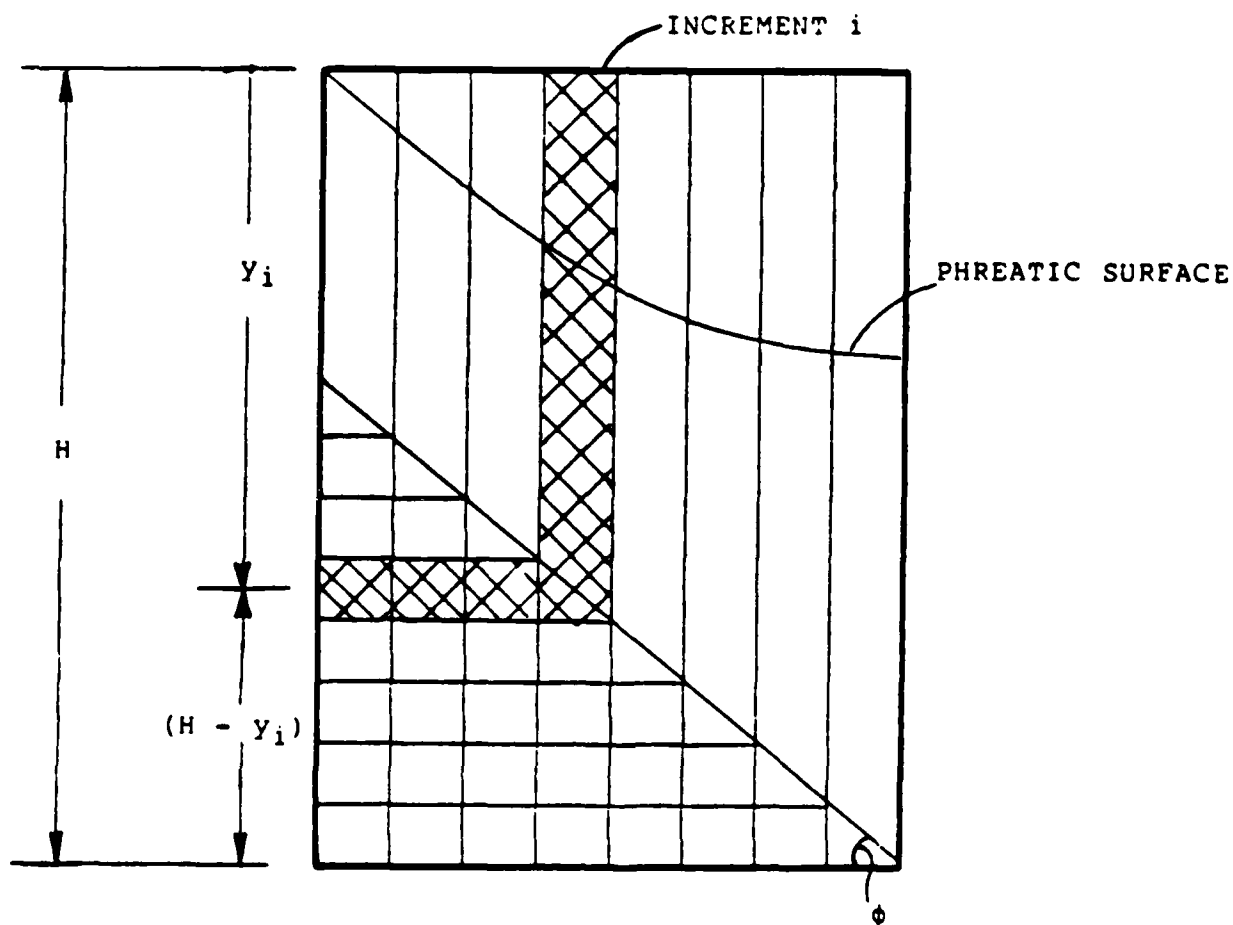

Figure 18. Increments used in computing M_{shear}

47

Cummings, rearranged to be consistent with notation in this report, is

$$M_{shear} = \frac{Hb^2 \gamma_e}{6} \left[3 \tan^2 \phi - \frac{b}{H} \tan^3 \phi \right] \tag{45}$$

where γ_e equals the effective unit weight of soil which is equal to the weighted average of γ_m above phreatic line and γ' below the phreatic line.

Interlock friction

77. Cummings' method also considers the contribution of interlock friction to resisting tilting of the cell. Figure 19a shows two portions of the cofferdam walls which will be analyzed for the effect of interlock friction. In Figure 19b, these portions of the walls have been isolated and shown in an elevation view. Three forces have been included in the free body diagram: (a) T_{cw} , the interlock tension in the crosswall; (b) LP* , the resultant of the fill pressure P* (P* is force per unit length of cofferdam acting on the main-cell walls); and (c) F , the friction force from the interlock of the cross-wall sheet pile adjacent to the connector pile. Following steps similar to those leading to Equation 30 leads to an expression for the friction force per unit length of cofferdam:

$$\frac{F}{L} = fP* = f \frac{T_{cw}}{L} \tag{46}$$

78. The moment per unit length of cofferdam, M_f , can be calculated by multiplying the friction force F/L of Equation 46 by the moment arm b (Figure 15) to obtain

$$M_f = fP*b = \frac{fbT_{cw}}{L} \tag{47}$$

Comments on horizontal shear method

79. The technical literature contains no reports of the failure of a full-sized cell by sliding on horizontal planes in the fill. The only positive experimental evidence for such a failure mode comes from Cummings' own model studies (1957), reported in the paper describing his theory, and from a TVA experiment using a cigar box with the top and bottom replaced by glass (TVA 1957). The walls of these models were all relatively stiff, and their

48
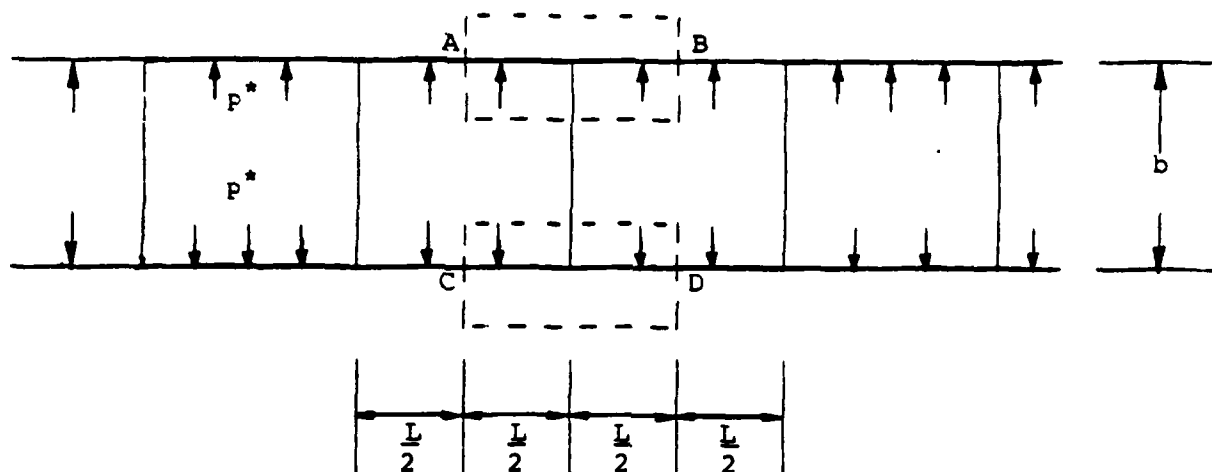
a. Portion of equivalent cofferdam selected for analysis
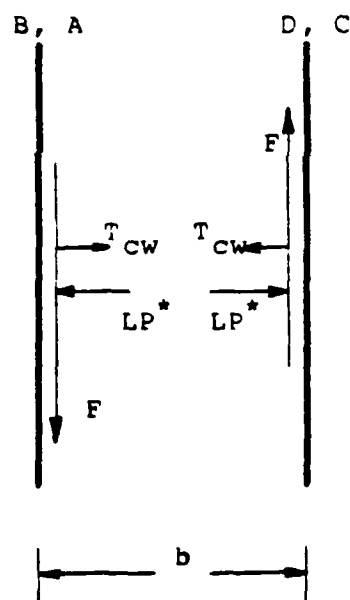
b. Elevation of portions
AB and CD

Figure 19. Free-body diagram for calculation of resisting moment
produced by friction in interlocks

small size raises serious concern that surface effects in the fill were far more important than they would be in a full-sized cell. Indeed, it is interesting to observe Erzen (1957) comments in a discussion published simultaneously with Cummings' paper. Erzen expressed concern that the stress distribution in the fill in Cummings' models was strongly influenced by the proximity of the walls, and as a result, he doubted Cummings' demonstration that distinct zones (active and passive) exist in the fill.

80. Heyman (1957), another discussor of Cummings' paper, stated that additional tests on cellular cofferdams were needed to determine where the actual plane of failure occurs. Aside from Cummings' own studies, no such studies have subsequently been reported in the literature.

81. In summary, then, the basic assumptions upon which Cummings' method rests--that is, a plane of rupture exists which makes an angle ϕ with the base and divides the fill into an active region and a region in which sliding occurs on horizontal planes--are not well supported by experimental evidence.

82. Even while Cummings' models provide the only experimental support for the horizontal-shear failure mode, the subsequent model studies of Maitland and Schroeder (Maitland 1977; Maitland and Schroeder 1979) provided evidence against it. These studies showed that Cummings' method predicted maximum resisting moments significantly larger than those actually observed at failure.

83. Figure 15, which was used in the derivation of the FS , shows all forces which are considered in Cummings' method. Note that these forces are considered to act on a single free "body" consisting of a unit width of the outboard wall and the inboard wall. Thus, although Cummings' method is often characterized as being based on a criterion of internal shear-failure of the fill, this characterization is misleading: the internal shear-failure mechanism is used only as a device to permit the calculation of the pressure of the fill on the wall. The actual FS is based on the assumption that the outboard and inboard walls behave as a rigid unit and a sum of all moments which act on this unit. The uncertainties involved in neglecting the interlock tensions for this flat-walled free body have been discussed previously in paragraph 18d.

PART VI: SLIP BETWEEN SHEETING AND FILL

Vertical Sheeting Slip from Overturning Moment

84. Under the action of the overturning moment, the sheeting slips vertically upward relative to the fill, and fill runs out at the heel. This is illustrated in Figure 20.
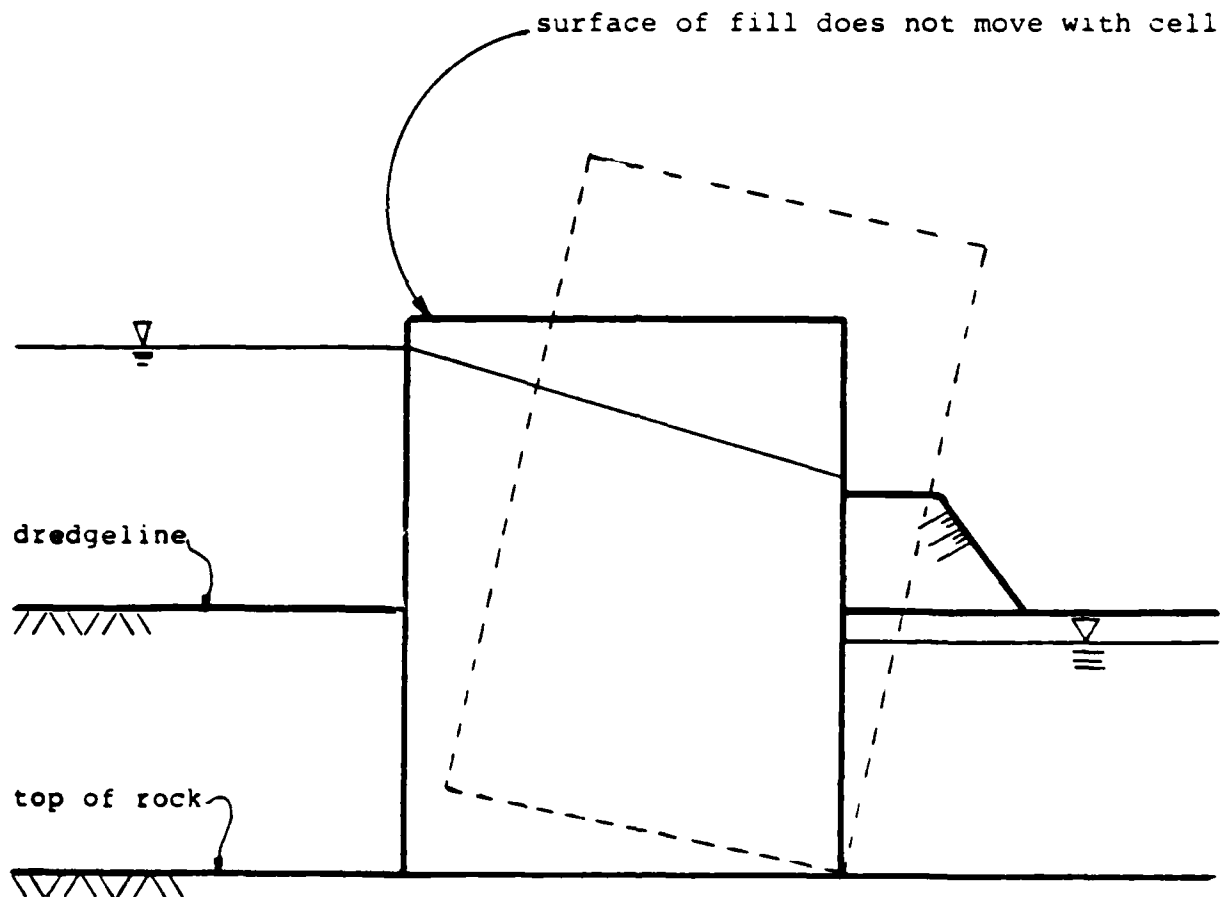

Figure 20. Illustration of slip between fill and sheeting

85. The FS against slip between sheeting and fill (Jumikis 1971; Lacroix, Esrig, and Lusher 1970; NAVDOCKS DM7 1971; USS 1972) is expressed as:

$$FS = \frac{\text{Maximum available resisting moment}}{\text{Driving moment}}$$

$$= \frac{b\{P'_a \tan (\delta) + [P_s + P_s (b/L)] \tan (\delta)\}}{M} \tag{48}$$

where

P_s = horizontal effective-force (per unit length) of the cell fill and foundation material within an equivalent cofferdam cell acting on a cell wall

δ = angle of friction between sheeting and soil

and the other quantities retain their previous meanings. All moments are computed with respect to the toe of the cell and are expressed per length of cofferdam.

Considerations in Calculations for Slip Between Fill and Wall

Moment calculations

86. Figure 21a shows the portion of the cofferdam selected as the free body, and Figure 21b shows the forces (per unit length of cofferdam) which are considered in the analysis. The driving forces acting on the body are given separately in an elevation view, Figure 22a. The factor of L has been introduced to convert from force-per-unit length to force. The resisting moment is considered to arise solely from friction forces. The effective forces which produce these friction forces are shown in Figure 22b. The friction forces themselves are illustrated in Figure 22c. Summing moments about point O in Figure 22c yields the resisting moment. Dividing the result through by L to obtain moment-per-length then yields the expression appearing in the numerator of Equation 48. It should be noted that the moment arm for the friction force on the crosswall is b/2 . However, the 2 in the denominator cancels with the factor of 2 introduced to account for the fact that friction acts on both sides of the crosswall.

87. The force P_s is calculated using an earth-pressure coefficient K between $1.2K_a$ and $1.6K_a$. The assumption is made in this failure mode derivation that the inboard sheeting does not slip with respect to the fill and the foundation material.

Alternative failure mode

88. The failure mode discussed thus far in PART VI is based on the assumption that the fill slips with respect to the entire sheet-pile shell of the cell--that is, all the walls act together as a unit. An alternative slip failure mode is conceivable. The crosswall may remain stationary relative to the fill, while the outboard wall alone slips upward (Figure 23). For this

a. Portion of equivalent cofferdam selected for analysis

P_a^i **pressure from overburden**

P_w **pressure from water outside cell**

P_s **pressure from fill acting on outboard wall**

P_s **pressure from fill acting on crosswall**

P_p **pressure from foundation soil and water on inside of cofferdam**
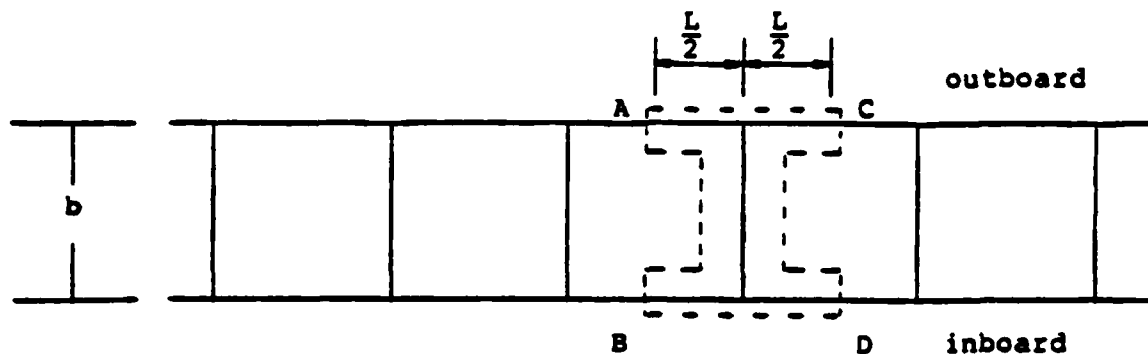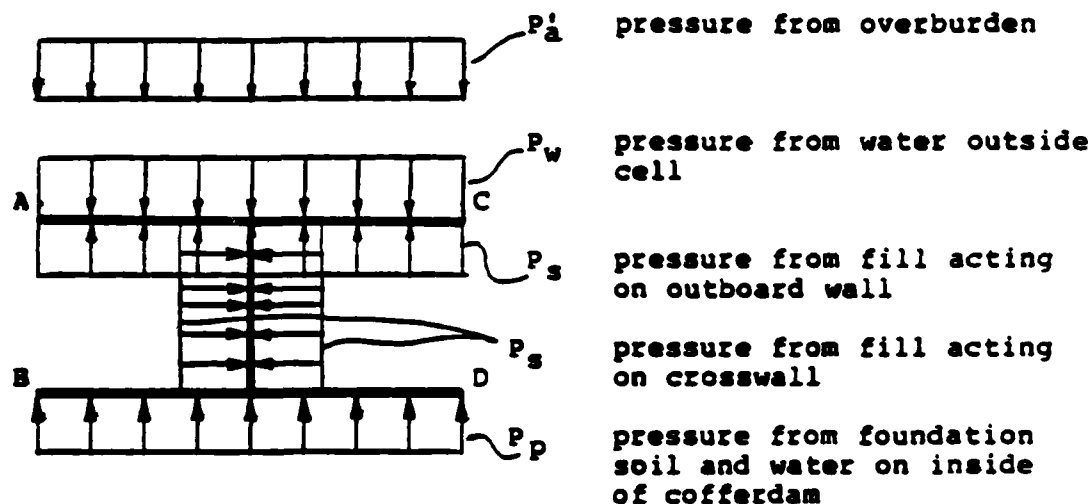
b. Forces considered in analysis

Figure 21. Free body for analysis of slip between fill and sheeting

failure mode, the relevant free body is the portion of the outboard wall shown in Figure 24; the driving forces acting on this free body are shown in Figure 24b, and the resisting forces in Figure 24c. The arrow labeled fT_{cw} in the latter figure represents the interlock-friction force from the crosswall.

89. In attempting to calculate a FS based on Figure 24, a difficulty arises. The ratio of resisting and driving moments depends strongly on the
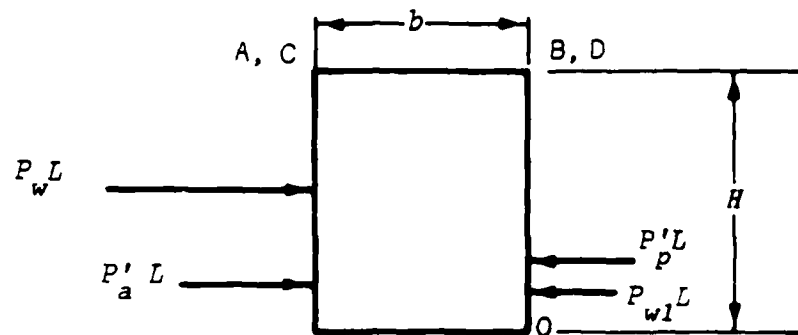
a. Driving force producing overturning moment about O
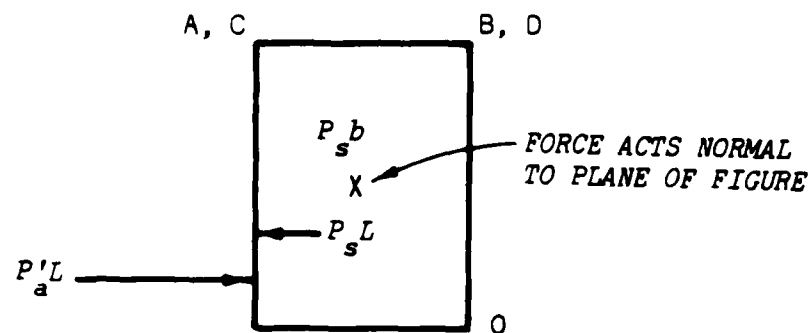
b. Effective forces producing friction forces shown in c
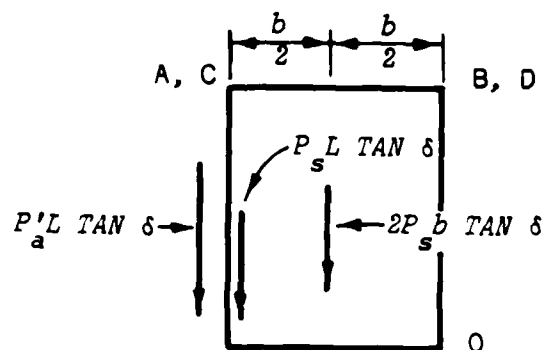
c. Friction forces producing resisting moment about O

Figure 22. Elevation views of free body of Figure 21
resultant forces shown
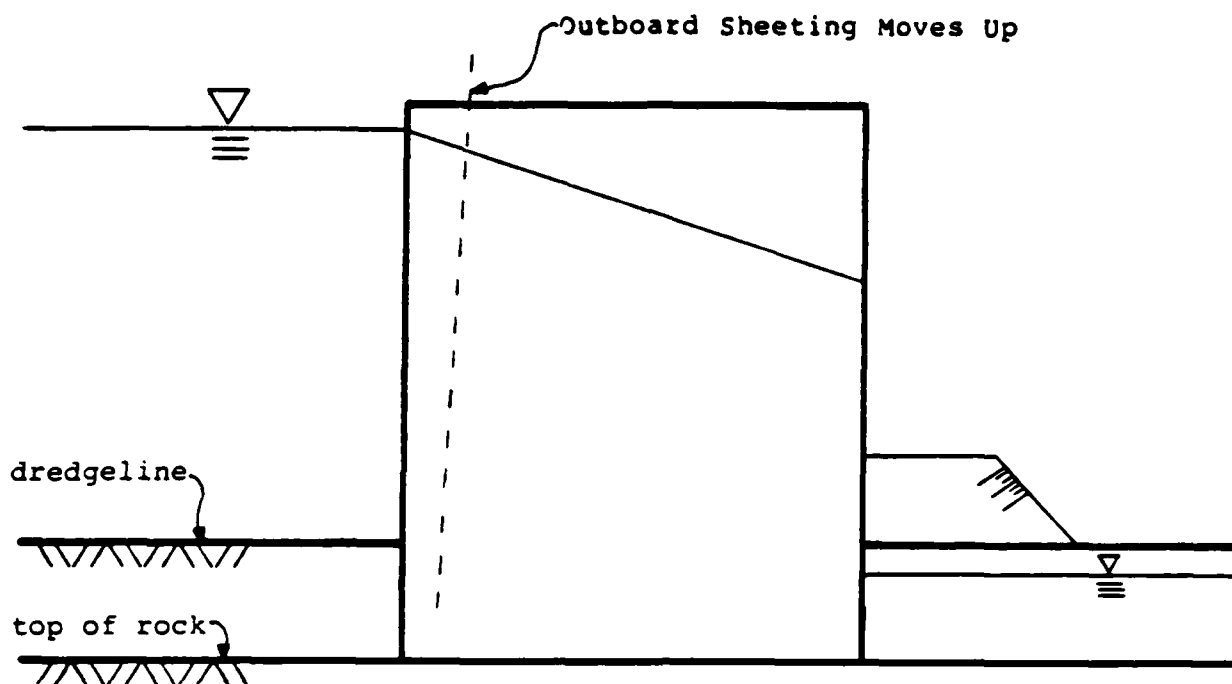
Figure 23. Alternative failure mode in which outboard sheeting
slips relative to fill and rest of piling

point about which the moments are computed, but no point is the obvious
choice. Although it is less apparent, this same comment also applies to the
slip failure mode previously discussed in which the entire sheet-pile shell
acts as a unit. The basic problem is that the design procedure does not
identify the driving forces which actually cause the failure. This matter is
discussed further in the next paragraphs.

Comments on failure mode

90. The error involved in using free bodies which neglect the curvature
of the walls has been discussed in paragraph 18. No reports exist in the
literature of a full-sized cell failing by this mode (ORD 1974; Grayman 1970).
If overburden is present on the rock foundation, the fill cannot escape the
cell until the bottom of the piling is above the dredgeline. Of course, scour
might have removed the overburden.

91. Apparently, the possibility of this failure mode originated from
model studies performed by TVA engineers (TVA 1957). The cell walls in their
models were very stiff. The effect of this excessive stiffness can be seen in
Figure 25, which has been reproduced from the TVA manual (1957). The front
portion of the walls is seen to act like a rigid body. Furthermore, if
bulging were present, the illustrator apparently did not consider it
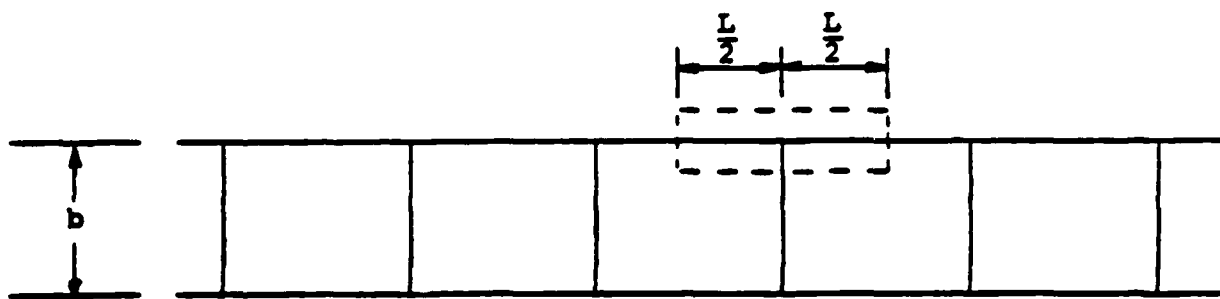
a. Portion of equivalent cofferdam selected for analysis
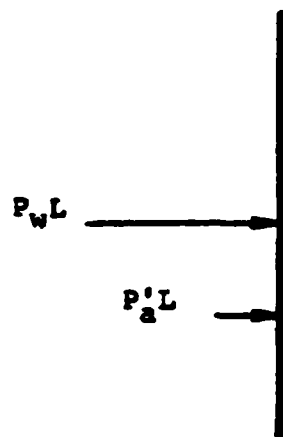
b. Elevation
view of free
body showing
driving forces
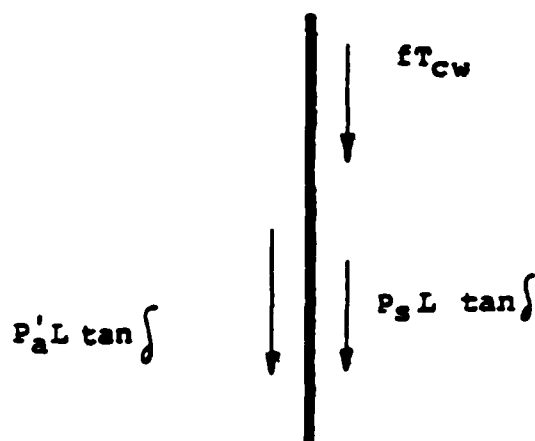
c. Elevation view of free
body showing resisting
forces

Figure 24. Driving and resisting forces acting on outboard sheeting

Figure 25. TVA model test showing
slip between outboard sheets and
fill (TVA Technical Monograph
No. 75)
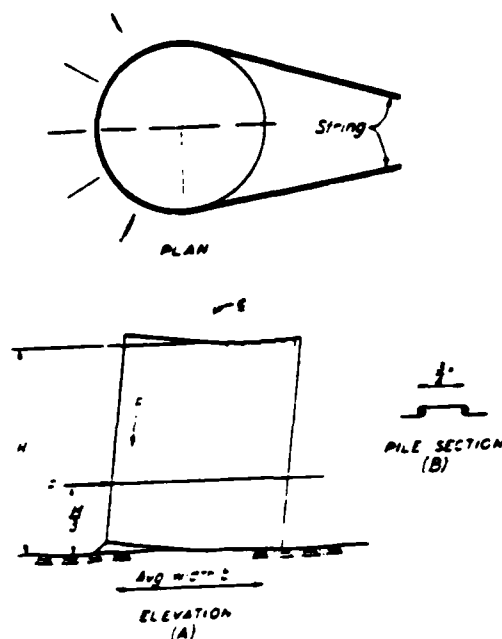
pronounced enough to include in the sketch. These observations raise doubts
as to whether the TVA models were flexible enough to permit the fill to de-
velop its maximum shearing resistance. That is, the failure mode observed in
the TVA experiments may occur only if the cell walls are very rigid. In a
full-sized cell, the large deformations occurring in the fill may lead to a
different failure mode such as a shear failure in the fill before slip between
the fill and the walls can happen.

92. The TVA model studies quite possibly exhibited slip between the
walls and the fill because of the loading device used (a string wrapped around
the cell). The loading device kept the load horizontal and did not allow it
to remain normal to the wall as tilting occurred, as would be the case with
water pressure on the outboard wall. The string may thus have exerted an
upward friction force on the walls which contributed significantly to their
upward motion.

Contribution of Cell Bulging

93. The TVA report and other discussions of slip between the fill
(Jumikis 1971; Lacroix, Esrig, and Lusher 1970) and the wall neglect the con-
tribution of cell bulging toward preventing this failure mode. This effect
may be discussed qualitatively by considering Figure 26, in which is shown a
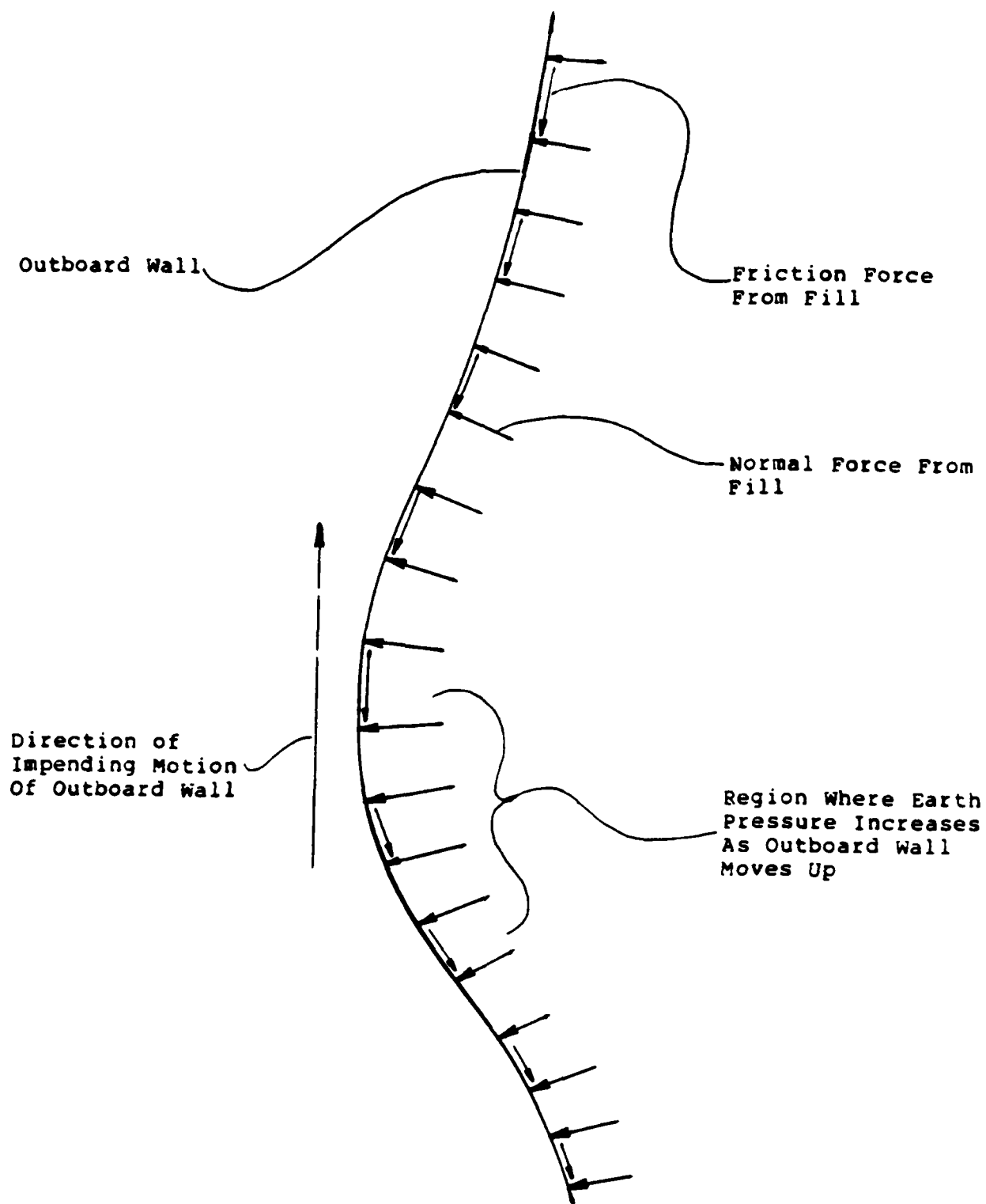
Figure 26. Effect of bulging in preventing slip between wall and fill

portion of a sheet-pile wall near the point of maximum bulging. According to the figure, as the wall tends to move upward, the normal component of the earth pressure acting on the lower side of the bulge tends to increase, and thus, the resistance to slip includes both friction and normal contributions. The derivations of safety factors based on straight rigid walls ignore this effect. Furthermore, the original TVA experiments were based on models with walls so rigid that significant bulging may not have occurred.

94. Since the free body is the entire sheet-pile shell, it appears arbitrary to base the resisting-moment calculation on the friction forces alone; the resisting moment produced by the differential head of water within the cell is ignored. Or, in the case of the alternative free body, Figure 24, the resisting moment of the horizontal force coming from the fill is not considered.

95. The magnitude of the FS is strongly dependent on the choice of the point about which moments are computed. Yet, there is no point for calculating moments which is clearly to be preferred over others. Use of the inboard toe as the reference point would appear to be a natural choice--if it can be assumed that the cell walls act like a rigid shell, rotating in a rigid-body manner about the toe, leaving the fill at rest. This assumption is questionable, however, since such a rotation could only occur if large bending stresses were transmitted by the cell walls. But, as was emphasized in paragraph 8, the cell walls transmit primarily membrane rather than bending stresses. Thus, a rigid-body rotation of the whole shell appears unlikely. On the other hand, if a rigid-body motion of only part of the piling occurs, it is difficult to know beforehand where the center of rotation will be and, thus, at which point moments should be summed.

96. The most important effect likely to cause pullout has been ignored. As the wall tilts toward the interior of the cofferdam, the normal component of the force from the fill inclines slightly upward, and tends to push the wall up, causing it to "ride up" on the fill (Figure 27). The implication of this observation is that a rational design procedure to prevent slip between the sheeting and the fill must be based on an analysis which accounts for the movement of the outboard wall under load. Such an analysis will, unfortunately, be nonlinear since the deflected position of the sheeting is not known beforehand.
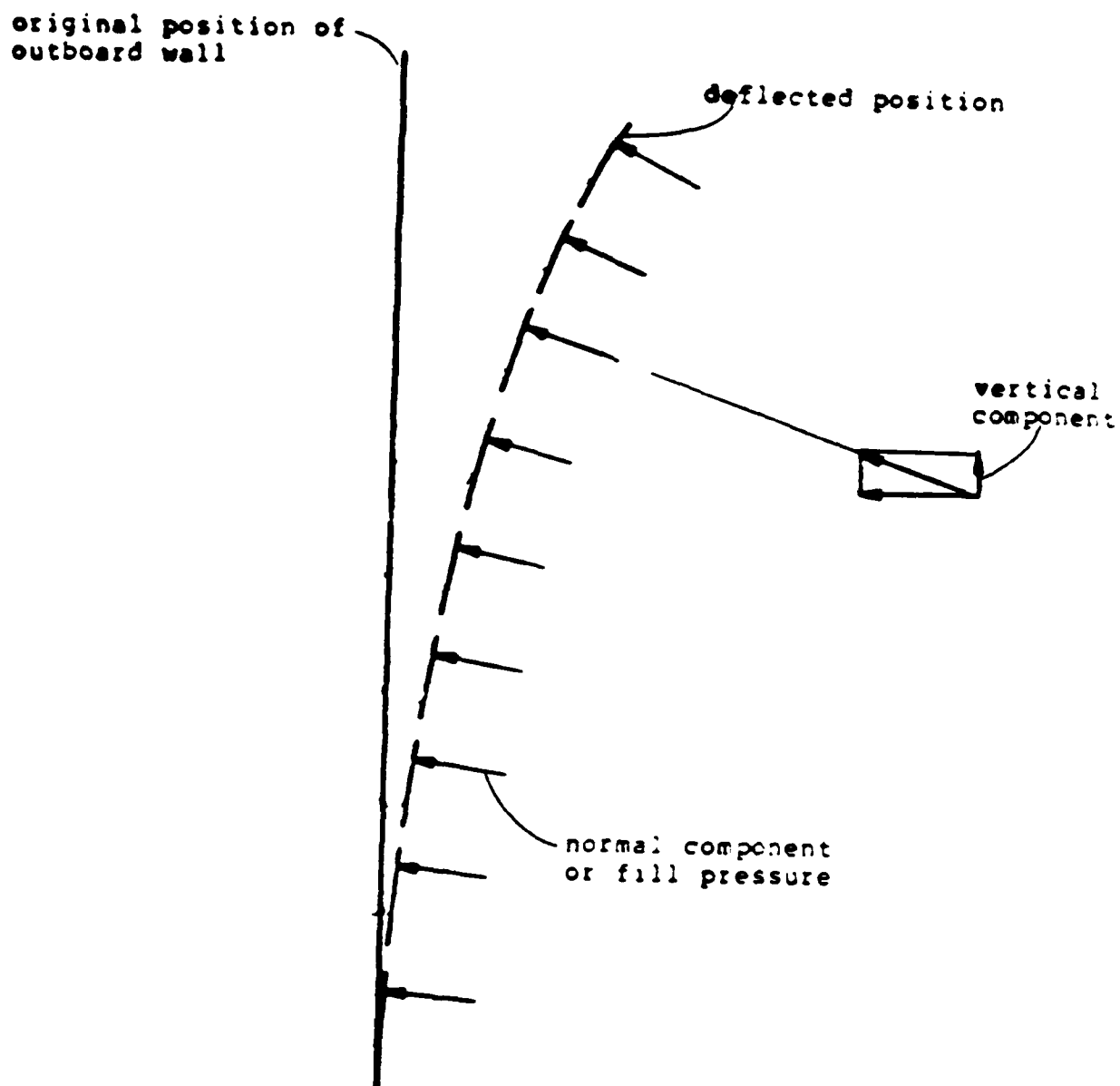
Figure 27.   Development of force component which tends to
produce upward slip of outboard wall

97. The above observations may be summarized as follows:

   a. It is not established that slip between fill and wall can occur in a full-sized cell.

   b. The only model studies in which slip between fill and wall occurred were the TVA studies and serious questions exist about the validity of the TVA models.

   c. The existing design rule is inadequate since it ignores a fundamental mechanism (the change in direction of the force from the fill) by which slip might occur.

   d. To clarify the mechanism by which slip might occur, an analysis should be performed which accounts for rotation of the piling.

PART VII: PULLOUT OF OUTBOARD SHEETING

Rotation about the Toe

98. The lateral forces acting on the cell cause it to rotate about the toe. These forces cause the outboard sheeting and the crosswall to pullout from the foundation. The failure mode resembles that shown in Figure 23, except that it is assumed that the common wall sheeting moves up with the outboard sheeting, and they both slip with respect to the cell fill and foundation material. The inboard sheeting is assumed not to slip with respect to the fill or foundation material and to rotate into the berm as the outboard and common wall sheets pullout.

99. The FS against pullout (DM7 1971; USS 1972) can be written as:

$$FS = \frac{\text{Maximum available resisting moment}}{\text{Driving moment}} = \frac{M_r b}{ML}$$

$$= \frac{b(Q_{uo}L + 0.5Q_{uc}b)}{L\left(\dfrac{P_w H_{wo}}{3} + \dfrac{P_a' d}{3} - P_p' H_p' - \dfrac{P_{wl} H_{wl}}{3}\right)} \tag{49}$$

where

Q_{uo} = ultimate sheet-pile pullout capacity (per unit length of cofferdam) of outboard sheeting

Q_{uc} = ultimate sheet-pile pullout capacity (per unit length) of common wall

H_{wo} = vertical distance from sheet-pile tips to the intersection of water level outside of cofferdam with outboard sheeting (Figure 28b)

H_p' = vertical distance from sheet-pile tips to line of action of P_p' (Figure 28c)

M_r = the resisting moment (per unit length of cofferdam) due to pull out of the equivalent cofferdam outboard and commonwall sheeting

M = the overturning or driving moment (per unit length of cofferdam) due to external forces on the cofferdam

The other quantities retain their previous meanings.
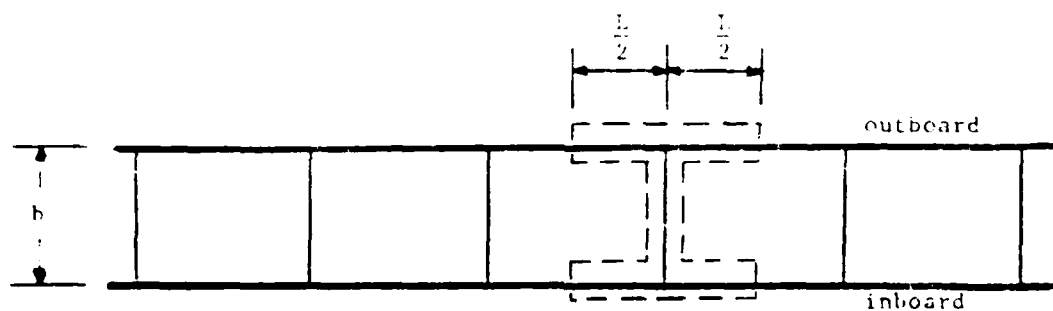
a. Portion of equivalent cofferdam selected for analysis
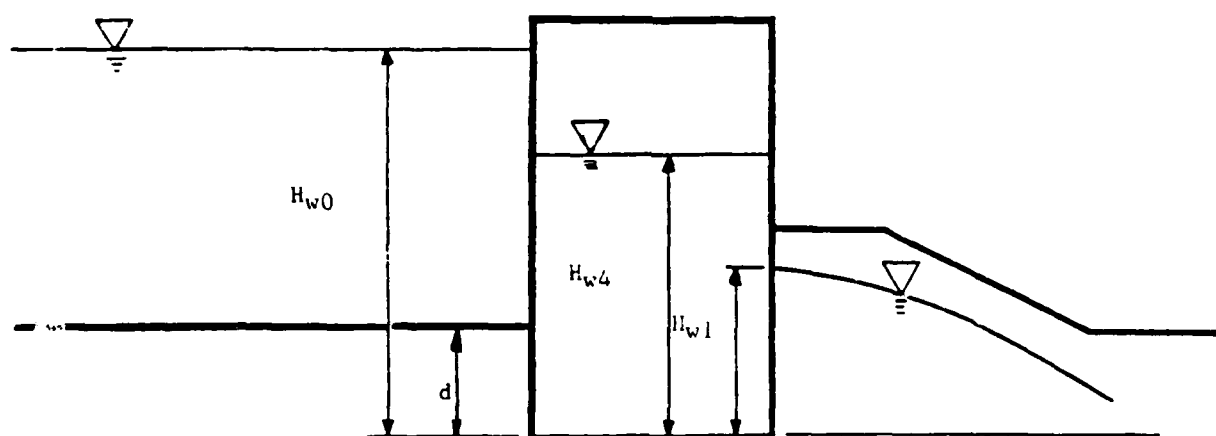
b. Definition of lengths used in pull out of outboard sheeting analysis
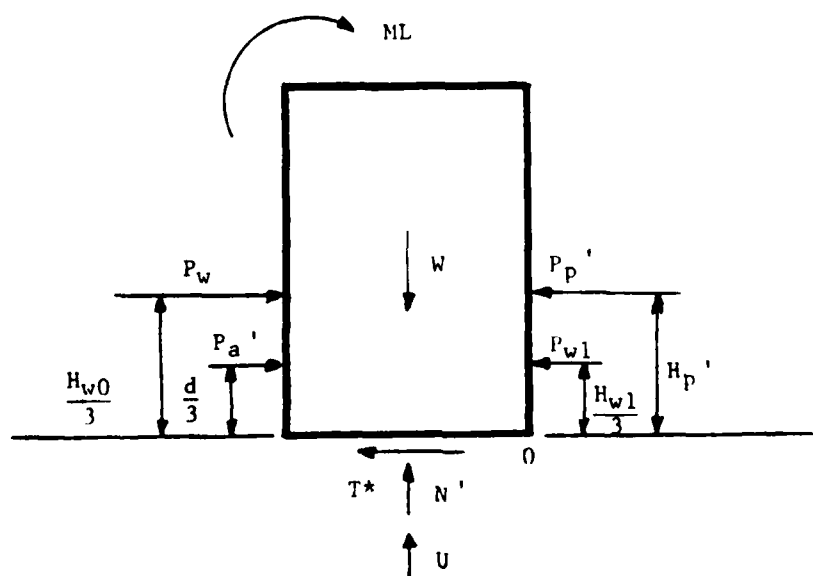
c. External forces considered in calculations
overturning moment

Figure 28. Free-body diagrams for pullout calculations (Continued)

63
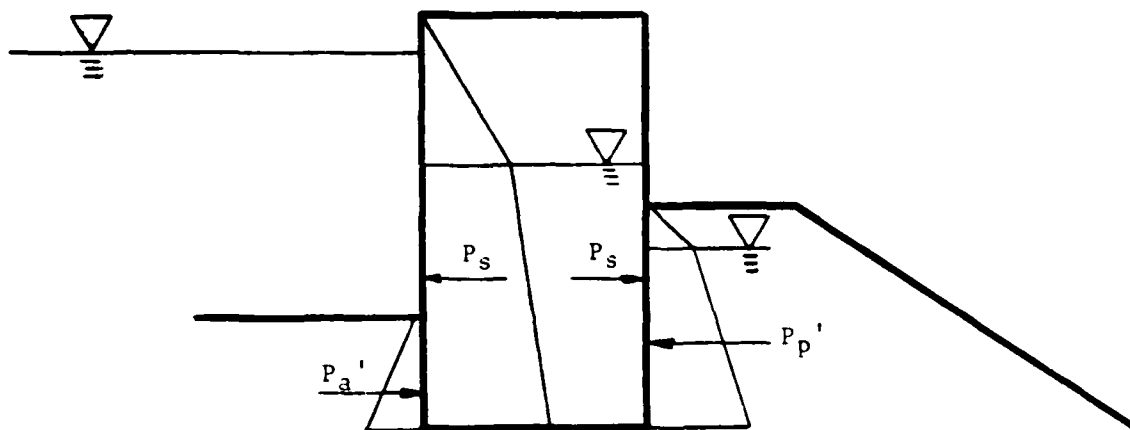
d. Effective soil pressure acting on sheet-pile walls
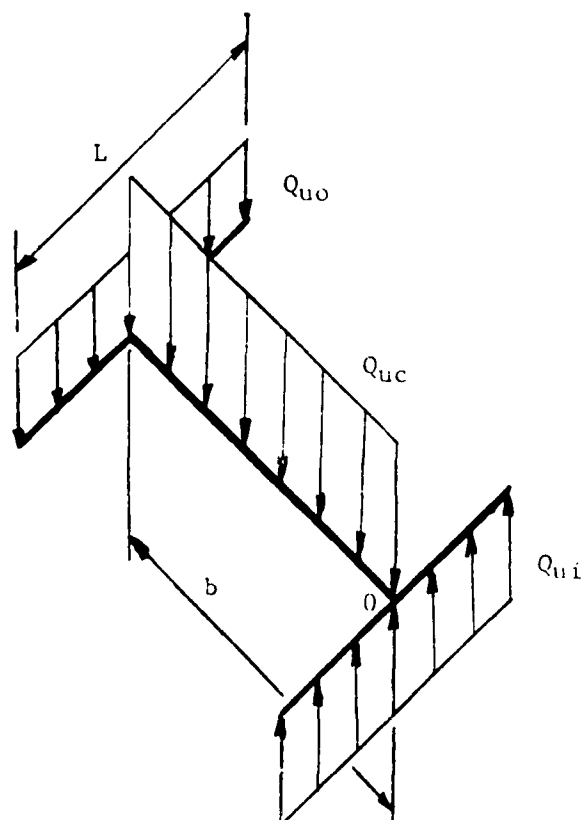
e. Forces resisting pull out of
equivalent cofferdam

Figure 28. (Concluded)

64

Considerations in Calculations for Pullout

Calculation of the driving moment

100. The portion of the cofferdam to be isolated as a free body is
shown in Figure 28a. The vertical distances used in calculating cofferdam
pull out are shown in Figure 28b. The overturning moment ML referred to as
the driving moment (calculated with respect to point 0) is shown acting in
Figure 28c along with the external forces which cause overturning. The forces
shown on Figure 28c and not previously defined are:

   U = resultant uplift force due to water pressure acting on the base of
   the cofferdam (per unit length of cofferdam)

   N' = resultant effective soil force acting on the base of the cofferdam
   (per unit length of cofferdam)

   T* = horizontal shear force on base of cofferdam (per unit length of
   cofferdam)

101. The assumption is made that the weight of the contents of the cell
(W), the resultant of the uplift force (U) and effective soil force (N') act
through the same point. This assumption allows the W , N' , and U terms
to be neglected when summing moments about point 0 . From horizontal
equilibrium the following equation is obtained:

$$P_w + P_a' = P_p' + P_{wl} + T*$$

Rearranging terms yields the equation:

$$P_p' = P_w + P_a' - P_{wl} - T* \tag{50}$$

Equation 50 must always be satisfied. The terms P_w , P_a' , and P_{wl} are
easily calculated (see Part IV). Let P_p^* be the horizontal effective-force
(per unit length of cofferdam) acting on the inner cofferdam wall when the
berm and foundation exert full passive earth pressure against the cofferdam.
It is assumed that P_p' is the smaller of P_p^* and the result of Equation 50
with T* taken as zero. When P_p' equals P_p^* and is less than Equation 50
with T* taken as zero, then T* is increased to maintain horizontal
equilibrium. Since T* passes through point 0 , it does not contribute to
the overturning moment. The justification for the above assumptions is that
for the outer and common wall to pullout, the inner wall will have to rotate a

large amount, mobilizing something approaching full passive pressure in the berm and foundation. At the same time the passive pressure mobilized must satisfy horizontal equilibrium as given by Equation 50. Note that T^* must be less than N' tan ϕ to prevent sliding along the base of the cell.

Calculation of resisting moment

102. The pull-out capacity Q_u of a pile depends on the skin friction arising from the material into which the pile is embedded and the skin friction between the cell fill and the sheet-piling. Figure 28d shows the earth pressure forces acting on the equivalent cofferdam walls. The force not previously defined is:

P_s = horizontal effective-force (per unit length) of the cell fill and foundation material within an equivalent cofferdam cell acting on a cell wall

The force P_s is calculated using an earth pressure coefficient K between $1.2K_a$ and $1.6K_a$. It should be noted that the force P_s acts on both sides of the common wall. The forces resisting pullout of the equivalent cofferdam section and being analyzed are shown in Figure 28e. The force not previously defined is

Q_{ui} = ultimate sheet-pile capacity (per unit length of cofferdam) of the inboard sheeting

The ultimate sheet-pile pullout capacities are computed as follows:

$$Q_{uo} = (P_a' + P_s) \tan \delta \tag{51}$$

$$Q_{uc} = 2P_s \tan \delta \tag{52}$$

103. It should be noted that the value of Q_{ui} is not needed to calculate the resisting moment about point 0 in Figure 28e because it passes through point 0. In developing Equation 49, the assumption is made in calculating the resisting moment that there is no interlock slip. It is also assumed that the outboard and common wall sheeting slip with respect to the cell fill in the analysis. If the assumption is made that the fill moves up with the cell during pull out then the method of calculating the resisting moment should be revised to take into account the weight of the fill. However, it seems unlikely that the fill would move up with the cell during pullout.

66

Comments on the design
procedure for preventing pull out

104. No full-sized cell nor model-test failures by this mode have been
reported in the literature.

PART VIII: PENETRATION OF THE INBOARD SHEETING (PLUNGING)

Effects of Friction Downdrag

105. The friction force from the fill drives the inboard sheeting further downward into the foundation, leading to tilting and also possible loss of fill from the top of the cell (Figure 29).
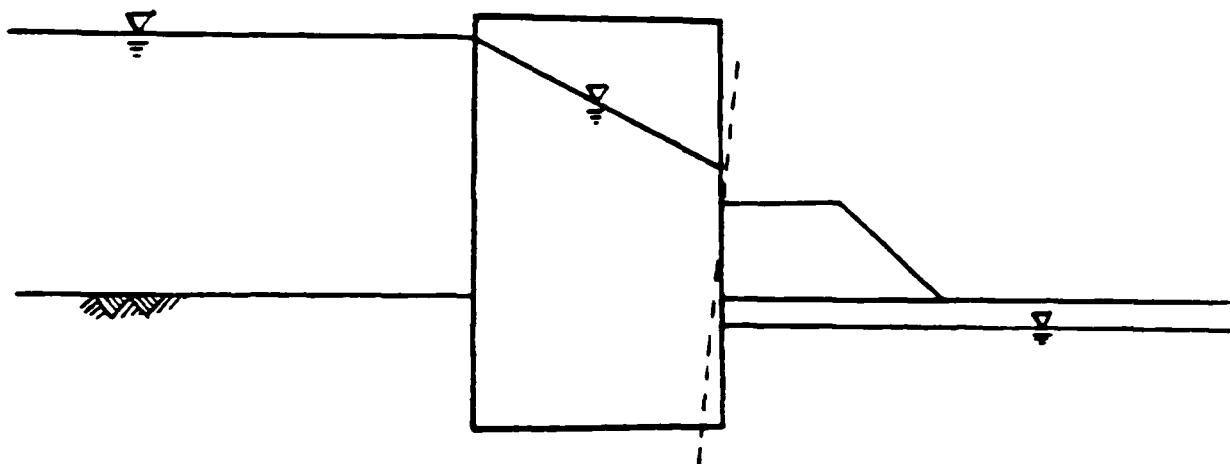
Figure 29.   Failure by excessive penetration of
inboard sheeting (plunging)

106. The FS against failure by penetration of the inboard sheeting (Lacroix, Esrig, and Lusher 1970; USS 1972) can be expressed as:

$$FS = \frac{\text{Maximum available resisting force}}{\text{Driving force}}$$

$$= \frac{(P'_p + P'_s) \tan (\cdot)}{P'_d \tan (\cdot)} \tag{53}$$

in which (Figure 30) P'_s is the horizontal effective force of the foundation soil acting on the interior of the inboard sheeting below the dredgeline. The other quantities retain their previous meanings. The forces are calculated for a unit length of cofferdam. Penetration is of concern for cells founded on deep soil foundations.

Considerations in Calculations for Penetration

107. The free body used in the factor of safety calculation is a portion of the inboard wall, as shown in Figure 30. The FS is based on a simple comparison of the downward friction force from the fill and the upward friction forces from the foundation soil.

108. The calculation of P_d' was described in paragraph 58. Lacroix, Esrig, and Lusher (1970) recommend using a value of $K = 0.4$ in this calculation. The calculation of P_p' was described in paragraphs 54 and 55 with exception that P_p' should not be less than the at-rest earth pressure. The calculation of P_s' requires the construction of a flow net to account for the effects of the hydraulic gradient (DM7 1971).

Comments on the Design Procedure for Preventing Penetration

109. Concern for preventing penetration apparently originated from the Terzaghi (1945) paper on cofferdams, in which he expressed the view that the friction force from the inboard wall acting on the fill contributed significantly to the overall resisting moment of the cell (Terzaghi 1945). Thus, assessing the wall's resistance to penetration was considered important in establishing the stability of the entire cell itself. Terzaghi was led to this view by his assumptions about the pressure distribution from the foundation acting upward on the base of the cell and by what he admitted was a "very crude approximation": the assumption that the lateral earth-pressure coefficient has the same value at all points in the fill. From their model studies, Schroeder and Maitland (1979) concluded that K does in fact vary significantly within the fill. This observation plus the additional observation that no failures by the penetration mode have been reported in model studies or in the field indicate that the need to design against sheet-pile penetration cannot be considered well-established.

110. The force $P_d' \tan (\phi)$ which causes the inboard wall to be driven downward is caused by settlement of the cell fill. As the inboard wall is driven downward into the foundation, the outboard wall and crosswall remaining stationary, friction forces must act in the interlock connecting the inboard wall and the crosswall. Since these forces aid the inboard wall in resisting
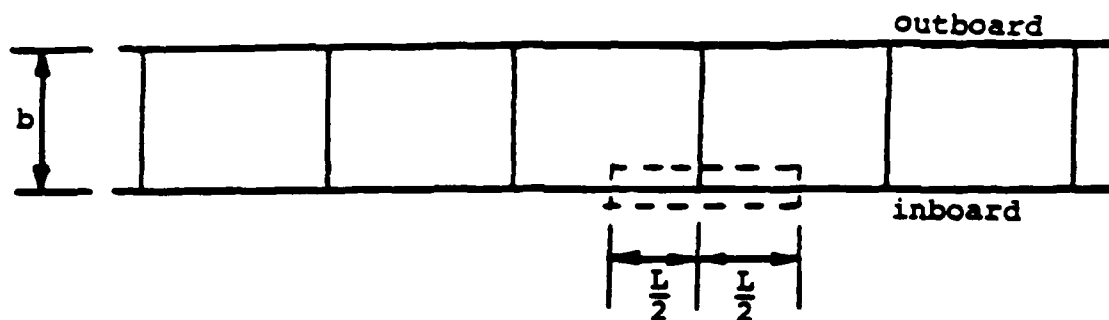
a. Portion of equivalent cofferdam selected for analysis
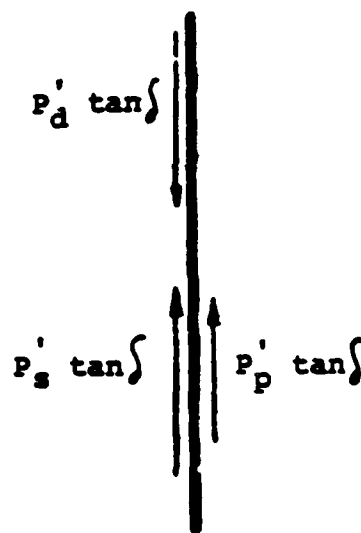
b. Elevation view
of free body show-
ing driving and
resisting forces
(per unit length
of cofferdam)

Figure 30. Free-body diagrams for penetration calculations

70

downward movement, neglecting them, as is done in the expression for the FS ,
is conservative.

111. As was discussed in paragraph 93, and shown in Figure 26, cell
bulging of the outboard wall tends to decrease the possibility of failure by
slip occurring between the fill and the sheeting. This is true since the
pressure on the sheeting from the fill in the bulge acts primarily in the
direction of the resisting forces, or downward. However, bulging of the in-
board wall tends to increase the possibility of failure by penetration because
the driving direction is downward in this case. A nonlinear analysis would be
required to evaluate this phenomenon, due to the unpredictable magnitude and
location of the bulging.

112. Based on model studies and field observations, Schroeder and Mait-
land (1979) concluded that the ability of the sheet-pile walls to mobilize
passive resistance is limited to the region above the plane of fixity. If
this recommendation is accepted, the at-rest value of the lateral earth-
pressure coefficient should be used to calculate effective forces acting below
the plane of fixity.

PART IX: BEARING FAILURE OF FOUNDATION

Effects of Lateral Forces on Bearing Capacity

113. Lateral forces acting on the cell combine with the weight of the
cell to produce an eccentric bearing force which exceeds the bearing capacity
of the foundation. Foundation material is pushed downward and out from under-
neath the cell (Figure 31).
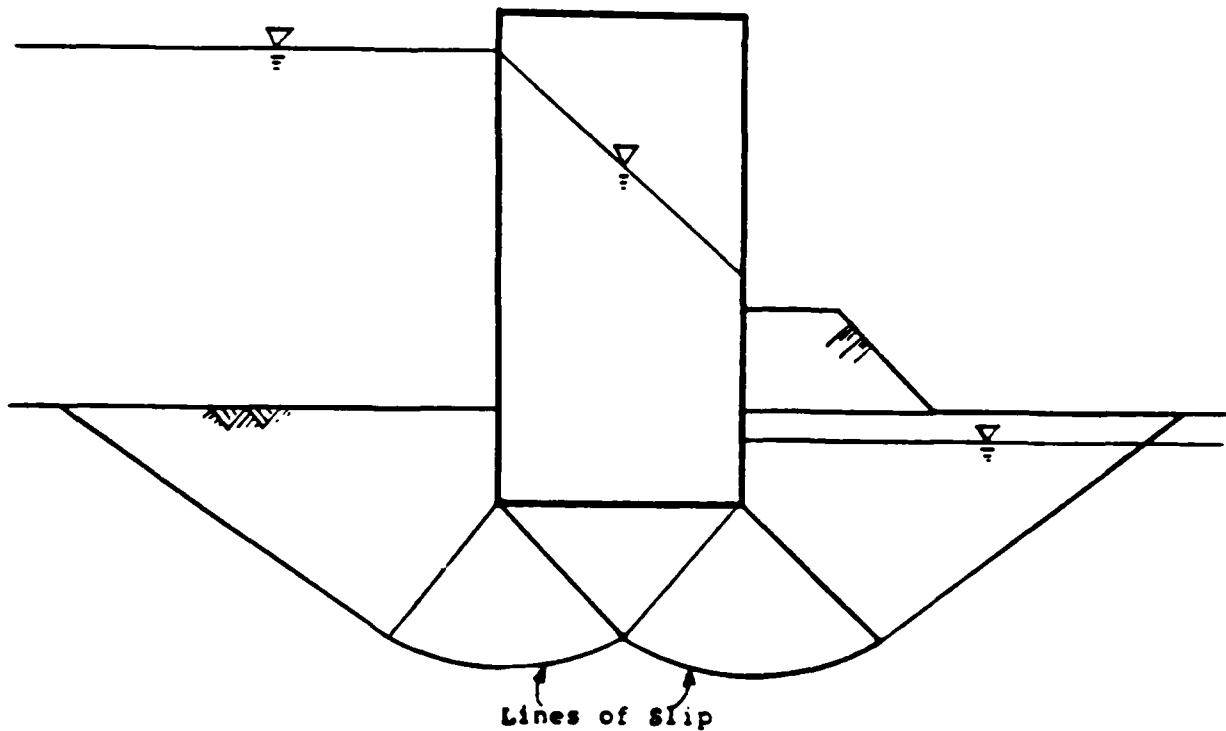
Figure 31. Bearing failure of foundation

114. The FS against bearing failure of foundation is shown below as:

$$FS = \frac{\text{Ultimate bearing capacity}}{\text{Effective bearing pressure}}$$

$$= \frac{q_{ult}}{q_{eff}} \tag{54}$$

where

q_{ult} = ultimate bearing capacity, calculated by dividing the effective width of the cofferdam into the total vertical load for which the foundation has the capacity

q_{eff} = effective bearing pressure, calculated by dividing the effective width into the resultant vertical force acting on the foundation

The cofferdam is analyzed as a strip footing of width b .

Considerations in Calculations for Avoiding
Bearing Failure of Foundation

Use of CBEAR

115. A comprehensive discussion of the theory and the calculations required for avoiding bearing failure is given in the user's guide to the CBEAR computer program (Mosher and Pace 1982), and thus will not be given here. Instead, the following remarks will be confined to indicating how the bearing-capacity design problem is formulated for the special case of a cellular cofferdam.

Cell foundation action

116. Because both vertical and horizontal forces act on the cell, the resultant force from the cell acting on the foundation is eccentric and inclined, that is, it does not act through the center of the base. Figure 32a shows a typical cell and foundation, while Figure 32b shows the isolated cell and the external forces acting on it. The resultant of these forces is shown acting on the foundation in Figure 32c at a distance e from the center of the cell. The magnitude of the vertical component of the resultant and the value of the eccentricity e are required if a bearing capacity analysis is to be performed.

117. The eccentricity is used to reduce the width b of the cofferdam to its effective value:

$$B' = b - 2e \tag{55}$$

118. The calculations should be based on all applicable water forces and the weights of fill and foundation soil.
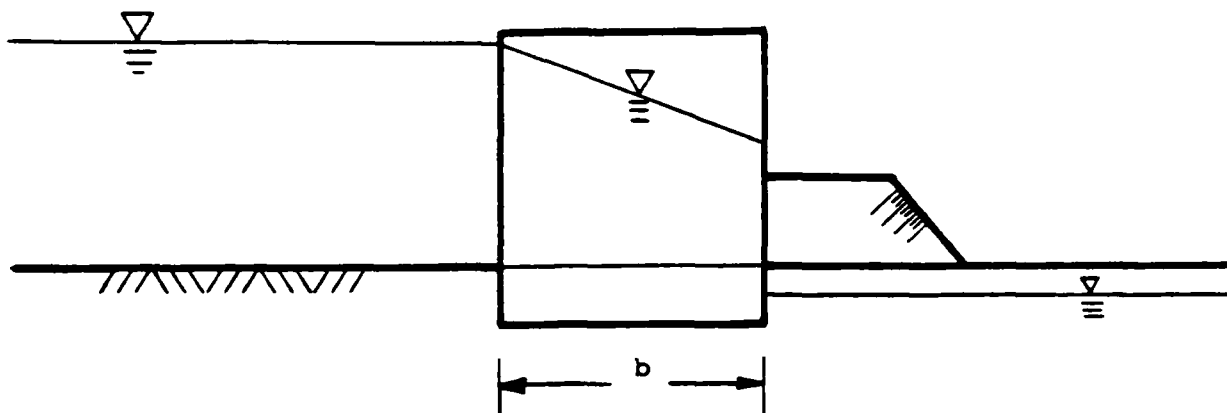
a. Cell founded on soil
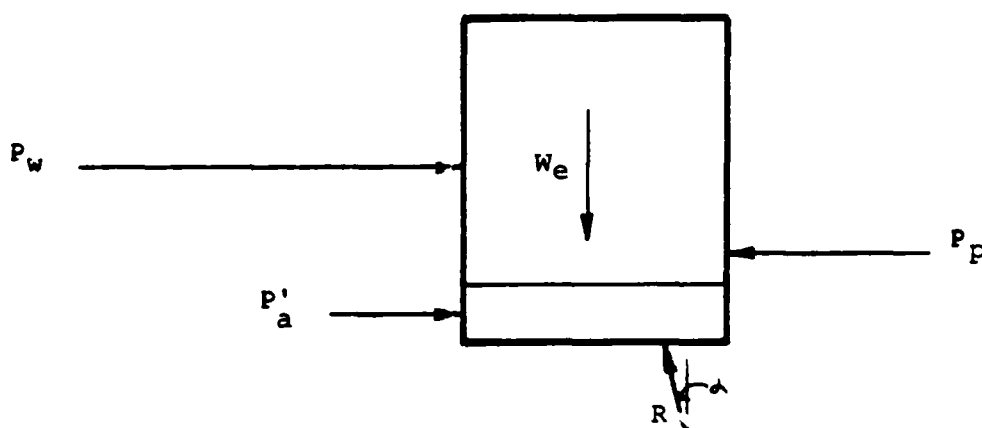
b. External forces acting on cell
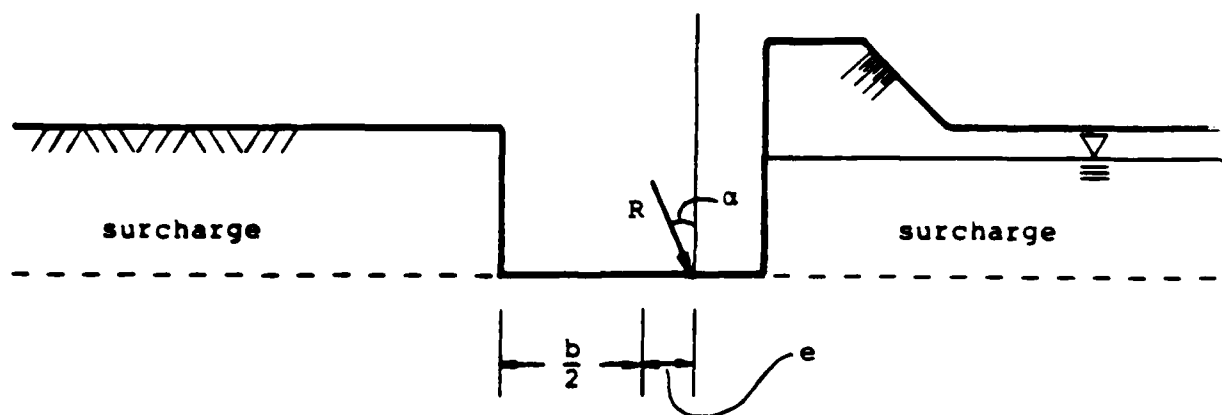
c. Force bearing on foundation

Figure 32. Calculation of bearing force R

74

PART X: SLIDING INSTABILITY

Effects of Lateral Force on Sliding

119. The horizontal forces acting on the cell cause it to slide on its base, or together with a portion of the foundation underneath the cell (Figure 33).
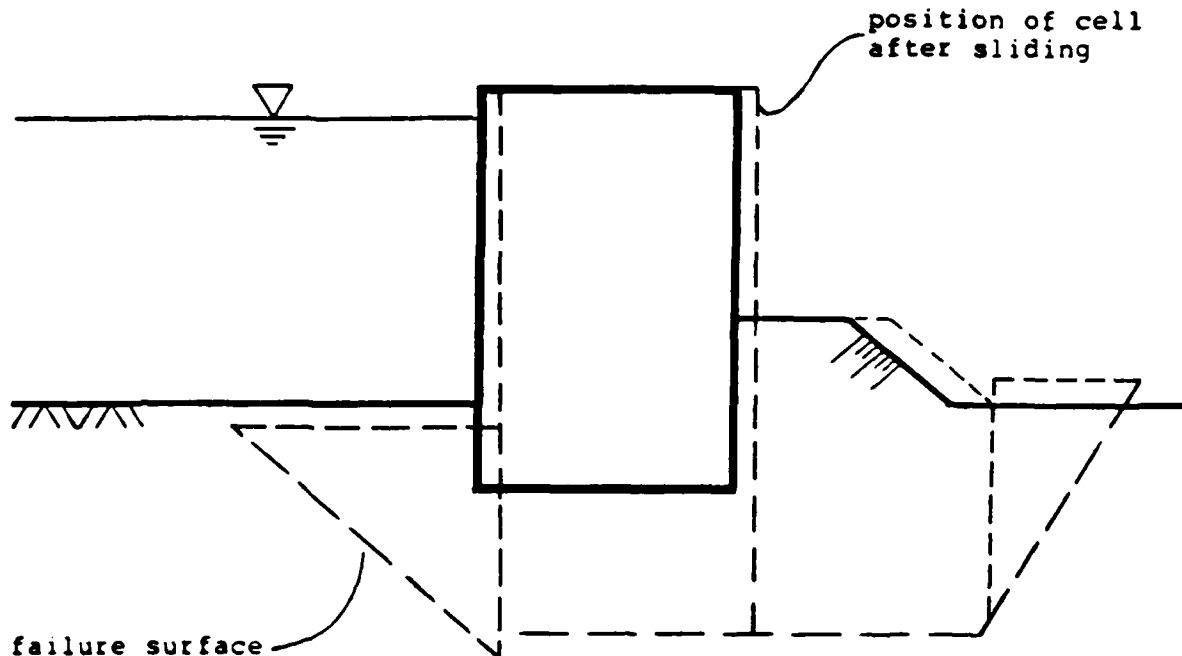
Figure 33. Failure by sliding instability

120. The FS against sliding instability for a cofferdam founded on rock, is computed from the equation:

$$FS = \frac{\text{Maximum available resisting force}}{\text{Driving force}}$$

$$= \frac{W_e f^* + P_{min}}{P_w + P'_a} \tag{56}$$

where

f^* = coefficient of friction of fill on rock

P_{min} = the smaller of (1) $P_p^* + P_{w1}$ or (2) the friction force acting from the rock on the bottom of the berm

75

the other quantities retain their previous meanings. The *sliding-stability of*
a cofferdam founded on <u>soil</u> is analyzed by the methods of wedge used for slope
stability. A FS is computed from the equation

$$FS = min \; \frac{\text{Maximum available shear resistance}}{\text{Shear force required to maintain equilibrium}}$$

in which the minimum is taken over all possible failure surfaces, and "shear"
refers to shear forces acting on the failure surface. To obtain the FS for
a given failure surface, a limit-equilibrium analysis is performed similar to
that performed for slope stability.

Considerations in Calculations for Sliding Instability

Rock foundation

121. A common recommendation in the literature (Lacroix, Esrig, and
Lusher 1970; USS 1972; Belz 1970; TVA 1957) is to take the coefficient of
friction f^* equal to $\tan (\phi)$ unless the rock surface is smooth, in which
case a value of 0.5 is advised.

Soil foundation

122. The wedge method is recommended for analyzing the slope-stability
problem corresponding to a cellular cofferdam founded on soil. Since a com-
prehensive discussion of the theory and the calculations required for applying
the wedge method is given in ETL 1110-2-256 and EM 1110-2-1902, it will not be
given here. Instead, the following remarks will be confined to indicating how
the wedge method is applied to the special case of a cellular cofferdam. To
begin the analysis, a set of surfaces in the foundation are chosen which are
candidates for the actual failure surface. Figure 34 shows a reasonable
choice for a typical cell with berm. The wedge method is then used to compute
a FS for each trial surface in turn. For example, in the figure a FS is
computed for surface 9-4-5-8, then for 9-4-5-7, for 9-4-5-6, and so on until
all combinations of surfaces have been considered. (Each trial failure sur-
face must include the surface 4-5 bounding the structural wedge.) The minimum
FS found by this procedure is the FS against sliding for the cell.
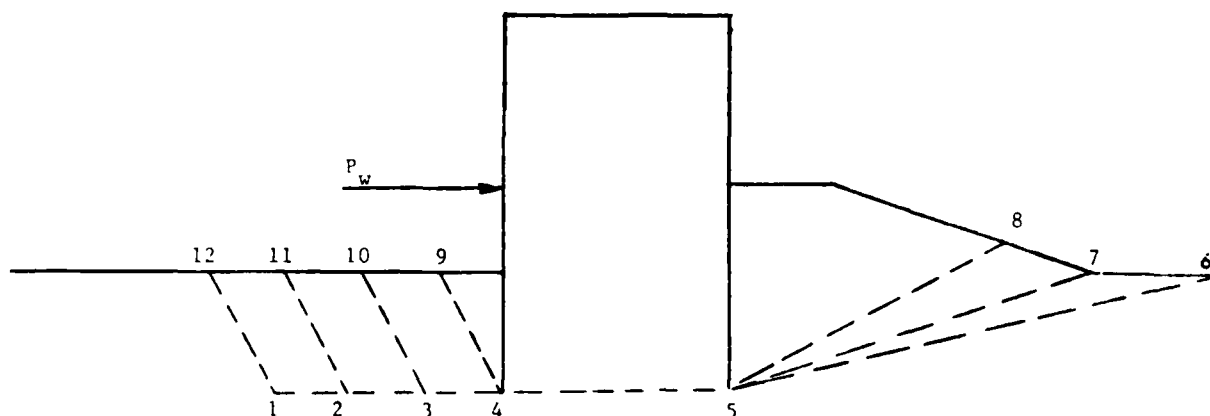
Figure 34. Trial failure surfaces for application of wedge method

Comments on failure by sliding

123. For a cofferdam founded on a rock foundation, an additional degree of conservatism is implicit in the FS expression, Equation 56, since the resisting force produced by the slight penetration of the sheet piles into the rock is neglected. Even if the rock surface is hard and penetration is very small, natural irregularities are usually present which contribute towards the resistance to sliding.

124. A conservative assumption which may be made is that only normal forces (no friction forces) are transmitted across the vertical boundaries of the wedges. In situations where sliding instability appears to be a significant possibility, a refined analysis may be considered which includes shear on all vertical boundaries.

125. The earth pressures on the cell walls computed by the wedge method are not necessarily good approximations to the actual earth pressures, since the former pressures may correspond to a relatively high FS against sliding.

126. If a weak stratum is present in the foundation soil, it should be included in the trial failure surfaces.

127. The wedge method gives an upper bound to the FS . Thus, there is no guarantee that the lowest FS has been found by the procedure described above. The reliability of the procedure depends on the analyst's experience and ability in predicting failure surfaces.

PART XI: SLIP ON CIRCULAR FAILURE SURFACE (HANSEN'S METHOD)

Alternative Mode of Failure

128. A circular failure surface forms between the tips of the outboard and inboard walls as shown in Figure 35. That portion of the cell above the surface rotates as a rigid body about the center of the circle. Sliding occurs between the fill and the walls and between some of the sheets in the crosswall (Lacroix, Esrig, and Lusher 1970; Ovesen 1962).
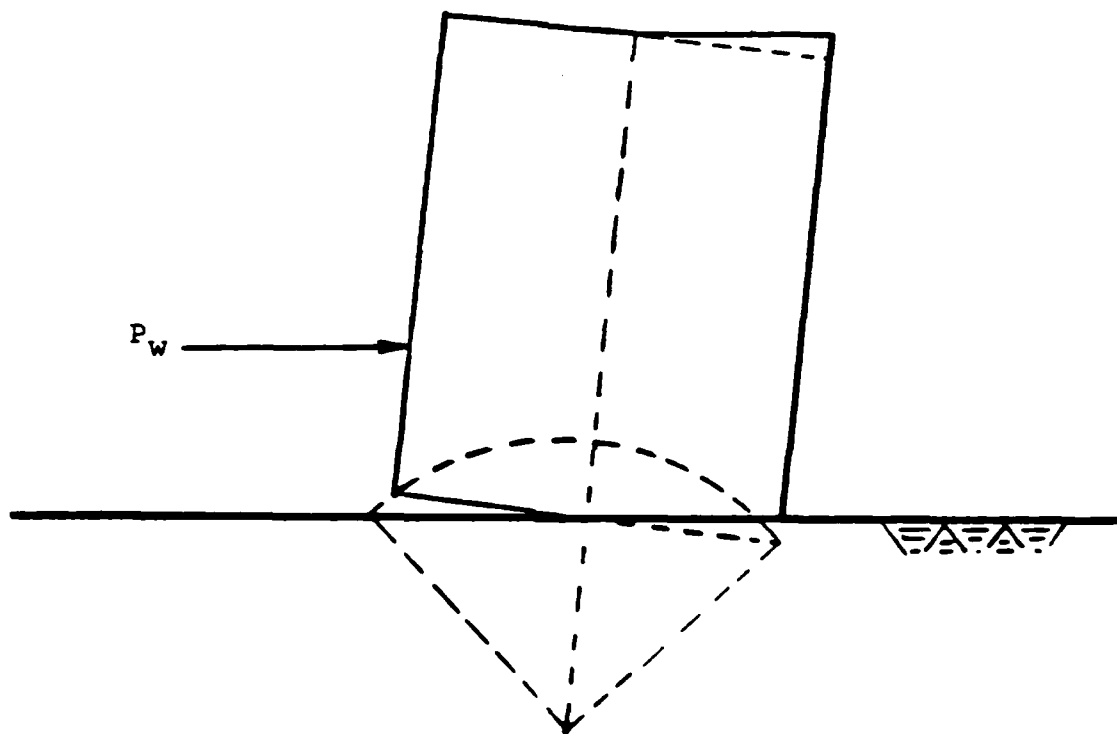
Figure 35. Failure by sliding on a circular rupture
surface (rock foundation)

129. The FS against slip on circular failure surface can be computed from the equation:

$$FS = \frac{\text{Maximum available resisting moment}}{\text{Overturning moment}}$$

$$= \frac{M_W}{M'} \qquad (57)$$

78

where

M_W = moment of effective weight of fill above the failure surface

M' = moment caused by the driving forces (Figure 11)

The moments are computed with respect to the center of the failure circle.

Considerations in Calculations for Hansen's Method

130. Hansen proposed two different methods for evaluating the stability of a cofferdam cell: the equilibrium method and the extreme method. The calculations required when using the equilibrium method are complicated. Fortunately, essentially the same results may be obtained by use of the extreme method, which is computationally simpler.

131. The extreme method is based on approximating the failure circle by a logarithmic spiral which obeys the equation

$$r = r_A e^{\theta \tan (\phi)} \tag{58}$$

where (Figure 36)

r = radial distance from point 0

θ = angle measured counterclockwise from line OA

r_A = radius corresponding to $\theta = 0$

e = base of natural logarithms

ϕ = angle of internal friction of fill

132. The logarithmic spiral defined by Equation 58 has the property that the resultant of the friction and normal force at each point on the rupture surface defined by the spiral passes through the pole of the spiral. Thus, if the moments acting on the free body are computed with respect to the pole, the resultant force acting on the rupture surface will not appear in the moment expression.

133. The analysis procedure is now straightforward. A sketch such as Figure 36 is made to scale, and a logarithmic spiral is plotted which passes through the inboard and outboard tips of the walls, but is otherwise arbitrary. The moments M_W and M' are computed (with respect to the pole of the spiral) and the FS evaluated from Equation 57. In evaluating M_W , which depends on the effective weight W' of the fill above the failure surface,
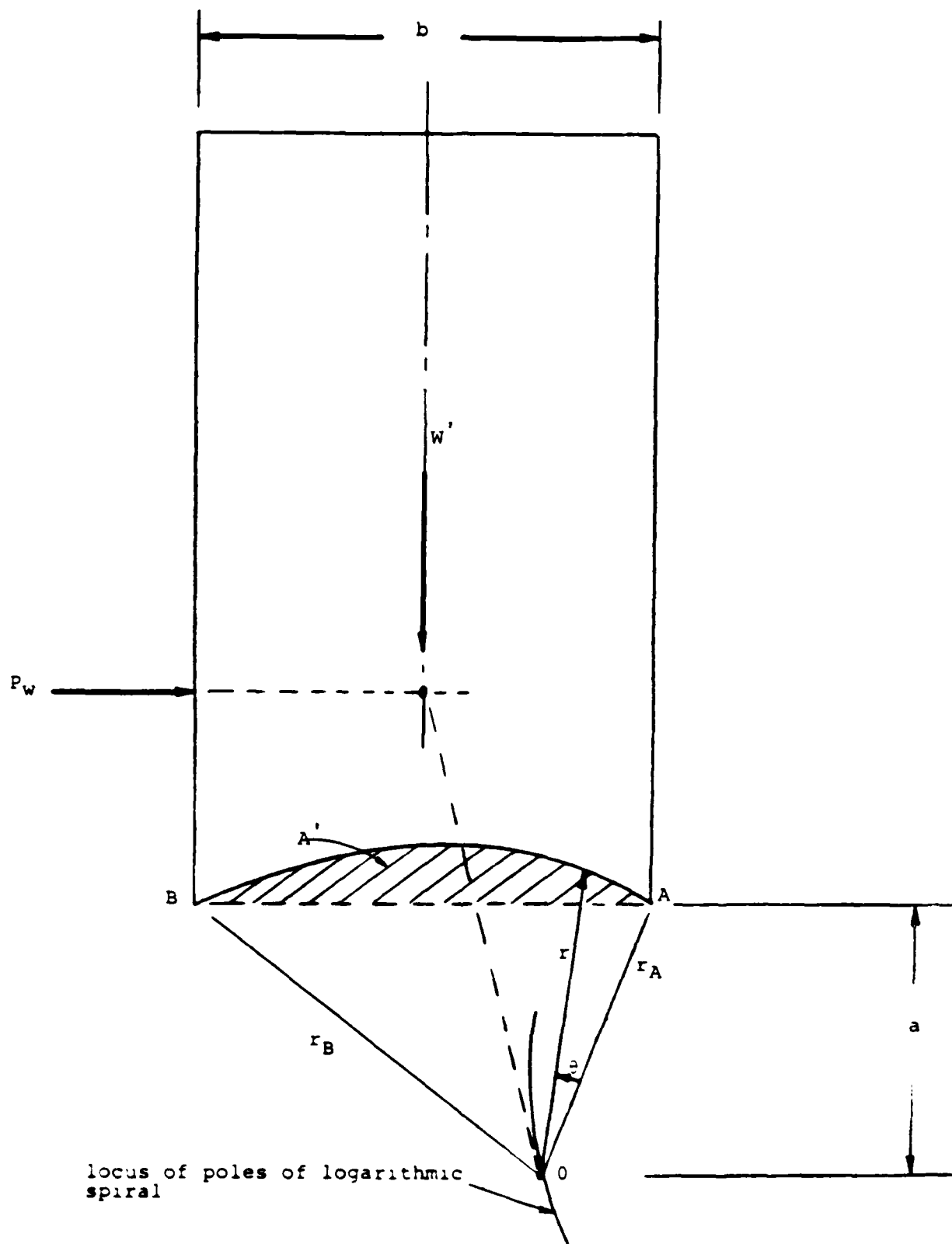
Figure 36. Free body for Hansen's method, rock foundation

work can be saved by applying the following equation for the cross-hatched area A' shown in Figure 36:

$$A' = \frac{(r_B)^2 - (r_A)^2}{4 \tan (\phi)} - \frac{ab}{2} \tag{59}$$

where

r_B = distance from pole to tip of outboard sheet

a = vertical distance from pole to base of cell

134. The pole for the most critical failure spiral may be found by repeating the above procedure with many different assumed spirals, and searching for the pole that yields the minimum value for the FS . A more direct approach is to make use of the fact that the pole of the failure spiral is on the locus of poles of those logarithmic spirals which pass through the tips of the sheet piles. The pole of the failure spiral can be found by drawing the tangent to this locus from the intersection of the force W' and the resultant of the driving forces (Figure 36).

Failure Modes for Cofferdams on Sand

135. Hansen hypothesized that two distinct failure modes are present for cofferdams on sand and must be investigated, an "X-mode" and an "A-mode" (Figure 37). Furthermore, the lateral forces E_a and E_p from the foundation soil must be taken into account in evaluating the moments appearing in the FS equation. Whether these additional moment contributions are to be added to the driving or to the resisting moment must be determined for each particular case. Ovesen (1962) and Hansen (1957) present tables and charts for calculating the lateral forces. If the sheet piles are embedded to great depth in the foundation, then tne possibility must be considered that plastic hinges form in the walls (Hansen 1957).

Comments on Hansen's Method

136. The method is based on a highly theoretical approach to soil mechanics. The following assumptions are made:

<u>a</u>. The fill is homogeneous, isotropic, cohesionless, obeys
    Coulomb's failure law, and follows the constitutive law for a
    rigid-plastic material.

<u>b</u>. In the rupture state, the dilatation is constant (same value
    of the ratio of volumetric-strain to maximum shear
    everywhere).

<u>c</u>. The axes of principal stress and principal deformation
    coincide.
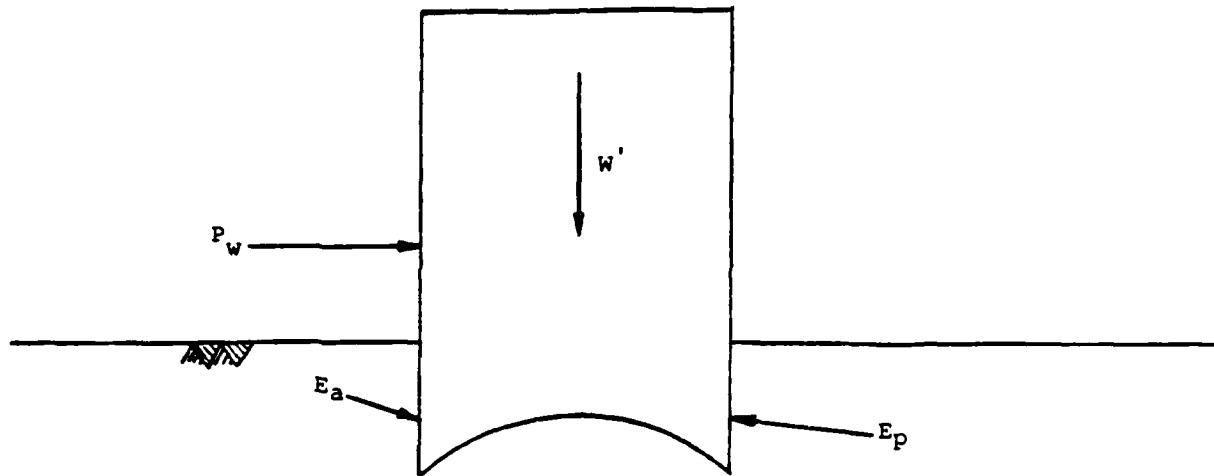
a. X-failure mode
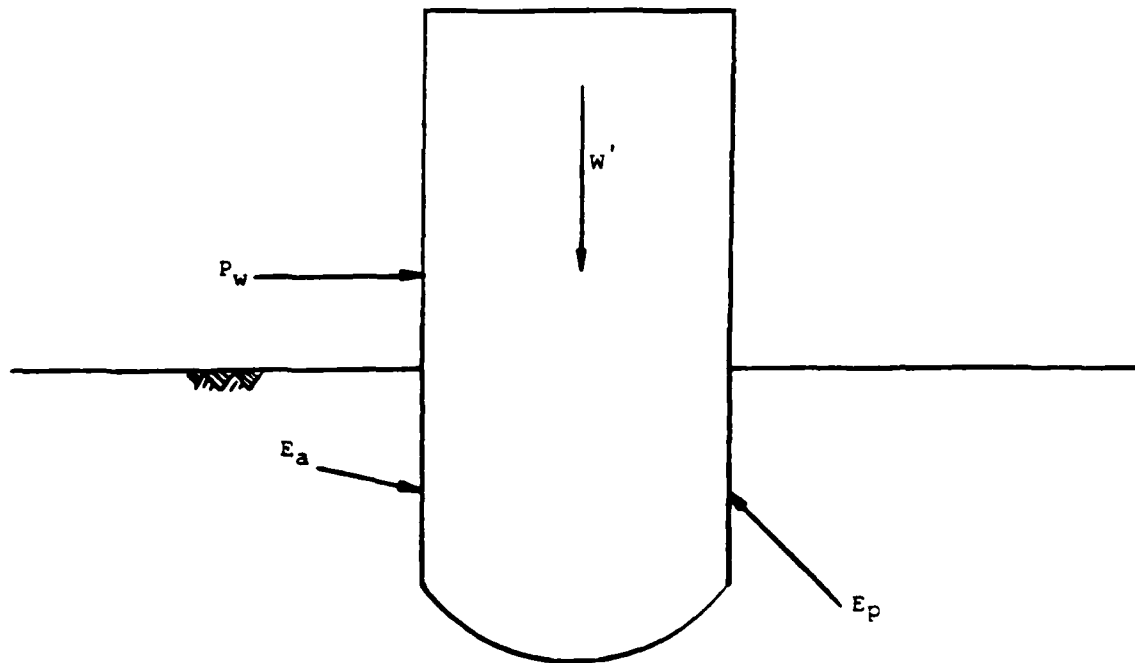
b. A-failure mode

Figure 37. Possible failure modes for cofferdams on sand
(Hansen's method)

137. If these assumptions are made, an analytical solution can be found. However, these are not the assumptions which are made by contemporary finite element analysts, for whom analytical simplicity is not a concern (Clough and Duncan 1977; Clough and Duncan 1978; Duncan et al. 1980; Duncan and Chang 1970). In particular, Hansen's assumptions do not allow the stress-strain law to vary from point to point in the fill according to the stress and deformation history which has been experienced locally. Thus, for example, the fill near the tip of the inboard wall is assumed to behave the same as the fill near the tip of the outboard wall, even though the compressive stress near the base of the inboard wall is much higher (Figure 10). Since the behavior of cohesionless material like sand is known to be strongly history dependent, Hansen's neglect of this feature is questionable.

138. Hansen's entire analysis is predicated on the existence of circular failure surfaces. Unfortunately, the model cells used by Ovesen (1962) to demonstrate the circular shape of the failure surface were only 20 cm high and 15 cm wide. Furthermore, the walls were made of two glass panes and two brass sheets which were "sufficiently rigid for the elastic deformations to be ignored" (Ovesen 1962). It appears that the walls in these models would carry a much higher proportion of the external load than would be carried by the walls of a full-sized cell, and thus the approximately circular rupture figures observed in these model tests may not represent what would happen in the field. It should be noted that Ovesen also carried out tests with larger models (72 cm in diameter), but did not observe the failure surface because of the nature of the test set up.

139. Hansen's method, as described above, gives a conservative estimate of the FS , since it does not include the stabilizing effects of the friction between the wall and fill and also, in the case of a cell founded on rock, neglects the reaction from the rock. Ovesen shows how these effects may be included.

140. The complexity of applying Hansen's method, especially for cells founded on soil, argues against its everyday use by the practicing engineer. It is based on highly theoretical concepts from solid mechanics with which most soils engineers have little familiarity. It requires computations sufficiently complicated that a computer program would be helpful, if not strictly necessary. Given these aspects of the method, most designers would probably prefer to use other methods.

PART XII: OVERTURNING

Cause of Overturning

141. The lateral force acting on the cell causes it to rotate about the toe and tip over into the interior of the cofferdam (Figure 38). The resultant of the weight of the fill and the lateral forces acting on the cell shall lie within the middle third of the cell base.
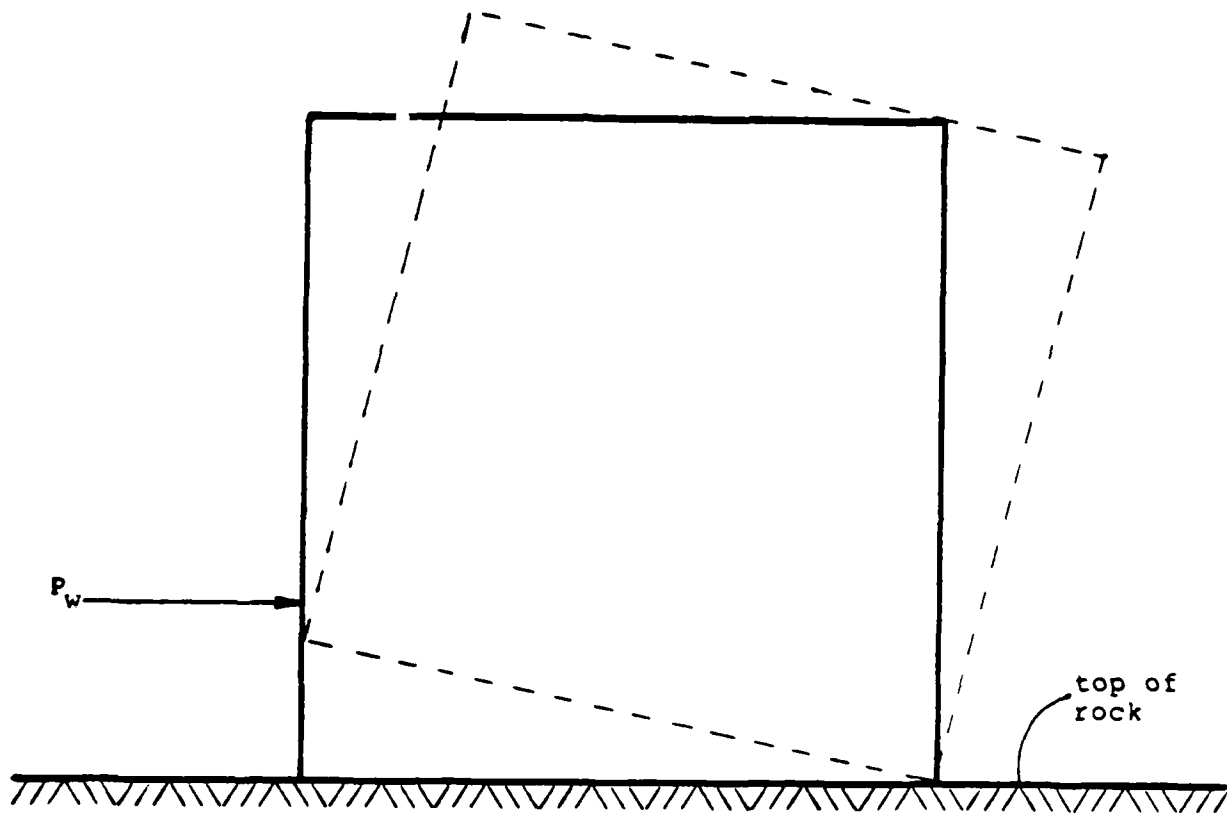
Figure 38. Failure by overturning

Considerations in Overturning Calculations

Assumed force distribution on cell base

142. If no lateral force were to act on the cell, the force distribution from the foundation acting upward on the cell would be the uniform pressure ACEB shown in Figure 39. When lateral force P_w is present, the pressure from the foundation is assumed to change to the linearly varying distribution CEBD. To investigate the possibility of overturning, the
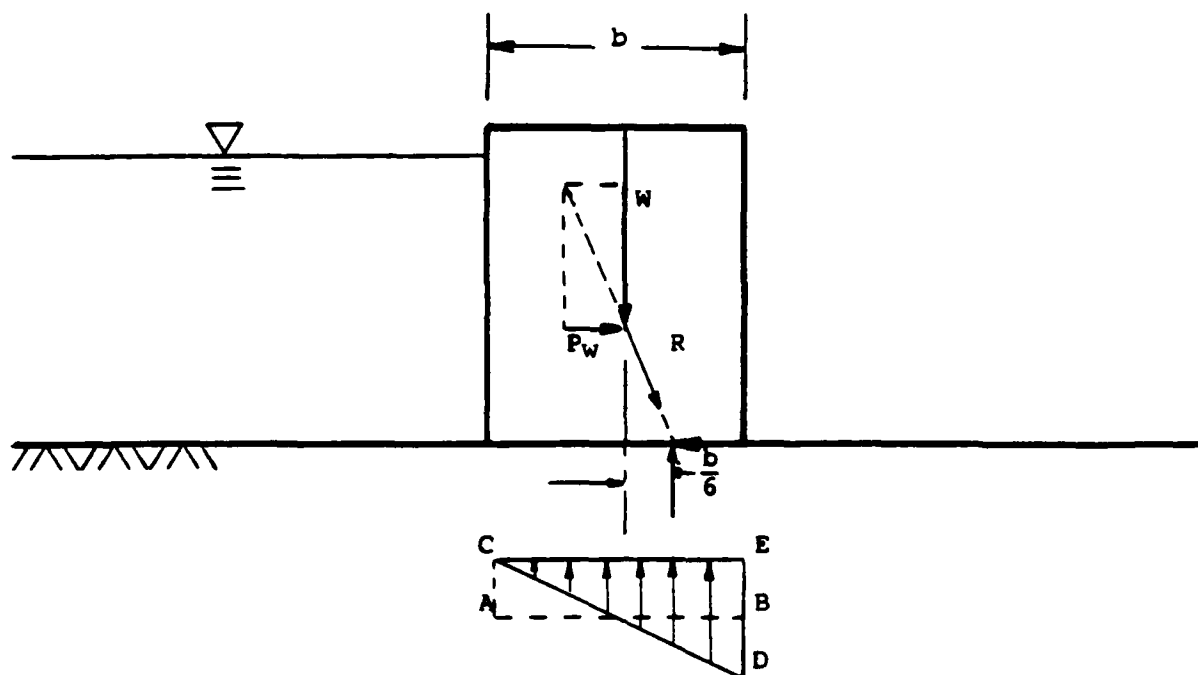
a. Stress distribution on base of cell
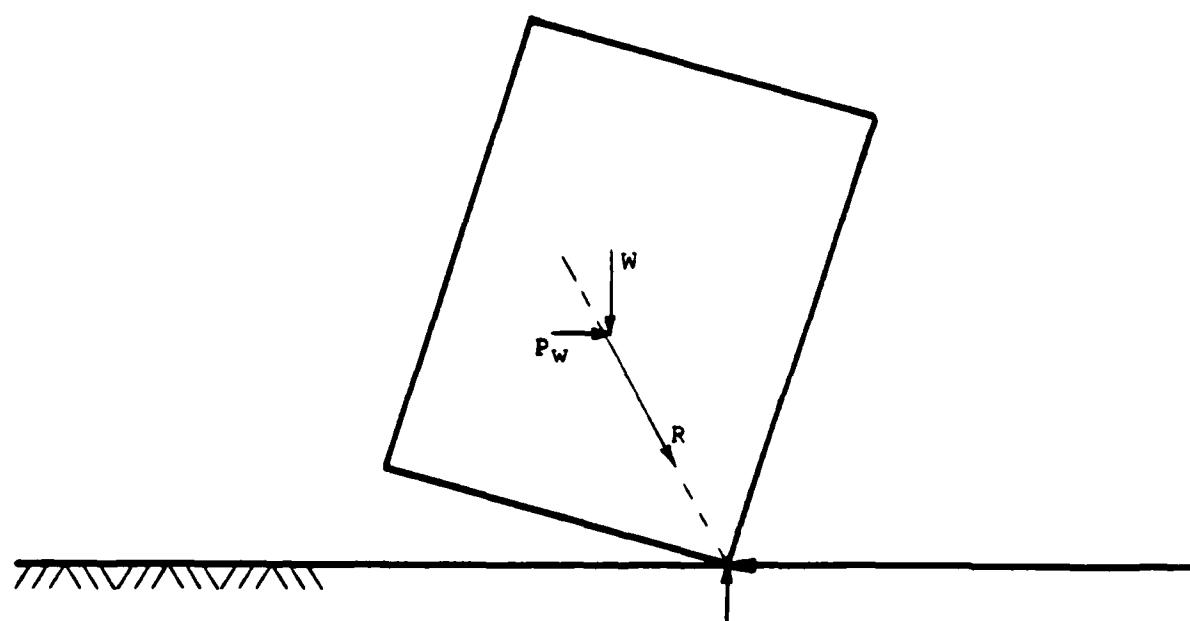
b. Impending tipping

Figure 39. Figure from foundation acting on base of cell

85

resultant R of the lateral force P_w and the weight W of the cell contents is computed, and the intersection of R with the cell base noted. For the conditions assumed in the sketch, the resultant intersects the base at a distance b/6 from the center, and the foundation and cell are beginning to lose contact at the heel, since the distributed force there is zero.

143. From 1908 until the publication of Terzaghi's paper (1945) on cofferdams, most cellular-cofferdam designs were based on the criterion of resistance to overturning. This criterion is now recognized as fundamentally incorrect (Belz 1970; TVA 1957; Cummings 1957; Schroeder and Maitland 1979). The fact that many cofferdams designed according to the criterion did not fail may be attributed to (a) cell heights were usually relatively low, compared to many modern cofferdams, and (b) cells filled with granular material are inherently quite stable because of the high shear resistance of the fill. It is important to realize that notable failures have occurred in cells filled by material deficient in shear resistance, such as clay. The requirement of designing against overturning did not prevent these failures (Cummings 1957).

Erroneous assumption

144. The basic difficulty with the approach of designing against overturning is that it is founded upon the assumption that a cellular cofferdam acts as a rigid, gravity-block structure which remains intact as it tips over. But, in fact, cofferdams are far from rigid, and failure by overturning is very unlikely to occur, since other failure modes, such as failure of the fill in shear, would occur first. These statements may be illustrated by consideration of Figure 39, in which overturning is shown to have proceeded to such an extent that the resultant now passes through the toe of the cell. Almost the entire base of the cell has lost contact with the foundation. But this situation is extremely unlikely, since once the base of the cell has lost contact with the foundation, the only means of supporting the weight of the fill is through arching. Arching is defined as vertical shear forces transmitted from the cell walls into the interior of the fill, and arching across the entire width of the cell is physically unrealistic. In place of arching, were the cell to reach the condition shown in Figure 39, a shearing failure of the fill would probably occur first. Indeed, the weakness of the overturning design rule is that it does not consider the shear resistance of the fill (Cummings 1957).

145. For the reasons just discussed, use of the criterion of designing against overturning is not recommended (Belz 1970; TVA 1957; Cummings 1957; Schroeder and Maitland 1979). However, the resultant base force must intersect the base at a distance less than $b/6$ from the center of the cell or the slip on vertical center plane in fill analysis presented in Part III will not be correct. If the resultant force falls outside of the distance $b/6$ from the center of the cell, the cell base pressure will go into tension. Since soil cannot take tension, the base pressure must be revised to reflect no tension pressure and the slip on vertical center plane in fill analysis must be revised. Also, if the resultant force falls outside of the distance $b/6$ from the center of the cell, the bearing area in the bearing capacity analysis is greatly reduced. For these reasons, even though the overturning analysis may not be fundamentally correct, the criteria should still be satisfied to make other analyses valid.

REFERENCES

Belz, C. A. 1970. "Cellular Structure Design Methods," Proceedings, Conference on Design and Installation of Pile Foundations and Cellular Structures, H. Y. Fang and T. D. Dismuke, eds., Envo Publishing Co., pp 319-338.

Clough, G. W., and Duncan, J. M. 1977. "A Finite Element Study of the Behavior of the Willow Island Cofferdam," Technical Report No. CE-218, Department of Civil Engineering, Stanford University, Stanford, Calif.

_____. 1978 (Dec). "Finite Element Analyses of Retaining Wall Behavior," Journal, Soil Mechanics and Foundations Division, American Society of Civil Engineers, Vol 97, No. SM2, pp 1657-1672.

Cummings, E. M. 1957 (Sep). "Cellular Cofferdams and Docks," Journal, Waterways and Harbors Division, American Society of Civil Engineers, Vol 83, No. WW3, Paper No. 1366, pp 13-45.

Dismuke, T. D. 1975. "Cellular Structures and Braced Excavations," Foundation Engineering Handbook, J. F. Winterkorn and H. Fang, eds., Reinhold, New York, pp 451-452.

Duncan, J. M., and Chang, C. Y. 1970 (Sep). "Nonlinear Analysis of Stress and Strain in Soils," Journal, Soil Mechanics and Foundations Division, American Society of Civil Engineers, Vol 96, No. SM5, Paper No. 7513, pp 1625-1653.

Duncan, J. M., et al. 1980 (Aug). "Strength, Stress-Strain, and Bulk Modulus Parameters for Finite Element Analyses of Stresses and Movements in Soil Masses," Report No. UCB/GT/80-01, University of California, Berkeley, Calif.

Erzen, C. Z. 1957 (Sep). Discussion of "Cellular Cofferdams and Docks," by E. M. Cummings, Journal, Waterways and Harbors Division, American Society of Civil Engineers, Vol 83, No. WW3, pp 37-43.

Esrig, M. 1970 (Nov). "Stability of Cellular Cofferdams Against Vertical Shear," Journal, Soil Mechanics and Foundations Division, American Society of Civil Engineers, Vol 96, No. SM6, Paper No. 7654, pp 1853-1862.

Grayman, R. 1970. "Cellular Structure Failures," Proceedings, Conference on Design and Installation of Pile Foundations and Cellular Structures, H. Y. Fang and T. D. Dismuke, eds., Envo Publishing Co., Lehigh Valley, pp 383-391.

Hansen, J. B. 1953. Earth Pressure Calculations, Danish Technical Press, Institution of Danish Civil Engineers, Copenhagen.

_____. 1957. "The Internal Forces in a Circle of Rupture," Bulletin No. 2, Danish Geotechnical Institute, Copenhagen.

Hansen, L. A., and Clough, G. W. 1982. "Finite Element Analyses of Cofferdam Behavior," Proceedings, Fourth International Conference on Numerical Methods in Geomechanics, Edmonton, Canada, Vol 2, pp 899-906.

Headquarters, Department of the Army. 1958 (Jul). "Design of Pile Structures and Foundations Manual," EM 1110-2-2906, Washington, DC.

_____. 1970 (Apr). "Stability of Earth and Rock-Fill Dams," EM 1110-2-1902, Washington, DC.

_____. 1974 (Apr). "Cellular Sheetpile Cofferdam Failures," Washington, DC.

_____. 1981 (Jun). "Sliding Stability for Concrete Structures," ETL 1110-2-256, Washington, DC.

Headquarters, Department of the Navy. 1971 (Mar). Soil Mechanics, Foundation and Earth Structures, NAVDOCKS Design Manual DM7, Bureau of Yards and Docks, Washington, DC.

Hetenyi, M. 1946. "Beams on Elastic Foundation," University of Michigan Press, Ann Arbor, Mich.

Heyman, S. 1957 (Sep). Discussion of "Cellular Cofferdams and Docks," by E. M. Cummings, Journal, Waterways and Harbors Division, American Society of Civil Engineers, Vol 83, No. WW3, pp 34-37.

Jumikis, A. R. 1971. Foundation Engineering, Intext Educational Publishers, Scranton, Pa.

Khuayjarernpanishk, T. 1975. Behavior of a Circular Cell Bulkhead During Construction, Ph. D. Dissertation, Oregon State University, Corvallis, Oreg.

Krynine, D. P. 1945. Discussion of "Stability and Stiffness of Cellular Cofferdams," by K. Terzaghi, Transactions, American Society of Civil Engineers, Vol 110, Paper No. 2253, pp 1175-1178.

Kurata, S., and Kitajima, S. 1967 (Sep). "Design Method for Cellular Bulkhead Made of Thin Steel Plate," Proceedings, Third Asian Regional Conference on Soil Mechanics and Foundation Engineering, Haifa, Vol I, Divisions 1-7.

Lacroix, Y., Esrig, M. I., and Lusher, U. 1970 (Jun). "Design, Construction and Performance of Cellular Cofferdams," Proceedings, ASCE Specialty Conference on Lateral Stresses in the Ground and Earth Retaining Structures, American Society of Civil Engineers, pp 271-328.

Maitland, J. K. 1977. Behavior of Cellular Bulkheads in Sands, Ph. D. Dissertation, Oregon State University, Corvallis, Oreg.

Maitland, J. K., and Schroeder, W. I.. 1979 (Jul). "Model Study of Circular Sheetpile Cells," Journal, Geotechnical Engineering Division, American Society of Civil Engineers, Vol 105, No. GT7, pp 805-821.

Matlock, H., and Reese, L. 1969. "Moment and Deflection Coefficients for Long Piles," Handbook of Ocean and Underwater Engineering, J. J. Myers, C. H. Holm, and R. F. McAllister, eds., McGraw-Hill, New York.

Moore, B. H., and Alizadeh, M. M. 1983 (Sep). "Design of Cellular Cofferdam Instrumentation," Proceedings, International Symposium of Field Measurements in Geomechanics, pp 503-512.

Mosher, R. L., and Pace, M. E. 1982 (Jun). "User's Guide: Computer Program for Bearing Capacity Analyses of Shallow Foundations (CBEAR)," US Army Engineer Waterways Experiment Station, Vicksburg, Miss.

Naval Research Laboratory. 1979 (Jan). "Trident Cofferdam Analysis," NRL Memorandum Report 3869, Naval Research Laboratory, Washington, DC.

Ovesen, N. K. 1962. "Cellular Cofferdams, Calculation Methods and Model Tests," Bulletin No. 14, Danish Geotechnical Institute, Copenhagen.

Rimstad, I. A. 1940. Zur Bemessung des Doppelten Spundwandbauwerkes, Akademiet for de Tekniske Videnskaber, Copenhagen.

Rossow, M. P. 1984 (Oct). "Sheetpile Interlock Tension in Cellular Cofferdams," Journal, Geotechnical Engineering Division, American Society of Civil Engineers, Vol 110, No. GT10, pp 1446-1458.

Schroeder, W. L., and Maitland, J. K. 1979 (Jul). "Cellular Bulkheads and Cofferdams," Journal, Geotechnical Engineering Division, American Society of Civil Engineers, Vol 105, No. GT7, pp 823-838.

Schroeder, W. L., Marker, D. K., and Khuayjarernpanishk, T. 1977 (Mar). "Performance of a Cellular Wharf," Journal, Geotechnical Engineering Division, American Society of Civil Engineers, Vol 103, No. GT3, Paper No. 12790, pp 153-168.

Scott, R. F. 1981. "Foundation Analysis," Prentice-Hall, Inc., Englewood Cliffs, New Jersey.

Sorota, M. D., and Kinner, E. B. 1981 (Dec). "Cellular Cofferdam for Trident Drydock: Design," Journal, Geotechnical Engineering Division, American Society of Civil Engineers, Vol 197, No. GT12, Paper No. 16758, pp 1643-1655.

Sorota, M. D., Kinner, E. B., and Haley, M. X. 1981 (Dec). "Cellular Cofferdam for Trident Drydock: Performance," Journal, Geotechnical Engineering Division, American Society of Civil Engineers, Vol 107, No. GT12, Paper No. 16733, pp 1657-1676.

Swatek, E. P. 1970. "Summary-Cellular Structure Design and Installation," Proceedings, Conference on Design and Installation of Pile Foundations and Cellular Structures, H. Y. Fang and T. D. Dismuke, eds., Envo Publishing Co., Lehigh Valley, pp 413-423.

Tennessee Valley Authority. 1957 (Dec). "Steel Sheet Piling Cellular Cofferdams on Rock," TVA Technical Monograph No. 75, Vol 1, pp 61-62, 66-67, and 69.

Terzaghi, K. 1945. "Stability and Stiffness of Cellular Cofferdams," Transactions, American Society of Civil Engineers, Vol 110, Paper No. 2253, pp 1083-1119.

Terzaghi, K. 1955 (Dec). "Evaluation of Coefficients of Subgrade Reaction," Geotechnique, Vol 5.

United States Steel. 1972. USS Sheet Piling Handbook, Pittsburgh, Pa., p 70.

US Army Engineer Division, Ohio River. 1974 (Apr). "An Analysis of Cellular Sheet Pile Cofferdam Failures," Cincinnati, Ohio, under sponsorship of the Civil Works Engineering Studies Program.

US Army Engineer District, St. Louis. 1983 (Nov). "Instrumentation Data Analyses and Finite Element Studies for First Stage Cofferdam," summary report for study of Lock and Dam No. 26 (Replacement).

White, A., Cheney, J. A., and Duke, M. 1971 (Aug). "Field Study of a Circular Bulkhead," Journal, Soil Mechanics and Foundations Division, American Society of Civil Engineers, Vol 87, No. SM4, Paper No. 2902, pp 89-124.

APPENDIX A: EXAMPLE PROBLEMS

1. The example problems illustrate how the material presented in this
theoretical manual is applied in the design of a cellular cofferdam. The
height of the cells is known, but the other dimensions must be determined.

Example Problem 1

Assumptions

1. cofferdam on bare rock
2. cell completely saturated
3. $H = 55$ ft*
4. $r = b/[2(0.875)]$ (initial estimate)
5. $L = 1.5b/2$ (initial estimate)
6. $b = 30$ ft (initial estimate)
7. $\theta = 45°$ (initial estimate)

Data for fill

$$\gamma_f' = 65 \text{ lbs/ft}^3$$

$\phi = 28.83°$ (implies $K_a = 0.3493$)

$\tan \delta = 0.4$

Data for sheet piles

$$t_{ult} = 16.0 \text{ k/in.} = 192,000 \text{ lb/ft}$$

$f = 0.3$

--------------------------------Bursting--------------------------------

$K = 1.2K_a = 1.2(0.3493) = 0.419$

Water level outside cell at $H/2$

Equation 13:

$$p_{max} = 0.419\{0 + 65[2(55/3) - 0]\} + 62.4[55 - (55/2)]$$

$$= 2,714.6 \text{ lb/ft}^2$$

* A table of factors for converting non-SI units of measurement to SI
(metric) units is presented on page 4.

Equation 12:

$$t_{max} = p_{max}r$$

$$= 2,714.6(b)/[2(0.875)]$$

$$= 1,551\ b(lb/ft)$$

Equation 3:

$$FS = (t_{ult})/t_{max}$$

$$= 192,000/(155b)$$

For $b = 30.0$, $FS = 4.1$
For $b = 60.0$, $FS = 2.1$

Crosswall
Equation 14:

$$t_{cw} = p_{max}L$$

$$= 2,714.6(1.5b/2)$$

$$= 2,035.9b\ lb/ft$$

$$FS = 192,000/(2,035.9b)$$

For $b = 30$, $FS = 3.1$
For $b = 60$, $FS = 1.6$

Alternative - "TVA Secant Equation"
Equation 15:

$$t_{cw} = p_{max}L\sec(\theta)$$

$$= 2,714.6(1.5b/2)\sec(45)$$

$$= 2,879.3(b) \text{ lb/ft}$$

$$FS = 192,000/(2,879.3b)$$

For b = 30.0 , FS = 2.2
For b = 60.0 , FS = 1.1

------------------------Slip on vertical centerplane------------------------

Equation 28:

$$M = (55)^3(62.4)/6 = 1,730,300 \text{ ft-lb/ft}$$

Equation 31:

$$K = \frac{\cos^2(28.83)}{2 - \cos^2(28.83)} = 0.623$$

Figures 12 & 30:

$$P_c' = P_d' = \gamma_f'KH^2/2$$

$$= 65(.623)(55)^2/2$$

$$= 61,217.2 \text{ lb/ft}$$

Equation 29:

$$S_m' = 61,217.2 \tan(28.83)$$

$$= 33,696 \text{ lb/ft}$$

Figure 13:

$$T_{cw} = 22.5 \left[\frac{1}{2} \times 2{,}465 \times 27.5 + \frac{1}{2}\, 9.17(2{,}465 + 2{,}714.7) \right.$$

$$\left. + \frac{1}{2}\, 2{,}714.7 \times 18.33 \right]$$

$$= 1856765 \text{ lbs}$$

Equation 30:

$$S_m'' = \frac{0.3 \times 1{,}856{,}765}{22.5}$$

$$= 24{,}755.1 \text{ lb/ft}$$

Equation 17:

$$FS = \frac{(33{,}696 + 24{,}755.1)(2b)}{3(1{,}730{,}300)}$$

$$= 0.0225b$$

For b = 30.0 , FS = 0.68
For b = 60.0 , FS = 1.35

--------------------------Slip on horizontal planes in fill--------------------------

Equation 28:

$$M = (55)^3(62.4)/6 = 1{,}730{,}300 \text{ ft-lb/ft}$$

Equation 46:

$$p^* = \frac{T_{cw}}{L} = \frac{1{,}856{,}765}{22.5} = 82{,}523$$

A4

Equation 47:

$$M_f = 0.3(82,523)30 = 742,706 \text{ ft-lb/ft}$$

For completely saturated fill, the integral in Equation 43 reduces to (Cummings 1957) ($c = b \tan \phi = 30.0 \tan (28.83) = 16.51$; $a = H - c = 55 - 16.51 = 38.49$):

Equation 45:

$$M_{shear} = 65 \left[\frac{38.49 \times 16.51^2}{2} + \frac{16.51^3}{3} \right]$$

$$= 438,484 \text{ ft-lb/ft}$$

Equation 32:

$$FS = \frac{742,706 + 438,484}{1,730,300} = 0.69$$

FS increases with b

--------------------------Slip between fill and sheets--------------------------

$$P'_a = 0$$

$$P_s = (0.419)65(55)^2/2 = 41,193 \text{ lb/ft}$$

Equation 48:

$$FS = \frac{b\{[41,193 + 41,193(b/(0.75b))]0.4\}}{1,730,300}$$

$$= 0.0222b$$

For b = 30, FS = 0.67
For b = 60, FS = 1.33

A5

Equation 56:

$$W_e = 65(55)b = 3,575 \text{ lb/ft}$$

$$P_w = 62.4(55)^2/2 = 94,380 \text{ lb/ft}$$

$$FS = \frac{\tan (28.83)(3,575b)}{94,380}$$

For b = 30.0 , FS = 0.63

For b = 60.0 , FS = 1.3
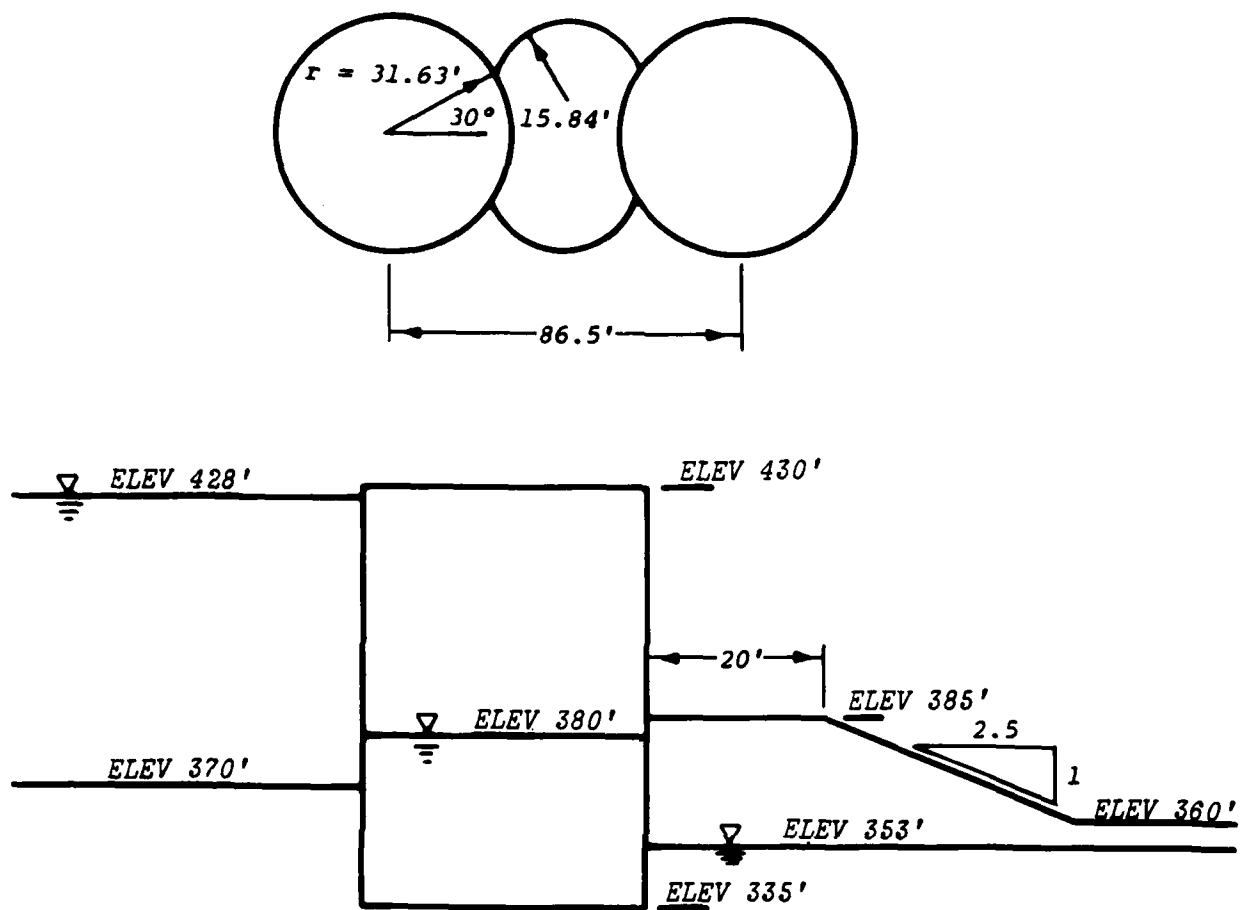
Foundation and fill material: sand

$\phi = 35°$

$\gamma_{sat} = 131 \; lb/ft^3$

$\gamma_m = 120 \; lb/ft^3$

$\gamma' = 68.6 \; lb/ft^3$

$c = 0$

$\delta = 2/3 \; \phi = 23.3°$

$L = 43.3 \; ft$

$b = 54.9 \; ft$

A7

Sheet pile properties

PS - 32

t_{ult} = 16,000 lb/in. = 16 k/in.

I = 3.6 in.^{4}

b_s = 15 in.

f = 0.3

Bursting (Part III)

$$K_a = \tan^2\left(45 - \frac{\phi}{2}\right) = 0.27$$

(CLAMSHELL FILLING)

ELEV 400

$$K = 1.6 K_a = 0.43$$

Water level inside and outside of cell at elevation 400 during clamshell filling.
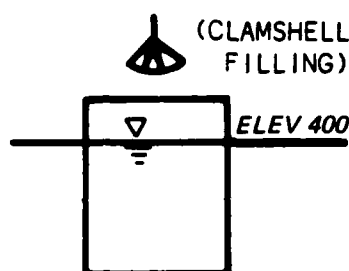
Note: If cell were filled hydraulically, water level inside cell would be at elevation 430, top of cell. With clamshell filling, water level inside and outside of the cell are near the same level for sand-filled cells on a sand foundation with good drainage.

Calculate plane of fixity

$$\ell_h = 5 \text{ tons/ft}^3 = 5.79 \text{ lb/in.}^3 \qquad \text{From Terzaghi 1955}$$

$$n_h = \frac{b_s}{d'} \ell_h \qquad \text{(Eq 8)}$$

$$d' = 3.1 \sqrt[5]{\frac{EI}{n_h}} \qquad \text{(Eq 4)}$$

Equations 4 and 8 can be rearranged to give

$$d' = 4.1 \sqrt[4]{\frac{EI}{b_s \ell_h}}$$

A8

$$d' = 4.1 \sqrt[4]{\frac{30,000,000(3.6)}{(15)(5.79)}} = 136.9 \text{ in.} = 11.4 \text{ ft}$$

Alternate method for plane of fixity

$$d' = \frac{K_a\left[\gamma_m(H_{fs} + d - H_{w4}) + \gamma'(H_{w4} - d)\right] + \Delta H_w \gamma_w}{\gamma'(K_p - K_a)} \qquad \text{(Eq 10)}$$

$$K_p = \tan^2\left(45 + \frac{\phi}{2}\right) = 3.69$$

$$H_{fs} = 60 \text{ ft}$$

$$d = 35 \text{ ft}$$

$$H_{w4} = 65 \text{ ft}$$

$$\Delta H_w = 0$$

$$d' = \frac{0.27[120(60 + 35 - 65) + 68.6(65 - 35)] + 0}{68.6(3.69 - 0.27)}$$

$$d' = 6.5 \text{ ft}$$

$$6.5 \text{ ft} < d' < 11.4 \text{ ft}$$

Terzaghi's values of ℓ_h are taken at an ultimate loading. Since the cell is not loaded at ultimate loading, we can use higher values of ℓ_h. Scott recommends to double, at least, Terzaghi's values of ℓ_h and K_{s1}.

$$d' = 4.1 \sqrt{\frac{30,000,000(3.6)}{(15)(2)(5.79)}} = 9.6 \text{ ft}$$

$$6.5 \text{ ft} < d' < 9.6 \text{ ft}$$

A9

Take $d' = 8$ ft

$\qquad x' = (H_{fs} + d')/3 = (60 + 8)/3 = 22.7$ ft $\hspace{4cm}$ (Eq 11)

Point of maximum interlock tension is

$\qquad 22.7 - 8 = 14.7$ ft above dredge line.

Alternately, point of maximum interlock tension is

$\qquad H_{fs}/4 = 60/4 = 15$ ft above dredge line

Use 15 ft above dredge line as point of maximum interlock tension.
Check cell embedment

$$d \geq 5[EI/n_h]^{1/5} \hspace{4cm} \text{(Eq 5)}$$

$$n_h = \frac{b_s}{d'} \ell_h = \frac{1.25 \text{ ft}}{8 \text{ ft}} (5.79) \frac{lb}{in.^3} = 0.9 \frac{lb}{in.^3} \hspace{2cm} \text{(Eq 8)}$$

$$d \geq 5 \sqrt[5]{\frac{30,000,000(3.6)}{2(0.9)}} = 179.7 \text{ in.} = 15 \text{ ft}$$

See note about doubling Terzaghi's values

$$d = 35 \text{ ft} > 15 \text{ ft}$$

$$P_{max} = K[120(30) + 68.6(15)]$$

$$P_{max} = 0.43[120(30) + 68.6(15)] = 1,990 \text{ lb/ft}^2$$

$$t_{max} = P_{max}r \hspace{4cm} \text{(Eq 12)}$$

$$t_{max} = 1,990(31.63) = 62,943.7 \text{ lb/ft} = 5.2 \text{ k/in.}$$

$$FS = \frac{t_{ult}}{t_{max}} = \frac{16 \text{ k/in.}}{5.2 \text{ k/in.}} = 3.1 \hspace{3cm} \text{(Eq 3)}$$

A10

Check common wall

$$t_{cw} = P_{max}L \qquad \text{(Eq 14)}$$

$$t_{cw} = 1,990(43.3) = 86,167 \text{ lb/ft} = 7.2 \text{ k/in.}$$

$$FS = \frac{t_{ult}}{t_{cw}} = \frac{16 \text{ k/in.}}{7.2 \text{ k/in.}} = 2.2$$

Slip on Vertical Center Plane (Part IV)

Water level outside of cofferdam at Elev 428 ft

Water level inside cofferdam cell at Elev 380*

Water level inside of cofferdam at Elev 353 ft

$$P_w = \frac{1}{2}(62.4)(93)^2 = 269,849 \text{ lb/ft}$$

$$P'_a = \frac{1}{2}(0.27)(35)^2(68.6) = 11,345 \text{ lb/ft}$$

$$P_{w1} = \frac{1}{2}(62.4)(18)^2 = 10,109 \text{ lb/ft}$$

$$K_p = \tan^2\left(45 + \frac{\phi}{2}\right) = 3.69 \text{ (for level backfill)}$$

$$K_p = \frac{\cos^2\phi}{\left[1 - \sqrt{\frac{\sin\phi\,\sin(\phi - \beta)}{\cos\beta}}\right]} = 1.72 \qquad \begin{array}{l}\text{(For a scoping backfill} \\ \text{with a scope of 1 to 2.5,} \\ \beta = 21.8°)\end{array}$$

---

* After I worked this example, I remembered a rule of thumb for selecting the
water level in a sand-filled cell on a sand foundation with good drainage.
The water level inside the cell is horizontal and is the average of the
water level inside and outside of the cofferdam.

$$\text{Water level inside of the cell} = \frac{428 + 353}{2} = 390.5 \text{ ft}$$

so I could have used Elev 390.5 ft instead of Elev 380.

Examining the geometry of the berm and the failure surfaces for the above assumptions indicates K_p is closer to 3.69 than 1.72, so use $K_p = 3.0$. Exact values of P_p' can be calculated using the trial wedge method.

$$P_p^* = \frac{1}{2}(3.0)(120)(32)^2 + 18(3.0)(120)(32) + \frac{1}{2}(18)^2(3.0)(68.6)$$

$$P_p^* = 184,320 + 207,360 + 33,340 = 425,020 \text{ lb/ft}$$

$$P_p' = P_w + P_a' - P_{wl} - T^* \qquad \text{(Eq 27)}$$

Let $T^* = 0$

$$P_p' = 269,849 + 11,345 - 10,109 - 0 = 271,085 \text{ lb/ft}$$

$$P_p' = 271,085 < 425,020 = P_p^*$$

Use $P_p' = 271,085 \text{ lb/ft}$

$$H_{wo} = 93 \text{ ft}$$

$$d' = 35 \text{ ft}$$

$$H_{wl} = 18 \text{ ft}$$

$$H_p' = \frac{184,320(32/3 + 18) + 207,360(9) + 33,340(18/3)}{425,020}$$

$$H_p' = 17.3 \text{ ft}$$

$$M = 269,849\left(\frac{93}{3}\right) + 11,345\left(\frac{35}{3}\right) - 271,085(17.3) - 10,109\left(\frac{18}{3}\right) \qquad \text{(Eq 28)}$$

$$M = 3,747,253 \text{ ft lb/ft}$$

A12

$$S' + S'' = \frac{3M}{2b} = \frac{3(3,747,253)}{2(54.9)} \qquad \text{(Eq 23)}$$

$$S' + S'' = 102,384 \text{ lb/ft}$$

$$K = \frac{\cos^2 \phi}{2 - \cos^2 \phi} = \frac{\cos^2 35}{2 - \cos^2 35} = 0.50 \qquad \text{(Eq 31)}$$

$$P'_c = \frac{1}{2}(0.5)(50)^2(120) + \frac{1}{2}(0.5)(45)[2(50)(120) + 45(68.6)]$$

$$P'_c = 244,729 \text{ lb/ft}$$

$$S'_m = P'_c \tan \phi = 244,729 \tan 35° \qquad \text{(Eq 29)}$$

$$S'_m = 171,361 \text{ lb/ft}$$
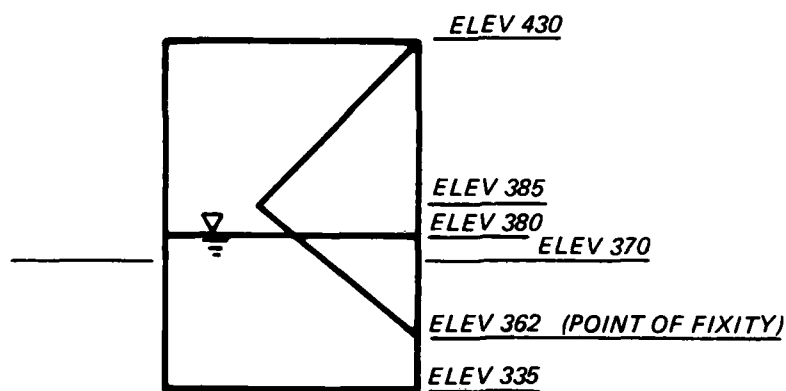
$$K = 0.43$$

$$T_{cw} = 43.3\left[\frac{1}{2}(0.43)(45)^2(120) + \frac{1}{2}(0.43)(45)(23)(120)\right]$$

$$T_{cw} = 3,418,448 \text{ lb}$$

$$S''_m = \frac{fT_{cw}}{L} = \frac{0.3(3,418,448)}{43.3} \qquad \text{(Eq 30)}$$

$$S''_m = 23,684 \text{ lb/ft}$$

$$FS = \frac{S'_m + S''_m}{\dfrac{3M}{2b}} = \frac{171,361 + 23,684}{102,384} \qquad \text{(Eq 17)}$$

$$FS = 1.91$$

Slip on Horizontal Planes in Fill (Part V)

$$M = 3,747,253 \text{ ft-lb/ft} \qquad \text{(Eq 28)}$$

$$\gamma_e = \frac{120(50) + 68.6(45)}{95} = 95.65 \text{ lb/ft}^3$$

$$M_{shear} = \frac{Hb^2\gamma_e}{6}\left(3\tan^2\phi - \frac{b}{H}\tan^3\phi\right) \qquad \text{(Eq 45)}$$

$$M_{shear} = \frac{95(54.9)^2(95.65)}{6}\left(3\tan^2 35° - \frac{54.9}{95}\tan^3 35°\right)$$

$$M_{shear} = 5,808,342 \text{ ft-lb/ft (Cummings Method)}$$

Alternate method for calculating M_{shear} (Incremental Method)   (Eq 44)

A14

ELEV 430

5'	5'	5'	5'	5'	5'	5'	5'	5'	5'	4.9'
w_1	w_2	w_3	w_4	w_5	w_6	w_7	w_8	w_9	w_{10}	w_{11}

ELEV 380

ELEV 373.44
ELEV 369.94
ELEV 366.44
ELEV 362.94
ELEV 359.44
ELEV 355.94
ELEV 352.44
ELEV 348.94
ELEV 345.44
ELEV 341.94
ELEV 338.44
ELEV 335

ϕ

A15
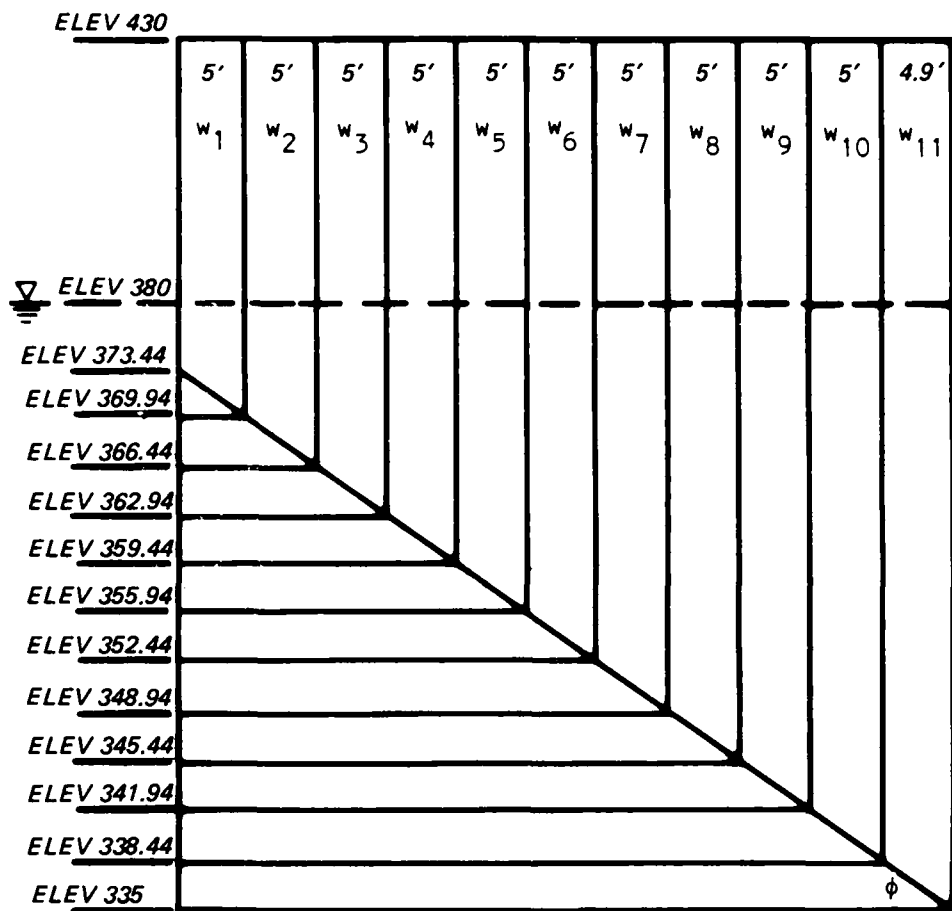
Item	Factor (Weight)	(Wt)(tan ϕ)	Arm	Moment
W_1	$\overbrace{[5(430 - 380)(120)]}^{30{,}000}$ $+ [5(380 - 369.94)(68.6)]$	23,422.35	36.69	859,366
W_2	$30{,}000 + [5(380 - 366.44) + 3.5(5)]68.6$	25,103.55	33.19	833,187
W_3	$30{,}000 + [5(380 - 362.94) + 3.5(10)]68.6$	26,784.74	29.69	795,239
W_4	$30{,}000 + [5(380 - 359.44) + 3.5(15)]68.6$	28,465.94	26.19	745,523
W_5	$30{,}000 + [5(380 - 355.94) + 3.5(20)]68.6$	30,147.14	22.69	684,039
W_6	$30{,}000 + [5(380 - 352.44) + 3.5(25)]68.6$	31,828.34	19.19	610,786
W_7	$30{,}000 + [5(380 - 348.94) + 3.5(30)]68.6$	33,509.54	15.69	525,765
W_8	$30{,}000 + [5(380 - 345.44) + 3.5(35)]68.6$	35,190.74	12.19	428,975
W_9	$30{,}000 + [5(380 - 341.94) + 3.5(40)]68.6$	36,871.93	8.69	320,417
W_{10}	$30{,}000 + [5(380 - 338.44) + 3.5(45)]68.6$	38,553.13	5.19	200,091
W_{11}	$30{,}000 + [4.9(380 - 335) + 3.44(50)]68.6$	39,859.66	1.72	68,559

$$\Sigma = 6{,}071{,}947 \text{ ft-lb/ft}$$

$M_{shear} = 6{,}071{,}947$ ft lb/ft (Incremental Method)

Alternate method for calculating M_{shear} (single increment)

$$M_{shear} = \tan (\phi) \, \Sigma[(\Delta W_e)_i \, (H - y_i)] \qquad \text{(Eq 44)}$$

$$M_{shear} = \tan 35° \, [50(54.9)(120) + 68.6(45)(54.9)] \left[\frac{1}{2} (54.9) \tan 35°\right]$$

A16

$$M_{shear} = 6,713,872 \text{ ft lb/ft (single increment)}$$

Use Eq 45 for M_{shear}

$$T_{cw} = 3,418,448 \text{ lb}$$

$$M_f = \frac{fbT_{cw}}{L} = \frac{0.3(54.9)(3,418,448)}{43.3} \qquad \text{(Eq 47)}$$

$$M_f = 1,300,273 \text{ ft-lb/ft}$$

$$FS = \frac{M_f + M_{shear}}{M} \qquad \text{(Eq 32)}$$

$$FS = \frac{1,300,273 + 5,808,342}{3,747,253}$$

$$FS = 1.90$$

Slip Between Sheeting and Fill (Part VI)

$$M = 3,747,253 \text{ ft-lb/ft}$$

$$P'_a = 11,345 \text{ lb/ft}$$

$$K = 1.6K_a = 1.6(0.27) = 0.43$$

$$P_s = \frac{1}{2}(0.43)(50)^2(120) + \frac{1}{2}(45)[2(0.43)(50)(120) + 0.43(68.6)(45)]$$

$$P_s = 645,000 + 145,967 = 210,467 \text{ lb/ft}$$

$$FS = \frac{b\left[P'_a \tan \delta + P_s + P_s \frac{b}{L} \tan \delta\right]}{M} \qquad \text{(Eq 48)}$$

A17

$$FS = \frac{54.9\left\{11,345 \tan 23.3° + 210,467 + 210,467\left[\left(\frac{54.9}{43.3}\right)\right] \tan 23.3°\right\}}{3,747,253}$$

$$FS = 3.08$$

Pullout of Outboard Sheeting (Part VII)

From Part IV

$$P_w = 269,849 \text{ lb/ft}$$

$$P'_a = 11,345 \text{ lb/ft}$$

$$P_{wl} = 10,109 \text{ lb/ft}$$

$$P'_p = 271,085 \text{ lb/ft}$$

$$H_{wo} = 93 \text{ ft}$$

$$d = 35 \text{ ft}$$

$$H_{wl} = 18 \text{ ft}$$

$$H'_p = 17.3 \text{ ft}$$

$$ML = L\left(P_w H_{wo}/3 + P'_a d/3 - P'_p H'_p - P_{wl} H_{wl}/3\right)$$

$$ML = 43.3[269,849(93)/3 + 11,345(35)/3 - 271,085(17.3) - 10,109(18)/3]$$

$$ML = 162,256,048 \text{ ft-lb}$$

A18

From Part VI

$$P_s = 210,467 \text{ lb/ft}$$

$$Q_{uo} = (P_a' + P_s) \tan \delta \qquad \text{(Eq 51)}$$

$$Q_{uo} = (11,345 + 210,467) \tan 23.3° = 951,527 \text{ lb/ft}$$

$$Q_{uc} = 2P_s \tan \delta \qquad \text{(Eq 52)}$$

$$Q_{uc} = 2(210,467) \tan 23.3 = 181,283 \text{ lb/ft}$$

$$M_r b = b\left(Q_{uo}L + \frac{1}{2} Q_{uc}b\right)$$

$$M_r b = 54.9\left[95,527(43.3) + \frac{1}{2}(181,283)(54.9)\right]$$

$$M_r b = 500,278,306 \text{ ft-lb}$$

$$FS = \frac{M_{rb}}{ML} \qquad \text{(Eq 49)}$$

$$FS = \frac{500,278,306}{162,256,048} = 3.08$$

Same value of FS as in Part VI because these two equations are the same.

Penetration of Inboard Sheeting (Part VIII)

From Part IV

$$P_p' = 271,085 \text{ lb/ft}$$
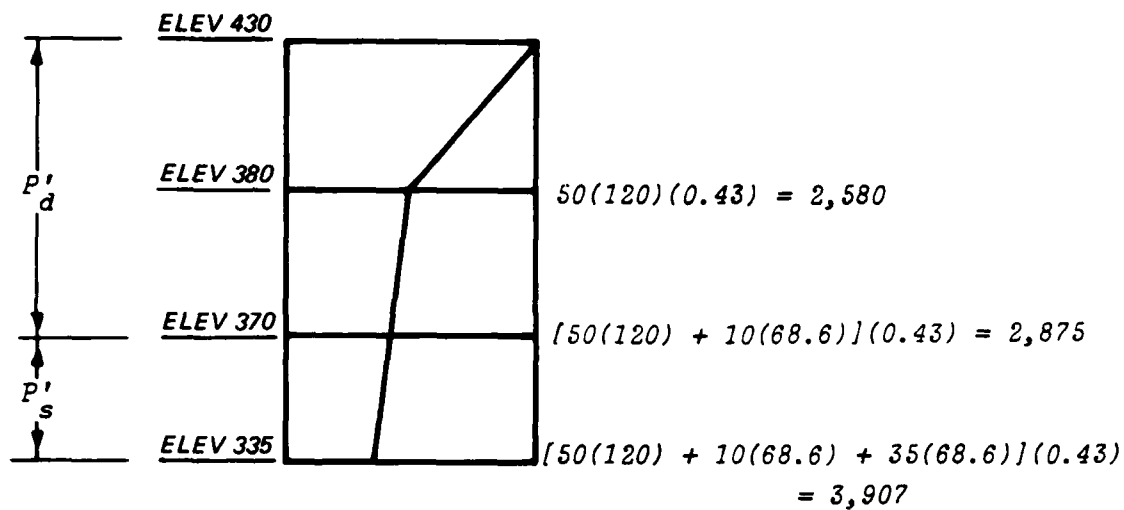
$$P'_d = \frac{1}{2}(0.43)(50)^2(120) + \frac{1}{2}(0.43)(10)[2(50)(120) + 10(68.6)]$$

$$P'_d = \frac{1}{2}(50)(2,580) + \frac{1}{2}(10)(2,580 + 2,875)$$

$$P'_d = 91,775 \text{ lb/ft}$$

$$P'_s = \frac{1}{2}(35)[2,875 + 3,907] = 118,685 \text{ lb/ft}$$

$$FS = \frac{(P'_p + P'_s)\tan\delta}{P'_d\tan\delta} \qquad\qquad (\text{Eq } 53)$$

$$FS = \frac{(271,085 + 111,685)\tan 23.3°}{91,775\tan 23.3°}$$

$$FS = 4.17$$

Bearing Failure of Foundation (Part IX)
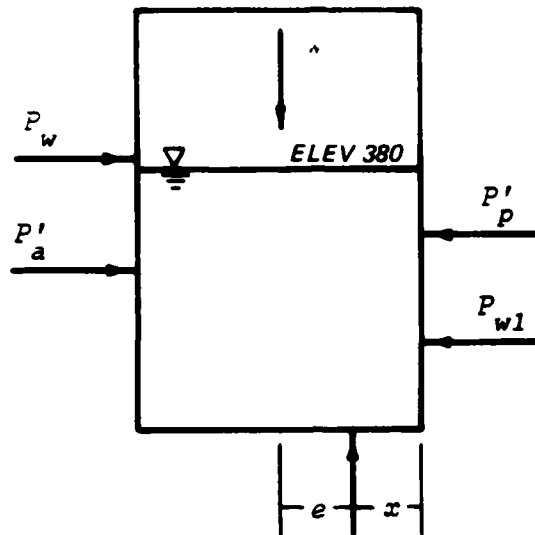
From Part IV

$$P_w = 269,849 \text{ lb/ft}$$

$$P'_a = 11,345 \text{ lb/ft}$$

$$P_{wl} = 10,109 \text{ lb/ft}$$

$$P'_p = 271,085 \text{ lb/ft}$$

$$H_{wo} = 93 \text{ ft}$$

$$d = 35 \text{ ft}$$

$$H_{wl} = 18 \text{ ft}$$

$$H'_p = 17.3 \text{ ft}$$

$$W = 54.9[50(120) + 45(68.6)] = 498,876 \text{ lb/ft}$$

$$R_v = W = 498,876 \text{ lb/ft}$$

$$R_H = 269,849 + 11,345 - 271,085 - 10,109 = 0$$

Find the eccentricity

$$R_v x = 498,876 \left(\frac{54.9}{2}\right) + 271,085(17.3) + 10,109 \left(\frac{18}{3}\right)$$

$$- 269,849 \left(\frac{93}{3}\right) - 11,345 \left(\frac{35}{3}\right)$$

$$R_v x = 9,946,893 \text{ ft-lb/ft}$$

$$x = \frac{9,946,893}{498,876} = 19.9 \text{ ft}$$

$$e = \frac{54.9}{2} - 19.9 = 7.51 \text{ ft}$$

Effective base width due to eccentricity

$$B' = b - 2e = 54.9 - 2(7.51) \qquad \text{(Eq 55)}$$

$$B' = 39.88 \text{ ft}$$

$$q_{act} = \frac{498,876}{39.88} = 12,509 \text{ lb/ft}^2$$

For $\phi = 35°$

$$N_\phi = \tan^2 \left(45 + \frac{35}{2}\right) = 3.69$$

$$N_q = e^{\pi \tan 35°}(3.69) = 33.3$$

A22

$$N_\gamma = (33.3 - 1) \tan [(1.4)(35)] = 37.2$$

$$\zeta_q = \zeta_\gamma = 1 + 0.1(3.69) \left(\frac{39.88}{\text{large number}} \right) = 1$$

$$\zeta_{qd} = \zeta_{\gamma d} = 1 + 0.1 \left(\frac{35}{39.88} \right) \tan \left(45 + \frac{35}{2} \right) = 1.17$$

$$\zeta_{qi} = \zeta_{\gamma i} = 1$$

$$\zeta_{qt} = \zeta_{\gamma t} = 1$$

$$\zeta_{qg} = \zeta_{\gamma g} = (1 - \tan \beta)^2 = ? \text{ Say } = 1$$

$$q_{ult} = 1(1.7)(1)(1)(1)(35)(68.6)(33.3)$$

$$+ \frac{1(1.17)(1)(1)(1)(39.88)(68.6)(37.2)}{2}$$

$$q_{ult} = 93,545 + 59,536 = 153,081 \text{ lb/ft}^2$$

$$FS = \frac{q_{ult}}{q_{eff}} = \frac{153,081}{12,509} \qquad \text{(Eq 54)}$$

$$FS = 12.2$$

Sliding Stability (Part X)

See Figure 34

A sliding stability analysis was made of an equivalent cofferdam as shown in Figure 34 using a computer program. The results of the analysis are as follows:

A23

Sliding Surface	FS
9 - 4 - 5 - 7	2.28
10 - 3 - 5 - 8	2.46
11 - 2 - 5 - 8	2.60

$$FS = 2.28$$

Overturning (Part XII)

From Part IX

$$e = 7.51 \text{ ft}$$

$$b = 54.9 \text{ ft}$$

$$\frac{b}{6} = \frac{54.9}{6} = 9.15 \text{ ft}$$

$$7.51 \text{ ft} < 9.15 \text{ ft}$$

APPENDIX B: NOTATION

a   Vertical distance from pole to base of cell (Figure 36)

A'   Area between circular failure surface and base of cell (Figure 36)

b   Equivalent width of cofferdam (width of fictitious straight-walled cofferdam of same plan area) (Figure 1)

b_s Width of a single sheet-pile

B   Total width of cellular cofferdam (Figure 1)

d   Depth of embedment (Figure 5)

d'   Depth to fixity (Figure 5)

e   Eccentricity of bearing force. Also, base of natural logarithms

E   Modulus of elasticity of the sheet-pile

E_s A horizontal spring modulus representing the behavior of the soil sheet-pile system

f   Coefficient of friction of interlocks (steel-on-steel)

f*   Coefficient of friction of fill on rock

F   Resultant friction force in interlocks of crosswall

F*   Shear force on horizontal planes within the fill (Figure 16)

FS   Factor of safety

H   Vertical distance from sheet-pile tips to top of cell

H_e Vertical distance from plane of fixity to top of cell (effective length of the sheet piles) (Figure 5)

H_p' Vertical distance from sheet-pile tips to line of action of P_p' (Figure 28c)

H_w Vertical distance from dredgeline to surface of water outside of cell (Figure 5)

H_{fs} Vertical distance from dredgeline to top of cell (free-standing height) (Figure 5)

H_{wc} Vertical distance from plane of fixity to intersection of phreatic surface with center line of cell (Figure 5)

B1

H_{wo} Vertical distance from sheet-pile tips to water level outside of cofferdam (Figure 28)

H_{w1} and H_{w2} Vertical distances from sheet-pile tips to intersection of phreatic surface with inboard sheeting (Figure 11)

H_{w3} Vertical distances from sheet-pile tips to intersection of phreatic surface with cell center line (Figure 11)

H_{w4} Vertical distance from sheet-pile tips to water level inside of cell

I Moment of inertia of the sheet-pile section

k_{s1} Basic value of coefficient of vertical subgrade reaction

K Lateral earth-pressure coefficient

K_a Active earth-pressure coefficient

K_p Passive earth-pressure coefficient

l_h Constant of horizontal subgrade reaction for anchored bulkhead with free earth support

L Average distance between crosswalls (Figure 1)

M Overturning moment (per unit length of cofferdam) (Equation 22)

M' Moment caused by the driving forces and effective weight about the center of the circle of rupture (Figure 36)

$M*$ Total moment acting on outboard sheet pile in Cummings' method

M_{ao} , M_{ai} Moments caused by active pressure of the fill acting on the inside of the outboard and inboard walls, respectively

M_f Moment caused by the friction force in the interlocks of the crosswall

M_r The resisting moment (per unit length of cofferdam) due to pullout of the equivalent cofferdam outboard and commonwall sheeting

M_{wo} Moment caused by water pressure acting on the <u>inside</u> of the outboard wall

M_{shear} Moment caused by the pressure of that portion of the fill which fails in shear on horizontal planes

M_W Moment of effective weight of fill above circular failure surface

ML	Overturning moment
n_h	Constant of horizontal subgrade reaction
N'	Resultant effective soil force acting on the base of the cofferdam (per unit length of cofferdam)
P*	Horizontal total force (per unit length of cofferdam) acting on inside of cell, in Cumming's method (Figure 19)
P'_a	Horizontal effective force (per unit length of cofferdam) of foundation soil on outboard sheeting, calculated using active earth-pressure coefficient (Figure 11 and Equation 26)
P'_c	Horizontal effective force (per unit length of cofferdam) acting on center plane of cell (Figure 12)
P'_d	Horizontal effective force (per unit length of cofferdam) of the fill acting on the inboard wall (Figure 30)
P'_p	Horizontal effective force (per unit length of cofferdam) of the foundation soil acting on the outside of the inboard sheeting
P^*_p	Horizontal effective force (per unit length of cofferdam) of berm and foundation soil on inboard sheeting, calculated using passive earth-pressure coefficient
P_s	Horizontal *effective force (per unit length)* of cell fill and foundation material within an equivalent cofferdam cell acting on a cell wall (Figure 28)
P'_s	Horizontal effective force (per unit length of cofferdam) of the foundation soil acting on the interior of the inboard wall (Figure 30)
P_w	Resultant force (per unit length of cofferdam) from water pressure acting on exterior of outboard wall (Figure 11)
P_{w1}	Resultant force (per unit length of cofferdam) from water pressure acting on exterior of inboard wall (Figure 11 and Equation 25)
P_{max}	Maximum lateral pressure acting against the wall
P_1 , P_2	Pressures used in derivation of Cumming's method (Figure 16)
Q	Force from foundation acting on half of fill (Figure 10)
Q_{uc}	Ultimate sheet-pile pullout capacity (per unit length) of the common wall
Q_{uo}	Ultimate sheet-pile pullout capacity (per unit length of cofferdam) of outboard sheeting

B3

r	Radius of cell. Also, radial distance (polar coordinate)
R	The resultant force of the horizontal and vertical forces acting on the cell
S'	Vertical shearing force (per unit length of cofferdam)
S''	Friction force (per unit length of cofferdam) from interlocks
S_m'	Maximum possible value of shearing force on vertical center plane of cell
S_m''	Maximum possible value of friction force from interlocks in crosswall
t_{cw}	Interlock tension (per unit length of sheet) in crosswall
t_{max}	Maximum interlock tension (per unit length of sheet) existing in the cell walls
t_{ult}	Maximum permissible interlock tension (per unit length of sheet) as specified by the sheet-pile manufacturer
T	Resultant tensile force in interlock of a single sheet pile
$T*$	Horizontal shear force on base of cofferdam (per unit length of cofferdam)
T_{cw}	Resultant tensile force in crosswall
U	Resultant uplift force due to water pressure acting on the base of the cofferdam (per unit length of cofferdam)
W	Weight of contents of cell
W'	Effective weight of fill above circular failure surface (Figure 37)
W_e	Effective weight of fill
x'	Distance from the plane of fixity to the point of maximum interlock tension
y	Distance measured downward from the top of the cell
δ	Angle of friction between soil and sheetpiling
Δ	Small increment
ΔH_w	Differential water head between inside and outside of the cell the water level inside of the cell minus the water level outside of the cell

γ' Effective unit weight of soil

γ_e Effective unit weight of soil = weighted average of γ_m above
         the phreatic line and γ' below the phreatic line

γ_f Unit weight of dry fill

γ_f' Submerged unit weight of fill

γ_m Unit weight of moist fill

γ_s' Submerged unit weight of foundation soil

γ_w Unit weight of water

θ Angle measured from the cofferdam axis to the connecting pile;
         also, angle in polar coordinate system

ϕ Angle of internal friction of fill